SYNTHESIS AND PROPERTIES OF POLYAMPHOLYTE AND THEIR APPLICATION TO CELL CRYOPROTECTION

By JING ZHAO, M.Sc.

A Thesis Submitted to the School of Graduate Studies in Partial Fulfilment of the Requirements for the Degree Doctor of Philosophy of Science

McMaster University

DOCTOR OF SCIENCE (2018) McMaster University

(Chemistry and Chemical Biology) Hamilton, Ontario

TITLE: Synthesis and Properties of Polyampholytes and their Application to Cell Cryoprotection

AUTHOR: Jing Zhao, B.Sc. and M.Sc. (Beijing Normal University, P.R. China)

SUPERVISOR: Professor Harald D.H. Stöver

NUMBER OF PAGES: xxvii, 199

Abstract

Polyampholytes are known as polymers comprising both cationic and anionic groups that can have pronounced isoelectric point behavior and strong responses to ionic strength, such as the anti-polyelectrolyte effect. This thesis focusses on exploring the solution properties of fully ionized random polyampholytes, their phase separation behavior, and their application in cell cryoprotection.

The reactivity ratios of different monomer pairs were measured by NMR to guide the subsequent formation of a series of polyampholytes with different charge ratios, molecular weights and compositions by free radical copolymerization with little compositional drift. The polyampholytes, comprising different ratios of *N*-(3-aminopropyl)methacrylamide hydrochloride (APM) and acrylic acid (AA), show phase separation at their isoelectric point, pH(I), anti-polyelectrolyte effects, and temperature responsive solubility. The latter include lower critical solution temperature (LCST) and upper critical solution temperature (UCST) behaviors, depending on composition and conditions. At the pH(I), liquid to solid phase separation is shown to be driven by a combination of electrostatic interactions and hydrogen bonding. The stoichiometric APM/AA polyampholytes with different molecular weights reveal significant molecular weight effects on polyampholyte properties, including their phase separation efficiency, anti-polyelectrolyte effect and LCST, but not their pH(I). High molecular weight polyampholytes were crosslinked into permanent hydrogels using THPC, and used to explore organic dye absorption from water.

Stoichiometric polyampholytes based on different monomers showed that the hydrophobicity of the comonomers also contributes to the polyampholyte phase separation. Depending on the balance of electrostatic interaction and polymer hydrophobicity,

polyampholytes may show no phase separation, liquid to liquid, and liquid to solid phase separations. Finally, polyampholytes made from *N*-[3-(dimethylamino)propyl methacrylamide (DMAPMA) and acrylic acid (AA) were used as macromolecular, non-penetrating cryoprotective agents for NIH 3T3 cells. The results show that to work as cryoprotective agents the polyampholytes need to have a moderate excess of negative charge at physiological conditions, with post-thaw cell viability further improved by high MW and with presence of about 10 mol% hydrophobic comonomer. As non-penetrating cryoprotective agents, these polyampholytes show good protection of the cell membrane from interstitial ice damage and 70-80% post-thaw cell viability, by bonding on cell surfaces and phase separating around the cells upon freezing. However, the absence of intracellular protection leads to low cell attachment and growth after thawing, which can be improved by introducing as little as 2% DMSO prior to freezing. As a result, polyampholytes cryoprotective agents can significantly decrease DMSO levels required for cell cryoprotection from 10% to 2%.

Acknowledgements

First I would like to express my sincere appreciation to my supervisor Dr. Harald D. H. Stöver for providing me a great Ph.D. life. He is the most amazing supervisor, who is enthusiastic, thoughtful and helpful and encourage me to explore the new research fields based on my interests. I learned a lot from him in the last five years, the diamond I learnt from his is his rigorous scholarship, I will follow this and be strict myself in my future work. More just a supervisor, Dr. Stöver is a best friend and the role model for me. Without him, I would not achieve what I have done.

I would also thank to my committee members: Dr. Giuseppe Melacini, Dr. Shiping Zhu, Dr. Emily D. Cranston and Dr. Ryan Wylie. Thank you for the insightful comments on my research and also for the hard question, which encourage me to widen and deepen my understanding of my research.

I would give my special thanks to Dr. Nicholas A.D. Burke for his enormous help during most of my Ph.D. life. My sincere thanks also goes to everyone in my group, Dr. Rachelle Kleinberger, Alison Stewart, Samantha Ros, Yuqing Zhao, Sheilan Sinjari， Christal Zhou, Derrick Hastings, Mitchell Jonson and also Krystle Pinto, Robert Fisher for your help and friendships over the years.

I would like to thank my parents and my wife Wenwen Xu for your unconditional love and support. Thanks for being by my side in my life. Finally, I want to thank all my friends for your help and friendship.

Table of Contents

List of Figures

List of Tables

List of Schemes

List of Abbreviations and Symbols

AA	Acrylic acid
AAm	Acrylamide
AMPS	2-Acrylamido-2-methylpropanesulfonate
APM	*N*-(3-Aminopropyl)methacrylamide Hydrochloride
BCS	Bovine calf serum
BSA	Bovine serum albumin
CAA	2-carboxyethyl acrylate
CTA	Chain transfer agent
DMAEMA	(2-Dimethylaminoethyl) methacrylate
DMAPMA	*N*,*N*-Dimethylaminopropyl acrylamide
DMEM	Dulbecco's modified eagle medium
FBS	Fetal bovine serum
FITC	Fluorescein isothiocyanate isomer 1
hBMSCs	Human bone marrow stromal osteoprogenitor cells
HEA	2-Hydroxyethyl methacrylate
HES	Hydroxyethyl starch
iPS cell	Induced pluripotent stem cell
LCST	Lower critical solution temperature
MAA	Methacrylic acid
MAETAc	2-Methacryloyloxyethyltrimethylammonium
MAPTAc	3-Methacryloyl aminopropyl trimethyl ammonium chloride
MES	2-methacryloyloxyethanesulfonate
NaSS	Sodium styrene sulfate
PBS	Phosphate-buffered saline
PDA49	Poly(DMAPMA-*co*-AA) with 49% DMAPMA in polymer
PDA_x-1/2/3	Poly(DMAPMA-*co*-AA), x= mol% of DMAPMA in polymer, 1,2,3 represents polymer with different molecular weights
PDAs50	Poly(DMAPMA-*co*-AMPS) with 50% DMAPMA in polymer

$PDAt_x$	Poly(DMAPMA-*co*-AA-*co*-*t*-BuAAm), x= mol% of *t*-BuAAm, ADMPAM:AA=30:70.
PDN50	Poly(DMAPMA-*co*-NaSS) with 50% DMAPMA in polymer
pH(I)	Isoelectric point
PMA50	Poly(APM-*co*-AA) with 50% APM in polymer
PMAx	Poly(APM-*co*-AA), x= mol% of APM in polymer
PMA-x	Poly(APM-*co*-AA) with 52% APM in polymer, x=Mw of the polymer
PMAs49	Poly(APM-*co*-AMPS) with 49% APM in polymer
PMcA52	Poly(MAPTAc-*co*-AA) with 52% MAPTAc in polymer
PMcAs54	Poly(MAPTAc-*co*-AMPS) with 54% MAPTAc in polymer
PMcN48	Poly(MAPTAc-*co*-NaSS) with 48% MAPTAc in polymer
PMN45	Poly(APM-*co*-NaSS) with 45% APM in polymer
PSPB	Poly[3-((3-methacrylamidopropyl) dimethylammonio) betaine-1-sulfonate]
$PSPBA_{60}$	Poly[3-((3-methacrylamidopropyl) dimethylammonio)betane-1-sulfonate-*co*-acrylic acid]
PVA	Poly(vinyl alcohol)
PVP	Polyvinylpyrrolidone
t-BuAAm	*N*-tert-butylacrylamide
THPC	Tetrakis (hydroxymethyl) phosphonium chloride
TMA	2-(Acryloyloxy)ethyl] trimethylammonium chloride
UCST	Upper critical solution temperature
Vazo-56	2,2'-Azobis(2-methylpropionamidine)dihydrochloride
VBTEAc	Vinylbenzyl trimethylammonium chloride
4VP	4-Vinylpyridine

Declaration of Academic Achievement

Chapter 2

I performed all experiments except the elemental analysis, which was carried out by Dr. Steve Kornic. I also wrote the manuscript, with edit and feedback provided by Dr. Burke and Dr. Stöver.

Chapter 3

I designed all experiments and performed: ^{1}H-NMR, GPC, fluorescent labelling of copolymers, measurement of phase separation efficiency, cloud points, dye binding and release, and most of coacervate crosslinking, microscopy measurements and some of the polymerizations and titrations. Krystle Pinto carried out most of the polymerizations, purifications, titrations and some of the coacervate crosslinking experiments and microscopy measurements. I also wrote the manuscript, with editorial help and feedback from Dr. Burke and Dr. Stöver.

Chapter 4

I designed all experiments, performed all measurements and synthesized most of polymers. Dr. Burke synthesized three of the polymers: PMAs49, PMcAs54 and PAPM. I also wrote the manuscript, with editorial help and feedback from Dr. Stöver.

Chapter 5

I designed all experiments and performed: synthesis of polybetaines, fluorescent labelling of APM, ^{1}H-NMR, GPC, DSC, most of the polyampholytes synthesis, cryomicroscopy experiments, and part of the cell culture and cryoprotection. Mitchell Johnson did some of

the cell culture, cryoprotection and cryomicroscopy experiments. Robert Fisher carried out part of the polyampholyte syntheses and cell cryoprotection experiments. I also wrote the manuscript, with editorial help and feedback from Dr. Stöver.

Chapter 1. Introduction

1.1 Introduction to Polyampholytes

Multi-responsive polymers, and materials incorporating them, have received considerable focus in recent decades. The properties of such polymers change reversibly in response to environment changes, e.g., pH, temperature, ionic strength, and light.[1-5] Zwitterionic polymers are one type of multi-responsive polymer that have unique solution properties including protein-like properties, anti-fouling behaviour and good cell compatibility, which has prompted ongoing interest.[6-8]

Both synthetic and natural origin polyampholytes have cationic and anionic groups on separate monomers units.[9] In contrast, polybetaines are zwitterionic polymers that carry both cationic and anionic groups on the same monomer units,[10] as shown in Scheme 1.1. The copolymer nature of polyampholytes allows easy access to polyampholytes with different charge ratios and corresponding isoelectric point (pH(I)), and can draw on a larger choice of commercial monomers, compared to polybetaines, for which there are fewer commercially available monomers and where the monomers have 1 to 1 charge ratio.

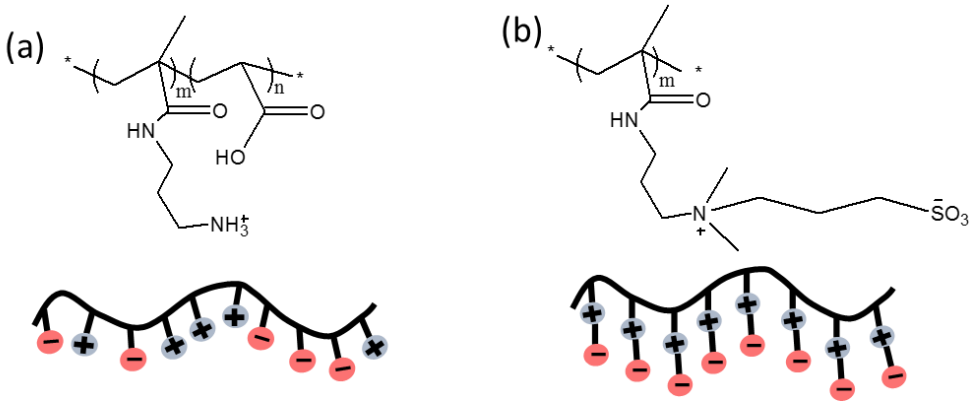

Scheme 1.1 Structures of (a) APM-AA polyampholyte (poly(*N*-(3-aminopropyl)methacrylamide hydrochloride-*co*-acrylic acid)), (b) poly[3-((3-methacrylamidopropyl)dimethylammonio)propane-1-sulfonate] and their charge distribution.

Polyampholytes show two special properties, the pH(I) and the anti-polyelectrolyte effect, illustrated in Scheme 1.2. The pH(I) is the pH value at which the net charge of a polyampholyte is zero, which often leads to polyampholyte chain aggregation or precipitation. The pH(I) for polyampholytes incorporating weak acids and bases depends on the molar ratio of the ionizable comonomers.[11,12] The anti-polyelectrolyte effect implies that addition of salts like NaCl causes the chains to expand and enhances their solubility, as salt can shield the electrostatic interactions within the polyampholyte.[9, 13] Some polyampholytes also show thermal phase separations, including a lower critical solution temperature (LCST) at certain [NaCl] and an upper critical solution temperature (UCST) in water / organic solvent mixtures.[11, 12, 14, 15]

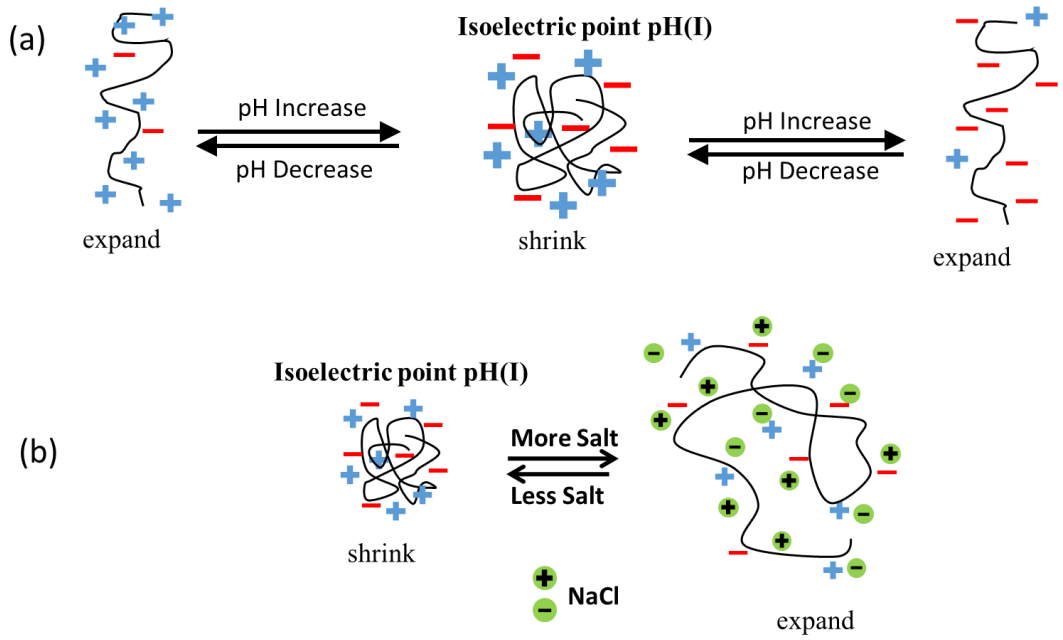

Scheme 1.2 Properties of polyampholytes (a) the pH(I), (b) the anti-polyelectrolyte effect.

Natural polyampholytes such as proteins, polypeptide, collagen and gelatin play important roles in physiological activity.[16-18] Proteins can be seen as pH responsive copolymers with nearly 20% of residues having cationic or anionic groups,[13] so it is not surprising that synthetic polyampholytes have been used as protein mimics.[8]

Synthetic polyampholytes are typically prepared by copolymerization of separate monomers containing acid and basic groups, as well as optionally other, neutral comonomers. Synthetic polyampholytes can be divided into four groups based on the anionic and cationic groups, e.g., polyampholytes with: strong acid and base, strong acid and weak base, weak acid and strong base, weak acid and base.[19] Polyampholytes containing weak acids and/or bases will show pH-dependent solubility,[14,19] while polyampholytes bearing permanent anionic and cationic charges will have a fixed net

charge, which is zero for a 50:50 polyampholyte.[10, 20] In terms of the sequence of monomers, synthetic polyampholytes can be random, alternating or block copolymers, with the sequence affecting the polyampholyte properties.[21]

1.2 Theoretical Research and Simulation Approaches of Polyampholytes

The structure of synthetic polyampholytes is usually much simpler than that of natural polyampholytes, so it is possible to use theoretical methods and simulation to predict the properties of polyampholytes,[21-30] which will help to design new polyampholytes, and understand the mechanism of phase transitions of synthetic or natural polymers.

For example, theoretical considerations allow the prediction of polyampholyte pH(I), based on composition and the pKa values of the acid and base groups involved.[31]

$$\mathrm{pH}(I) = \mathrm{p}K_a - log\left\{{}^{R}\!/_{2} \times \left[-{}^{(1-R)}\!/_{R} + \sqrt{\left({}^{(1-R)}\!/_{R}\right)^2 + {}^{4}\!/_{R} \times 10^{(pK_a - pk_{b)}}}\right]\right\} \quad (1)$$

$$\mathrm{pH}(I) = \mathrm{p}K_b + log\left\{{}^{1}\!/_{2} \times \left[{}^{(1-R)}\!/_{R} + \sqrt{\left({}^{(1-R)}\!/_{R}\right)^2 + {}^{4}\!/_{R} \times 10^{(pK_a - pk_{b)}}}\right]\right\} \quad (2)$$

where R is the ratio of acidic to basic group, pK_a and pK_b are the negative logarithms of the dissociation constants of the acidic and basic groups. The equations (1) and (2) are particularly use to obtain the pH(I) values of the acid and base rich polyampholytes, respectively. For stoichiometric polyampholytes (R=1), the equation can be simplified to

$$\mathrm{pH}(I) = {}^{(pk_a + pk_b)}\!/_{2} \quad (3).$$

Equations (1) to (3) provide a fast and efficient way to predict the pH(I) of natural and synthetic polyampholytes.

Debye-Hückel theory can be used to describe the electrostatic interactions among charges on polyampholyte chains, including the resulting polyampholyte chain conformations and anti-polyelectrolyte effects. Early research of polyampholyte conformation suggested that stoichiometric random polyampholytes adopt a collapsed globular conformation at their pH(I).[26] Further research extended this study to non-stoichiometric polyampholytes. While neutral polyampholytes collapse at pH(I) into a globule because of the electrostatic interactions, adding salt will screen these electrostatic interactions. There is a θ (theta) salt concentration at which the net interaction is zero due to shielding, with coil expansion at salt concentration above θ. However, polyampholyte with large amounts of net charge will behave like simple polyelectrolytes.[27]

Molecular dynamics simulations were used to correctly predict that randomly charged multi-chain polyampholytes collapse at low temperature, and swell at high temperature.[22] Low charge density non-stoichiometric polyampholytes behave similar to neutral polyampholytes, however, high charge asymmetry polyampholytes behave in the opposite way, swelling at low temperature and collapsing at high temperature. The effect of salt involves two steps, the addition of small amounts of salt lead to precipitation of the polyampholytes by weakening the electrostatic repulsion between chains; while the addition of larger amounts of salt will help these precipitates redissolve by disrupting the electrostatic attraction.

Simulation was also used to model the effects of the primary structures[21, 28] (e.g., block, alternate, random) and showed that these structures play an important role in

polyampholyte properties. The ionization of one monomer will become easier if the neighboring monomer has the opposite charge or at least no charge. Conversely, neutralization of an ionized monomer next to an oppositely charged monomer is not easy. The net charge of polyampholytes comprising weak acids and bases hence tends to be zero in a certain pH range around the pH(I), due to these neighboring effects.[32]

Such theoretical research of polyampholytes reveal the basic properties of polyampholytes, the pH(I) and anti-polyelectrolyte effects, and can help guide the design of polyampholytes with certain properties.[33]

1.3 Properties of Synthetic Polyampholytes

Synthetic polyampholytes contain anionic, cationic and sometimes neutral monomers. Many have properties similar to those predicted by theory, such as chain shrinkage or phase separation at pH(I), or enhanced solubility upon addition of salt, but there are exceptions. For example, there are no examples of polyampholyte solubility increasing with increasing temperature at pH(I) in water, which is predicted by theory,[27] and the LCST and UCST of polyampholytes at certain conditions have not been well studied by theoretical work. Synthetic polyampholytes can be grouped by the strengths of the electrostatic interaction on the polyampholyte chains. The polymer composition and [NaCl] strongly affects key propeties of polyampholytes: polyampholytes containing both permanent cationic and anionic groups do not show pH responses, while polyampholytes with one weak and one permanent ionic group will show pH responses in terms of, e.g., viscosity, but only

polyampholytes with both weak cationic and anionic groups have pH(I) and associated phase separation.

In earlier studies, low charge density polyampholytes were prepared by copolymerizing neutral monomers such as acrylamide (AAm) with monomers having permanent cationic and anionic charges based on quaternary ammonium groups 3-methacryloylaminopropyltrimethylammonium chloride (MAPTAC), 2-methacryloyloxyethyltrimethylammonium (MAETAc) and sulfonates 2-acrylamido-2-methylpropanesulfonate (AMPS), 2-methacryloyloxyethanesulfonate (MES), such as in copolymers comprising MAPTAc/AMPS/AAm and MAETAc/MES/AAm.[34,35] These copolymers contain 0.3 to 5 mol% ionic pairs with stoichiometric charge ratio and show a U-shaped salt dependent viscosity, in agreement with theory.[22] High charge density binary polyampholytes made using only permanent cationic and anionic monomers such as MAETAc/AMPS show different properties than low charge density ones.[29,30] Solutions of these binary polyampholytes shows decreased transmittance as the charge ratio approaches 1:1 stoichiometry. Their solution transmittance also shows [NaCl] dependence in that all polyampholyte solutions become clear at high [NaCl], while off-stoichiometric polyampholytes show U-shape titration curves but the transmittance of stoichiometric polyampholytes monotonously increases with [NaCl].

Unlike polyampholytes with permanent cationic and anionic charges, weak acid and weak base polyampholytes will show pH responses. The alternating sequence polyampholyte formed from (4-Vinylpyridine) 4VP and AA shows U-shape titration curves with increasing pH and keeps zero net charge over a broad pH range, from pH 6 to 9.[32, 36]

Zhang and Hoogenboom reported UCST behavior for polyampholyte made from 1:1 (2-Dimethylaminoethyl) methacrylate (DMAEMA) and AA, in water/ethanol mixtures.[15] Our group prepared polyampholytes with weak acid (MAA) and week amine (APM) with or without hydrophilic comonomer hydroxyethylacrylamide (HEA) and measured the effect of pH, composition, NaCl concentration and temperature on their solubility.[12,37] The pH(I) moves to higher pH with increasing weak base comonomer content, and the stoichiometric copolymers have a broad titration curve covering 2 to 3 pH units, while the curve of other ratios are much narrower. Increasing [NaCl] increased the degree of hydration at pH(I), with high enough [NaCl] keeping the polyampholyte soluble. Such soluble stoichiometric copolymers in NaCl solution will show LCST behavior upon heating. Adding hydrophilic comonomer such as HEA to such stoichiometric polyampholytes leads to increased solubility, reflected e.g. in lower [NaCl] required to keep the polyampholyte soluble at pH(I).

Polyampholytes that comprise permanent cationic monomers together with a mixture of both permanent and weak anionic monomers can show properties reflective of both ionic monomers, such as anti-polyelectrolyte effect and pH response. At low charge density, however, the resulting weaker electrostatic interactions only cause viscosity changes but not visible phase separation as function of pH and [NaCl].[38-40]

Polyampholyte hydrogels share many of the fundamental properties of the corresponding linear polyampholytes. For example, a series of polyampholyte microgels prepared using MAETAc and APMS with 43 to 54 mol% AMPS show [NaCl] dependent swelling behaviors that with the increasing of [NaCl] concentrations, the microgels with high charge unbalanced deswells, the charge balanced microgel swells and others between them show

U-shape swelling curves. Their elastic moduli showed [NaCl] dependence too complex to be interpreted by the authors.[41] Polyampholyte microgels with weak acid and base were reported to have composition-dependent pH(I).[42] Stoichiometric polyampholyte hydrogels made from AMPS/MAPTAc or NaSS/VBTA showed that increasing the hydrophobic nature of the monomer, of the solution (ethanol / water ratio) or the temperature may cause first order phase transitions of polyampholytes.[43] Polyampholytes were also used to prepare hydrogels with high mechanical strength,[20,44] attributed to cooperation of weak and strong electrostatic interactions between cationic and anionic groups on polyampholyte chains, which are dependent on the number of ion pairs, the strong interactions comes from the polymer fragment with multi-ion pairs and the weak interactions contains less ion pairs. Stoichiometric polyampholyte hydrogels at pH(I) can also bond with both cationic or anionic hydrogels, and even with biological tissue.[45] The weaker acid and base containing polyampholyte hydrogels show pH responsive swelling.[46]

Kitano et al. explored the effect of polyampholytes on water structure.[47,48] They found that MAA, DMAPMA and butyl methacrylate based symmetrical polyampholytes had little effect on the water structure, compared to polyelectrolytes. This was attributed to the electrostatic interaction between cationic and anionic groups decreasing the interaction between the charged groups and water, and supports the notion that such polyampholytes can prevent non-specific adsorption.

Polyampholytes can be used to form block copolymers, where one or more blocks contain both anionic and cationic charges. Block polyampholytes can be used to prepare responsive micelles, due to the pH and temperature-tunable solvation of one or more blocks.[49-51]

In summary, synthetic polyampholytes show many properties predicted by theory, such as the anti-polyelectrolyte effect, and pH(I). Their properties depend strongly on composition and the nature of the comonomers. In particular, while stoichiometry polyampholytes show standard behaviors, off-stoichiometric polyampholytes show properties that resemble those of polyelectrolytes. Polyampholytes with permanent cationic and anionic charges do not have pH(I) and show only weak phase separation or viscosity changes in response to changes in, e.g., pH. In contrast, high charge density polyampholytes made from weak acid and base groups often have strong macroscopic phase separation, visible as transmittance changes. Polyampholyte hydrogels and block copolymers show pH or [NaCl] responsive swelling or self-assembly. Some of polyampholytes show LCST and UCST behavior under certain conditions. These temperature responses can come from the electrostatic interactions,[11,12,14,37] but can also include hydrophobic contributions.[49,50,52]

1.4 General Applications of Polyampholytes

Given their multi-responsiveness in aqueous media at or near physiological conditions, polyampholytes have been examined for many industrial and biomedical applications. This part will introduce (non-biomedical) industrial applications of polyampholytes, with the next part focusing on biomedical applications.

In the petroleum industry, polyampholytes are used to depress the pour point[53] and improve oil recovery.[54] Polyampholytes can inhibit wax deposition and improve the viscosity of crude oils. The possible reason is that polyampholytes can form inverse micelles in oil,

where the hydrophobic parts cocrystallize with paraffin and the charged parts prevent these crystals from growing further.

Like polyelectrolytes, polyampholytes can be used for water purification. Some polyampholytes hydrogels have an ability to adsorb organic dyes[55-57] (such as methylene blue, methyl orange, crystal violet and indigo carmine), heavy metals[58] (like Cd(II) and Pb(II)) and aromatic compounds[59] from water. Amphoteric cellulose can be used to improve paper strength.[60] Polyampholytes have adjustable cationic and anionic groups, as well as hydrophobic groups on backbones or side groups, so they can bond with cationic, anionic groups, and also form hydrophobic interactions. The multiple interactions provide polyampholytes the ability to strongly bind a broad type of molecules.

1.5 Biomaterials Applications of Polyampholytes

The application of polyampholytes in the area of biomedicine and biomaterials arouse more and more interest in recent years. Polyampholytes generally have good compatibility with different cells and tissues.[19]

Polyampholytes can have electrostatic interactions, hydrogen bonding, hydrophobic interactions and van der Waals interactions, which are all relevant for interactions with cells, proteins, and tissues. At pH(I), the zero net charge of polyampholytes provides a non-fouling surface, a useful baseline property not easily reached by other materials. In addition, polyampholytes are explored for drug delivery,[61,62] protein conjugation and cell adhesion,[63] injectable hydrogel[64] and as cryoprotective agents.[19]

Polyampholytes have many advantages as a non-fouling material. Polyampholytes offer structural diversity and can be further functionalized for special applications. Besides, cation-rich polyampholytes were found to have antibacterial properties or can be loaded with antibacterial drugs.[65] The [2-(acryloyloxy)ethyl]trimethylammonium chloride (TMA)/ 2-carboxyethyl acrylate (CAA) stoichiometric polyampholyte hydrogels show zero net charge and non-fouling properties towards proteins, while being able to be conjugated with proteins that confer the ability to form specific interactions with, e.g., cells.[63]

P(Glu-*co*-Lys) microgels have been synthesized for anti-cancer drug delivery systems. The key for this work was adjusting the pH(I) between 7.4 and 6.8 by adjusting the ratio of cationic and anionic groups. The resulting microgels have negative charge and are colloidally stable in blood at pH 7.4, however, they adopt a cationic surface charge upon encountering the low pH (6.8) in tumors, which increases their uptake. As the result, drug loaded P(Glu-*co*-Lys) microgels were shown to inhibit the proliferation of cancer cells.[66]

Another interesting application of polyampholytes is to improve the thermo-stability of proteins grafted with the polyampholytes.[67,68] This effect is attributed to polyampholytes forming reversible polymer-protein interactions upon heating that prevent the protein-protein interactions believed to cause the non-reversible aggregation and denaturation of protein.[69] As well, polyampholytes have recently been shown to serve as DMSO-free cryoprotective agents for cell storage, as discussed below. The study of polyampholyte cell cryoprotective action and mechanism is a key focus for this thesis.

1.6 Polyampholytes as Cryoprotective Agent

Cryopreservation is a method of long time storage of bio-samples (cells, tissues, and organs) at low temperature. It plays an increasingly important role for cell researchers, cell banks and storing valuable cells for cytotherapy. Direct freezing of cells in media will cause pervasive cell death through ice crystal formation both inside and outside of cells, as well as through osmotic pressure changes.[70] In order to successfully freeze and recover bio-samples, cryoprotective agent is an efficient way to protect cells. Many natural cryoprotective agents are found in certain vertebrates, plants, fungi, and bacteria, including antifreeze proteins (e.g. northern cod) and sugars. The simplified mechanism of antifreeze proteins is through inhibition of ice growth and recrystallization, and through protection of cells membranes by interacting with proteins.[71]

However, use of antifreeze proteins is limited by supply and immunological concerns regarding downstream cell transplantation.[72,73] Current cryoprotective agents are hence typically small, cell-penetrating molecules, such glycerol and DMSO. They are widely used in research, industry and cell banks, and give good cell viability for most cell lines. In early research, glycerol (10-20 wt%) was used to protect cock spermatozoa at -80 ^{o}C,[74] and now it is the standard cryoprotective agent (20-40%) for red blood cell storage.[75] DMSO was found to successfully freeze most kinds of cell lines including many stem cells.[76-79]

The mechanism of cryoprotection with glycerol and DMSO are different. High concentrations of glycerol lead to water vitrification, where the water is kept in a glassy state instead of forming ice crystals. In contrast, DMSO leads to decrease of the size of ice crystals. Both mechanisms decrease the damage from inter-and intra-cellular ice crystals,

so both of them need to gain access to the interior of the cells and are hence called permeant cryoprotective agents.[78] In order to reach good post-thaw viability, significant concentrations of either glycerol (10-40 %) or DMSO (5-10 %) are needed. However, these concentrations are not well tolerated by cells for very long, as chemical toxicity is concentration, time and temperature dependent. Therefore, both need to be removed from cells immediately after thawing. As well, there is concern about cell death or abnormal differentiation of stem cells, e.g. granulocytes, neuron-like cells, and cardiac myocytes[80-82] associated with these cryoprotectants. Finally, removal of, e.g. glycerol, from frozen red blood cell samples can take up to an hour due to fairly slow extraction of intracellular glycerol, which significantly delays readying blood samples needed during, e.g. surgery.[83] As well, storage of red blood cells in glycerol requires storage at -65 ^{o}C or lower, and is limited post-thaw storage period, e.g. 24h after thawing.[75]

Cryostorage of hES stem cells requires additives such as 50% FBS in addition to DMSO or glycerol in order to achieve good post-thaw viabilities[84.85] but these additives increase the cost and would not be acceptable for subsequent human medicine. As the result, it is important to develop new cryoprotective agents to avoid some of the limitations associated with the currently available slate of agents.

Except DMSO and glycerol, there are some non-permeant cryoprotective agents like trehalose, dextran, and PVP.[86,87] Recently, polyampholytes are found to have cryoprotective properties. Compared with DMSO and glycerol, polyampholyte cryoprotective agents have lower to no cytotoxicity, are active in lower concentration (around 10% wt) and without addition of animal-derived proteins like fetal bovine serum (FBS).

Polyampholytes were found to work as a DMSO free cryoprotective agent. Matsumura's group studied polyampholyte prepared by modifying ε-poly-L-Lysine (ε-PLL) with succinic anhydride, which introduced carbonic acid groups. The polyampholyte had low molecular weight (4000 Da) due to the bacterially produced ε-PLL precursor, 65 % carboxylic acid and 35 % primary amine groups, and gave 90 % post-thaw viability for various types of cells with 7.5 % wt polymer, 300 mM NaCl and without FBS,[88] this polyampholyte also successfully froze hBMSCs for 24 months at -80 °C.[89] This polyampholyte was used to successfully freeze different types of cells on different conditions, for example, for iPS cells, the cryoprotective solution contained 7.5% wt polyampholyte, 6.5 M ethylene glycol, and 0.75 M sucrose.[90] It was also used for mouse oocytes in presence of ethylene glycol,[91] for two-dimensional cell monolayers (10% wt polyampholyte, 6.5 M ethylene glycol, 0.5 M sucrose),[92] in form of hydrogels with dextran,[93] and for mouse embryos.[94] However, in others work, stoichiometric polyampholytes gave the highest cell viability, and increasing the molecular weight and hydrophobicity were also associated with higher viability.[95]

One of the mechanisms of cryoprotection is called ice-recrystallization inhibition, whereby the cryoprotective agent can prevent or minimize the formation of larger, more dangerous ice crystals during the thawing process.[78] Polyvinylalcohol (PVA) was found to have molecular weight dependent ice-recrystallization inhibition, with higher molecular weight offering more protection.[96] Low concentration PVA (0.1 wt% 9k Da) in presence of 21.5 wt% hydroxyethylstarch (HES) showed good post-thaw viability of red blood cells, reflecting significant reduction of extracellular ice crystal damage.[97] Stoichiometric polyampholyte showed similar freeze-protection properties for red blood cells in presence

of HES.[98] In addition, polyampholytes were found to protect cell membranes during freezing.[99]

However, even where polymeric cryoprotective agents work as well as DMSO, there are some mechanism issues to solve. Some studies reported best results for polyampholytes with 30% cationic content works best[88-94] while others show polyampholytes with 50% cationic content work and those with 30% cationic content do not.[95,99] Finally, in yet other studies, the 50 to 50 stoichiometric polyampholytes work in presence of HES.[98] While these polyampholytes have different structures, they should share similar charge-related properties. Yet, if their compositions are different, like 30:70 versus 50:50 ratio, the first one at physiological pH has net anionic charge and should behave like a polyelectrolyte, while the second one should have zero net charge and behave like a polyampholyte.

Another issue is a lack of clear rationalization for the selection of additives to polyampholyte cryoprotectants. These additives include additional NaCl,[88-95,99] EG and sucrose,[90-92] and HES.[99] They are needed for effective cryoprotection, but the mechanism of their function is not clear. Similarly, the actual mechanism of cryoprotection of the polyampholytes is not clear. There are two possible mechanism: the anti-freezing properties[97,98] that the polyampholyte cryoprotective agent can significantly decrease the ice crystal size and protect cells from the mechanical damage of ice; and direct protection of the cell membrane where polyampholytes coat on the surface of cell membrane and prevent ice crystal penetration,[99] but they do not explain all observations. DMSO and glycerol are permeable cryoprotective agents, which work both inside and outside of cells, but polyampholytes are confined to the outside of cells.[88,91,100] The dehydration of cytosol through the increasing osmotic pressure around cells during slow freezing is held

responsible for minimizing intracellular formation of ice crystals, but dehydration can both protect and kill cells during freezing.[78] Hence, additional research and development of polyampholyte CPA are needed.

1.7 Summary and Research Objectives

Polyampholytes contain both cationic and anionic groups that together provide their special properties: the pH(I), anti-polyelectrolyte effects, and temperature responsive solubility including LCST and UCST. These properties produce many interesting applications. Hence improved understanding of polyampholyte behavior is interesting and useful for the design of new polyampholyte based materials. This thesis focuses on polyampholyte phase separation and explores the mechanism of polyampholytes used as cryoprotective agents.

In synthesizing polyampholytes, the overall ratio of comonomers and comonomer sequence are important. The reactivity ratios of different monomer pairs were measured by ^{1}H-NMR. With the help of reactivity ratios, the polyampholytes were synthesized by free radical copolymerization with a low compositional drift.

The second chapter describes a new, fully charged polyampholyte comprised of weak acid and base monomers, APM and AA. The pH(I), ionic strength and temperature response of the copolymers were measured as function of copolymer composition, [NaCl], and pH. These polyampholytes share some properties of other polyampholytes like the pH(I) and anti-polyelectrolyte behaviour for stoichiometric polyampholytes. However, at pH(I), non-stoichiometric polyampholytes at low pH with protonated (non-charged) AA have different properties like the anti-polyelectrolyte effect with low [NaCl] and salting out at high [NaCl].

The polyampholytes have liquid to liquid and liquid to solid phase separation, where both electrostatic interaction and the hydrogen bonding between AA units play important roles in the polyampholyte phase separation.

The third chapter focusses on the stoichiometric APM/AA polyampholytes and explores the effect of molecular weight on the liquid to liquid separation. There is not enough understanding of the effect of molecular weight on polyampholytes, especially for the fully charged polyampholytes with weak acids and bases. The polyampholytes phase separate at pH(I), and form coacervates. Coacervation is a common phenomenon of liquid-liquid phase separation of the charged polymers, where the polymer-rich phase forms the coacervates by electrostatic interactions.[101,102] Such liquid-liquid phase separation has very recently been observed in a variety of new biological contexts, including the adhesives used by sandcastle worms and barnacles,[103] proteins used to form the hard beaks of squids,[104, 105] as well as in intracellular reversible thermal phase separation of unstructured mammalian proteins.[106, 107]

The properties of polyampholytes are dependent on the pH, [NaCl], polymer concentration and molecular weight. The polyampholytes with high molecular weight have high phase separation efficiency, need high [NaCl] to dissolve the coacervates, and when molecular weight is high enough, the phase separation efficiency is independent on polymer concentration. However, with decreasing molecular weight, the phase separation efficiency decreases and finally disappears. We also crosslinked the coacervates with THPC to form microgels and explored the organic dye absorption of polyampholytes.

Even though there are many theoretical and experimental studies on polyampholytes, there remain many interesting questions. For example, in different studies, polyampholytes all

contain quaternary ammonium and sulfonate groups, but one of them forms strong physical gel,[20, 44, 45] one of them shows phase separation at pH(I),[29] and yet another only shows viscosity changing at different pH, but no phase separation.[108] Chapter four explores how electrostatic interactions and polymer hydrophobicity affect polyampholyte properties, by employing six monomers. The results show both the electrostatic interaction and polymer hydrophobicity affect the polyampholytes properties.

The last chapter, five, explores the mechanism of polyampholyte cryoprotective activity. The reason of developing a polyampholyte cryoprotective agent is to replace the DMSO and glycerol which are currently used, but failed or caused some problems for some cells. Polyampholytes are the only polymers that show good cryoprotection of cells with nuclei. This chapter describes that the polyampholyte cryoprotective agents need have appropriate molecular and excess negative charges, 70 : 30 of AA : DMEPAM, and conforms the hydrophobic groups will improve the cell viability. The freezing / thawing processes were measured by optical and fluorescence cyromicroscopy. The possible mechanism is polyampholytes decrease the ice size and coat on the surface of cells during freezing, which can protect cells from ice and help cells to dehydrate; during thawing, the polymer rich phase melts first, which covers cells and protects them from ice recrystallization.

Overall, this thesis develops several new polyampholytes, and describes their solution properties with various conditions and explores some of them as cryoprotective agents.

1.8 References

1. Woodfield, P. A.; Zhu, Y.; Pei, Y.; Roth, P. J. *Macromolecules* **2014**, *47*, 750-762.

2. Käfer, F.; Liu, F.; Stahlschmidt, U.; Jérôme, V.; Freitag, R.; Karg, M. Agarwal, S. *Langmuir* **2015**, *31*, 8940-8946.

3. Dai, S.; Ravi, P.; Tam, K. C. *Soft Matter* **2008**, *4*, 435-449.

4. Zhao, B.; Moore, J. S. *Langmuir* **2001**, *17*, 4758-4763.

5. Hribar, K. C., Lee, M. H., Lee, D.; Burdick, J. A. *ACS NANO*, **2011**, *5*, 2948-2956.

6. Brzozowska, A. M.; Parra-Velandia, F. J.; Quintana, R.; Zhu, X.; Lee, S. S. C.; Lim, C.; Jańczewski, D.; Teo, S. L. M.; Vancso, J. G. *Langmuir*, **2014**, *30*, 9165-9175.

7. Liu, P., Emmons, E.; Song, J. *J. Mater. Chem. B*, **2014**, *2*, 7524-7533.

8. Xia, Y.; Gao, M.; Chen, Y.; Jia, X.; Liang, D. *Macromol. Chem. Phys.* **2011**, *212*, 2268-2274.

9. Das, M.; Kumacheva, E. *Colloid Polym. Sci.* **2006**, *284*, 1073-1084.

10. Shao, Q.; Jiang, S. *Adv. Mater.* **2015**, *27,* 15-26.

11. Zhao, J.; Burke, N. A. D.; Stöver, H. D. H. *RSC Adv.* **2016**, *6*, 41522-41531.

12. Dubey, A.; Burke, N. A. D.; Stöver, H. D. H. *J. Polym. Sci. Pol. Chem.* **2014**, *53*, 353-365.

13. Ciferri, A.; Kudaibergenov, S., Ciferri, A.; Kudaibergenov, S. *Macromol. Rapid. Comm.* **2007**, *28*, 1953-1968.

14. Ogawa, K.; Nakayama, A.; Kokufuta, E. *Langmuir* **2003**, *19*, 3178-3184.

15. Zhang, Q.; Hoogenboom, R. *Chem. Commun.* **2015**, *51*, 70-73.

16. Bianchi, E.; Conio, G.; Ciferri, A.; Puett, D.; Rajagh, L. *J. Biol. Chem.* **1967**, *242*, 1361-1369.

17. Subbotin, A. V.; Semenov, A. N. *Polym. Sci. Ser. C+* **2012**, *54*, 36-47.

18. Levin, Y.; Barbosa, M. C.; Tamashiro, M. N. *Euro. Phys. Lett.* **1998**, *41*, 123-127.

19. Zurick, K. M.; Bernards, M. *J. Appl Polym. Sci.* **2014**, *131*, 40069 (1-9).

20. Sun, T.; Kurokawa T.; Kuroda, S. Ihsan, A. B.; Akasaki, T.; Sato, K.; Haque, Md. A.; Nakajima, T.; Gong, J. *Nat. Mater.* **2013**, *12*, 932-937.

21. Ulrich, S.; Seijo, M.; Stoll, S. *J. Phys. Chem. B* **2007**, *111*, 8459-8467.

22. Tanaka, M.; Tanaka, T. *Phys. Rev. E* **2000**, *62*, 3803-3816.

23. Kantor, Y.; Li, H.; Kardar, M. *Phys. Rev. Lett.* **1992**, *69*, 61-64.

24. Dobrynin, A. V.; Rubinstein, M. *J. Phys. II* **1995**, *5*, 677-695.

25. Kantor, Y.; Kardar, M. *Phys Rev E Stat Phys Plasmas Fluids Relat Interdiscip Topics* **1995**, *51*, 1299-1312.

26. Edwards, S. F.; King, P. R.; Pincus, P. *Ferroelectrics* 1980, *30*, 3-6.

27. Higgs, P. G.; Joanny, J. F. *J. Chem. Phys.* **1991**, *94*, 1543-1554.

28. Cheong, D. W.; Panagiotopoulos, A. Z. *Mol. Phys.* **2005**, *103*, 3031-3044.

29. Corpart, J. M; Candau, F. *Macromolecules* **1993**, *26*, 1333-1343.

30. Corpart, J. M; Selb, J.; Candau, F. *Polymer* **1993**, *34*, 3873-3886.

31. Patrickios, C. S. *J. Colloid Interface Sci.* **1995**, *175*, 256-260.

32. Burke, S. E. & Barrett, C. J. *Langmuir* **2003**, *19*, 3297-3303.

33. Narayanan Nair, A. K.; Uyaver, S.; Sun, S. *J. Chem. Phys.* **2014**, *141*, 134905.

34. Salamone, J. C.; Ahmed, I.; Rodriguez, E. L.; Quach, L.; Watterson, A. C. *J. Macromol. Sci., Pure Appl. Chem.* **1988**, *A25*, 811-837.

35. Ohlemacher, A.; Candau, F.; Munch, J. P.; Candau, S. J. *J. Polym. Sci., Part B: Polym. Phys.* **1996**, *34*, 2747-2757.

36. Masuda, S.; Minagawa, K.; Tsuda, M.; Tanaka, M. *Eur. Polym. J.* **2001**, *37*, 705-710.

37. Abdilla, A.; Shi, S.; Burke, N. A. D.; Stöver, H. D. H. *J. Polym. Sci., Part A: Polym. Chem.* **2016**, *54*, 2109-2118.

38. Fevola, M. J.; Bridges, J. K.; Kellum, M. G.; Hester, R. D.; Mccormick, C. L. *J. Polym. Sci., Part A: Polym. Chem.* **2004**, *42*, 3236-3251.

39. Fevola, M. J.; Kellum, M. G.; Hester, R. D.; McCormick, C. L. *J. Polym. Sci., Part A: Polym. Chem.* **2004**, *42*, 3252-3270.

40. Ezell, R.; Gorman, I.; Lokitz, B.; Treat, N.; McConaughy, S.; McCormick, C. *J. Polym. Sci., Part A: Polym. Chem.* **2006**, *44*, 4479-4493.

41. Nisato, G.; Munch, J. P.; Candau, S. J. *Langmuir* **1999**, *15*, 4236-4244.

42. Deng, L.; Zhai, Y.; Guo, S.; Jin, F.; Xie, Z.; He, X.; Dong, A. *J. Nanopart. Res.* **2009**, *11*, 365-374.

43. Takeoka, Y.; Berker, A. N.; Du, R.; Enoki, T.; Grosberg, A.; Kardar, M.; Oya, T.; Tanaka, K.; Wang, G. Q.; Yu, X. H.; Tanaka, T. *Phys. Rev. Lett.* **1999**, *82*, 4863-4865.

44. Luo, F.; Sun, T.; Nakajima, T.; King, D. R.; Kurokawa, T.; Zhao, Y.; Ihsan, A. B; Li, X.; Guo, H.; Gong, J. *Macromolecules* **2016**, *49*, 2750-2760.

45. Roy, C. K.; Guo, H.; Sun, T.; Ihsan, A. B.; Kurokawa, T.; Takahata, M.; Nonoyama, T.; Nakajima, T.; Gong, J. *Adv. Mater.* **2015**, *27*, 7344-7348.

46. Tan, B. H.; Ravi, P.; Tam, K. C. *Macromol. Rapid. Commun*. **2006**, *27*, 522-528.

47. Kitano, H.; Nagaoka, K.; Tada, S.; Gemmei-Ide, M.; Tanaka, M. *Macromol. Biosci.* **2008**, *8*, 77-85.

48. Kitano, H.; Gemmei-Ide, M. *J. Biomater. Sci. Polym. Ed.* **2010**, *21*, 1877-1893.

49. Han, X.; Feng, J.; Dong, F.; Zhang, X.; Liu, H.; Hu, Y. *Mol. Phys.* **2014**, *112*, 2046-2057.

50. Zhang, X.; Ma, J.; Yang, S.; Xu, J. *Soft Materials* **2013**, *11*, 394-402.

51. Xiong, Z.; Peng, B.; Han, X.; Peng, C.; Liu, H.; Hu, Y. *J. Colloid Interface Sci*. **2011**, *356*, 557-565.

52. Deen, G. R.; Wei, T. T.; Fatt, L. K. *Polymer*, **2016**, *104*, 91-103.

53. Kudaibergenov, S. E.; Didukh, A. G.; A. G.; Z. E.; Ibraeva, L. A.; Bimendina, Rullens, F.; Devillers, M.; Laschewsky, A. *J. Appl Polym. Sci.* **2005**, *98*, 2101-2108.

54. Ezell, R. G.; McCormick, C. L. *J. Appl. Polym. Sci.* **2007**, *104*, 2812-2821.

55. Shao, H.; Wang, C.; Chen, S.; Xu, C. *J. Polym. Sci., Part A: Polym. Chem.* **2014**, *52*, 912-920.

56. Kudaibergenov, S. E.; Tatykhanova, G. S.; Klivenko, A. N. *J. Appl. Polym. Sci.* **2016**, *133*, 43784, (1 of 9).

57. Dalaran, M.; Emik, S.; Güçlü, G.; İyim, T. B.; Özgümüş, S. *Desalination*, **2011**, *279*, 170-182.

58. Copello, G. J.; Diaz, L. E.; Campo Dall' Orto, V. *J. Hazard. Mater.* **2012**, *217-218*, 374-381.

59. Morisada, S.; Suzuki, H.; Hirokawa, Y.; Nakano, Y. *J. Appl. Polym. Sci.* **2011**, *119*, 2968-2973.

60. Song, J.; He, A.; Jin, Y.; Cheng, Q. *RSC. Adv.* **2013**, *3*, 24586-24592.

61. Barcellona, M. N.; Johnson, N.; Bernards, M. T. *Langmuir* **2015**, *31*, 13402-13409.

62. Mishra, R. K.; Ramasamy, K.; Ban, N. N.; Majeed, A. B. A. *J. Appl. Polym. Sci.* 2013, 128, 3365-3374.

63. Schroeder, M. E.; Zurick, K. M.; McGrath, D. E.; Bernards, M. T. *Biomacromolecules* **2013**, *14*, 3112-3122.

64. Jain, M.; Matsumura, K. *Mater. Sci. Eng., C* **2016**, *69*, 1273-1281.

65. Li, M.; Jiang, S. *Angew. Chem. Int. Ed.* **2014**, *53*, 1746-1754.

66. Huang, Y.; Tang, Z.; Zhang, X.; Yu, H.; Sun, H.; Pang, X.; Chen, X. *Biomacromolecules*, **2013**, *14*, 2023-2032.

67. Liu, E. J.; Sinclair, A.; Keefe, A. J.; Nannenga, B. L.; Coyle, B. L.; Baneyx, F.; Jiang, S. *Biomacromolecules* **2015**, *16*, 3357-3361.

68. Lucius, M.; Falatach, R.; McGlone, C.; Makaroff, K.; Danielson, A.; Williams, Nix, C.; J. C.; Konkolewicz, D.; Page, R. C.; Berberich, J. A. *Biomacromolecules*, **2016**, *17*, 1123-1134.

69. Muraoka, T.; Adachi, K.; Ui, M.; Kawasaki, S.; Sadhukhan, N.; Obara, H.; Tochio, H.; Shirakawa, M.; Kinbara, K. *Angew. Chem. Int. Ed.* **2013**, *52*, 2430-2434.

70. Hunt, C. J. *Transfus. Med. Hemother*. **2011**, *38*, 107-123.

71. Fletcher, G. L.; Hew, C. L.; Davies, P. L. *Annu. Rev. Physiol.* **2001**, *63*, 359-390.

72. Liu, S.; Wang, W.; von Moos, E.; Jackman, J.; Mealing, G.; Monette, R.; Ben, R. N. *Biomacromolecules*, **2007**, *8*, 1456-1462.

73. Wang, T.; Zhu, Q.; Yang, X.; Layne Jr., J. R.; Devries, A. L. *Cryobiology* **1994**, *31*, 185-192.

74. Polge, C.; Smith, A. U.; Parkes, A. S. *Nature*, **1949**, *164*, 666-666.

75. Miloš Bohoněk (2012). Cryopreservation of Blood, Blood Transfusion in Clinical Practice, Dr. Puneet Kochhar (Ed.), ISBN: 978-953-51-0343-1, InTech, Available from: http://www.intechopen.com/books/blood-transfusionin-clinical-practice/cryopreservation-of-blood.

76. Berz, D.; McCormack, E. M.; Winer, E. S.; Colvin, G. A.; Quesenberry, P. *Am. J Hematol*. **2007**, *82*, 463-472.

77. Slichter, S. J.; Jones, M.; Ransom, J.; Gettinger, I.; Jones, M. K.; Christoffel, T.; Pellham, E.; Bailey,S. L.; Corson, J.: Bolgiano, D. *Med. Rev.* **2014**, *28*, 212-225.

78. Methods in Molecular Biology, 2007 vol. 368: Cryopreservation and Freeze-Drying Protocols, Second Edition Edited by: J. G. Day and G. N. Stacey © Humana Press Inc., Totowa, NJ page 39

79. Pegg, D. E. *J. clin. Path.* **1976**, *29*, 271-285.

80. Young, D. A.; Gavrilov, S.; Pennington, C. J.; Nuttall, R. K.; Edwards, D. R.; Kitsis, R. N.; Clark, I. M. *Biochem. Biophys. Res. Commun.* **2004**, *322*, 759-765.

81. Oh, J. E.; Raja, K. K.; Shin, J. H.; Pollak, A.; Hengstschlager, M.; Lubec, G. *Amino Acids* **2006**, *31*, 289-298.

82. Jiang, G.; Bi, K.; Tang, T.; Wang, J.; Zhang, Y.; Zhang, W.; Ren, H.; Bai, H.; Wang, Y. *Int. Immunopharmacol.* **2006**, *6*, 1204-1213.

83. Briard, J. G.; Jahan, S.; Chandran, P.; Allan, D.; Pineault, N.; Ben, R. N. *ACS Omega*. **2016**, *1*, 1010-1018.

84. Reubinoff, B. E.; Pera, M. F.; Vajta, G.; Trounson, A. O. *Human Reprod,* **2001**, *16*, 2187-2194.

85. Zhou, C. Q.; Mai, Q. Y.; Li, T. Zhaung, G. J. *Chin. Med. J. (Engl)* **2004**, *117*, 1050-1055.

86. Pellerin-Mendes, C.; Million, L.; Marchand-Arvier, M.; Labrude, P.; Vigneron, C. *Cryobiology* **1997**, *35*, 173-186.

87. Thirumala, S.; Wu, X.; Gimble, J. M.; Devireddy, R. V. *Tissue Eng. Part C Methods*, **2010**, *16*, 783-792.

88. Matsumura, K.; Bae, J. Y.; Hyon, S. H. *Cell Transplantation.* **2010**, *19*, 691-699.

89. Matsumura, K.; Hayashi, F.; Nagashima, T.; Hyon, S. H. *J. Biomat. Sci-Polym. E* **2013**, *24*, 1484-1497.

90. Matsumura, K.; Bae, J. Y.; Kim, H. H.; Hyon, S. H. *Cryobiology* **2011**, *63*, 76-83.

91. Watanabe, H.; Kohaya, N.; Kamoshita, M.; Fujiwara, K.; Matsumura, K.; Hyon, S. H.; Ito, J.; Kashiwazaki, N. *PLOS ONE* **2013**, *8*, e83613.

92. Matsumura, K.; Kawamoto, K.; Takeuchi, M.; Yoshimura, S.; Tanaka, D.; Hyon. S. H. *ACS Biomater. Sci. Eng.* **2016**, *2*, 1023-1029.

93. Jain, M.; Rajan, R.; Hyon, S. H.; Matsumura, K. *Biomater. Sci.* **2014**, *2*, 308-317.

94. Hyon, S. H.; Ito, J.; Kashiwazaki, N.; Shibao, Y.; Fujiwara, K.; Kawasaki, Y.; Matsumura, K. *Cryobiology* **2014**, *68*, 200-204.

95. Rajan, R.; Jain, M.; Matsumura, K. *J. Biomater. Sci. Polym. Ed.* **2013**, *24*, 1767-1780.

96. Congdon, T.; Notman, R.; Gibson M. I. *Biomacromolecules* **2013**, *14*, 1578-1586.

97. Deller, R. C.; Vatish, M.; Mitchell, D. A.; Gibson, M. I. *Nat. Commun.* **2014**, *5*, 3244.

98. Mitchell, D. E.; Cameroncd, N. R.; Gibson, M. I. *Chem. Commun.* **2015**, *51*, 12977-12980.

99. Rajan, R.; Hayashi, F.; Nagashima, T.; Matsumura, K. *Biomacromolecules*, **2016**, *17*, 1882-1893.

100. Ahmed, S.; Hayashi, F.; Nagashima, T.; Matsumura, K. *Biomaterials*, **2014**, *35*, 6508-6518.

101. Wang, Q.; Schlenoff, J. B. *Macromolecules* **2014**, *47*, 3108-3116.

102. Perry, S. L.; Sing, C. E. *Macromolecules* **2015**, *48*, 5040-5053.

103. Seo, S.; Das, S.; Zalicki, P. J.; Mirshafian, R.; Eisenbach, C. D.; Israelachvili, J. N.; Waite,J. H.; Ahn, B.

K. *J. Am. Chem. Soc*. **2015**, *137*, 9214-9217.

104. Cai, H.; Gabryelczyk, B.; Manimekalai, M. S. S.; Grüber, G.; Salentinig, S.; Miserez, A. *Soft Matter*, **2017**, *13*, 7740-7752.

105. Wei, W.; Tan, Y.; Martinez Rodriguez, N. R.; Yu, J.; Israelachvili, J. N.; Waite, J. H. *Acta Biomater*. **2014**, *10*, 1663-1670.

106. Vrhovski, B.; Jensen, S.; Weiss A. S. *Eur. J. Biochem*. **1997**, *250*, 92-98.

107. Nott, T. J.; Petsalaki, E.; Farbe,r P.; Jervis, D.; Fussner, E.; Plochowietz, A.; Craggs, TD.; Bazett-Jones, D.; Pawson, T.; Forman-Kay, J. D.; Baldwin, A. J. *Mol. Cell.* **2015**, *57*, 936-47.

108. McCormick, C. L.; Salazar, L. C. *Macromolecules* **1992**, *25*, 1896-1900.

Chapter 2. Preparation and Study of Multi-Responsive Polyampholyte Copolymers of *N*-(3-Aminopropyl)methacrylamide Hydrochloride and Acrylic Acid

Jing Zhao, Nicholas A.D. Burke, Harald D.H. Stöver

Published in *RSC Adv.*, **2016**, *6*, 41522-41531.

Contributions: I performed all experiments except the elemental analysis, which was carried out by Dr. Steve Kornic. I also wrote the manuscript, with edit and feedback provided by Dr. Burke and Dr. Stöver.

2.1 Abstract

A series of polyampholytes was prepared by free radical batch-copolymerization of *N*-(3-aminopropyl)methacrylamide hydrochloride (APM) and acrylic acid (AA). The drifts in monomer feed ratio during copolymerization were monitored by ^{1}H-NMR, and used to extract the reactivity ratios of 0.68 (APM) and 0.48 (AA). The phase separation in aqueous solutions of copolymers containing between 4 to 90 mol% APM were studied by potentiometric turbidity titration. The obtained isoelectric point (pH(I)) values agree well with theoretical values for weak polyampholytes. The influence of ionic strength on the phase separation during potentiometric turbidity titrations was measured for three different copolymer compositions and the effect on solubility was most pronounced for the stoichiometric (1:1 APM:AA) polyampholyte, reflecting the greatest number of electrostatic interactions at pH(I). Aqueous solutions of this stoichiometric polyampholyte

showed LCST-type cloud points upon heating, which varied as a function of pH, ionic strength and polymer concentration. The cloud point increased with ionic strength, and showed U-shaped dependence on pH, being constant within ±1.5 pH units of the pH(I). Some non-stoichiometric, high AA-content polyampholytes also were temperature responsive at pH(I), except that the phase transition was of the UCST-type, reflecting the increasing importance of hydrogen bonding on polymer solubility.

2.2 Introduction

Polyampholytes are polymers that carry cationic and anionic groups on separate monomer units.[1-6] They are characterized e.g. by their isoelectric point and often exhibit anti-polyelectrolyte properties. The isoelectric point, pH(I), is the pH value at which the net charge of the polyampholyte in aqueous solution is zero, and where electrostatic interactions between the cationic and anionic groups can cause intra and inter-molecular chain aggregation, often leading to macroscopic phase separation, a phenomenon well-known in peptide chemistry.[7] The anti-polyelectrolyte properties include chain expansion and increased solubility upon addition of sodium chloride and other salts, caused by shielding of the electrostatic attractions within the polyampholyte. Some zwitterionic polymers and block copolymers also show thermal phase separations including lower critical solution temperature (LCST), and upper critical solution temperature (UCST) behaviour.[8-12]

Synthetic polyampholytes can be seen as protein mimics,[13] since they have structures and properties similar to proteins, natural polyampholytes that typically contain nearly 20%

charged monomers.[2] The response of synthetic and natural polyampholytes to pH, temperature and ionic strength suggest biomedical applications.[14]

Synthetic polyampholytes may be random, alternating or block copolymers, with the sequence strongly affecting the polyampholyte properties.[15] Their often simpler structure, compared to natural polyampholytes, facilitates the use of theory and simulation to predict their properties and interpret their phase transitions.[15-21]

Polyampholytes have found industrial application, e.g., in water purification,[22] paper strength enhancement[23] and oil recovery.[3] They recently have attracted a lot of attention for use in non-fouling surfaces, reservoirs or membranes for drug delivery, protein conjugation, and as cryoprotective agents.[24-31]

There are relatively few reports on the influence of pH, ionic strength and temperature on weak acid/weak base polyampholytes.[8,9,26] Our group recently described the preparation and solubility of polyampholytes composed of different ratios of *N*-(3-aminopropyl)methacrylamide (APM) and methacrylic acid (MAA), as function of pH, ionic strength and temperature.[32] Some of these p(APM-*co*-MAA) polyampholytes had broad regions of insolubility about their pH(I), e.g., ~4 pH units (7 ± 2) for the 50:50 copolymer. This copolymer needed 550 mM NaCl to be solubilized at pH 7, preventing many potential applications in, e.g., cell encapsulation.

We decided to replace MAA with the more polar acrylic acid (AA) in order to increase the polyampholyte solubility near its pH(I). The current paper describes the preparation and properties of APM-AA polyampholytes made by copolymerization of APM with AA, over a wide range of comonomer ratios (Scheme 2.1). The reactivity ratios of the two monomers

were determined by following the copolymerization by NMR.[33] The effects of polymer composition, pH, ionic strength and temperature on the solubility of the polyampholytes were studied over a broad range of conditions. This information should prove useful in future applications of these polymers as biomaterials (e.g., synthetic extracellular matrices).

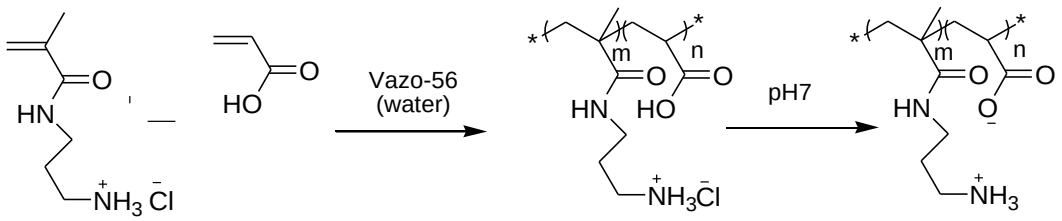

Scheme 2.1 Polyampholyte prepared by free radical copolymerization of APM and AA.

2.3 Experimental Section

2.3.1 Materials

Acrylic acid (AA, 99%) was obtained from Sigma-Aldrich, and distilled before use. *N*-(3-Aminopropyl)methacrylamide hydrochloride (APM.HCl) from Polysciences. Ethylene carbonate (98%), 2-(cyclohexylamino)ethanesulfonic acid (CHES, 99%) and 2,2'-azobis(2-methylpropionamidine) dihydrochloride (Vazo-56) from Sigma-Aldrich were used as received. Deuterium oxide (D_2O) was purchased from Cambridge Isotope Laboratories (Andover, MA). Sodium hydroxide and hydrochloric acid solutions (0.10 and 1.0 M) were obtained from LabChem Inc.

2.3.2 Small-Scale Model Copolymerizations to Determine Reactivity Ratios

Solution copolymerizations were carried out at 55 °C in a water bath, on a 1 mL scale in D_2O in 5 mm NMR tubes, with 10% (w/v) total monomer loading, 1 mol% initiator (Vazo-56, relative to total monomer), and ethylene carbonate (10 mg/mL) as internal NMR integration standard. The monomer ratios used were APM:AA = 10:90, 20:80, 30:70, 40:60, 50:50, 60:40, 75:25 and 90:10. The resulting aqueous solutions had pH values in the range of 2.4 to 2.5. Samples were placed in the water bath for specific lengths of time, then rapidly cooled in ice water and analyzed by ^{1}H-NMR on a Bruker Avance 200 spectrometer, at room temperature. This sequence of heating and analysis was repeated until monomer conversion had reached about 80%. The lengths of the heating segments were varied with comonomer ratio in order to limit the conversion for each segment to about 10-30%: 10 mins for APM:AA=90:10 and 75:25, 5 mins for 60:40, 4 mins for 50:50, 3 mins for 40:60, 30:70 and 20:80, and 2 mins for 10:90. The areas of the vinyl signals of AA at 5.8-6.5 ppm and APM at 5.3-5.7 ppm relative to the internal standard were used to determine the conversion of the two monomers in each time step. Their reactivity ratios were then calculated by fitting the instantaneous monomer and copolymer compositions to the terminal model of the copolymerization equation.

2.3.3 Larger Scale Copolymerizations

Larger scale polymerizations were carried out in a similar fashion, using 1 g total monomer in 20 mL screw cap glass vials, dissolved in 10 mL distilled water instead of D_2O. The comonomer feed ratios were APM:AA = 4:96, 6:94, 8:92, 10:90, 30:70, 50:50, 60:40,

70:30 and 90:10. The vials were heated at 55 °C in an oven fitted with a set of horizontal steel rollers that rolled the vials at 4 rpm. The progress of the copolymerizations was monitored by removing small aliquots by syringe, diluting these with D_2O, and determining conversion by ^{1}H-NMR on Bruker Avance 200 and 600 instruments. Polymerizations were stopped at 60-80% conversion and the cooled reaction mixtures were dialyzed against distilled water in cellulose tubing (Spectra/Por, 3.5 kDa MW cutoff, Spectrum Laboratories) for 4 days with daily water changes. The pH of the dialysis bath was kept at 3 for copolymers with pH(I) higher than 3, and at 8 for copolymers with pH(I) close to 3, by adding hydrochloric acid or sodium hydroxide to the aqueous medium at every water change. The purified polymers were isolated by freeze drying. Typical isolated yields of freeze-dried copolymer were near 60%.

The nomenclature for copolymers is based on PMA_x, where M, A and x stand for APM, AA, and the average mol% APM in the polymer, respectively. The x value was taken as the average of: a) values predicted from the comonomer feed and the reactivity ratios, and values from b) elemental analysis, and c) ^{1}H-NMR analysis (Table 2.1).

2.3.4 ^{1}H-NMR Analysis of PMA_x

^{1}H-NMR analyses of the copolymers were carried out on a Bruker AV 600 spectrometer, using 10 mg of purified polymer dissolved in 1 mL of D_2O. The mol ratios of APM and AA in the copolymer were calculated by comparing the areas of the two down-field APM methylene groups (between 2.5 and 3.5 ppm, 4H) with the combined area of the other signals of APM and AA at 0.5 to 2.5 ppm (7H for APM and 3H for AA).

2.3.5 Elemental Analysis

Elemental analyses were performed by the Combustion Analysis and Optical Spectroscopy Facility (McMaster University) using a Therm Flash EA 1112 elemental analyzer. The carbon to nitrogen ratio was used to determine the APM:AA ratio in the polymers.

2.3.6 GPC Analysis

The molecular weights (MWs) of poly(APM-*co*-AA) copolymers were estimated using an aqueous gel permeation chromatography (GPC) system consisting of a Waters 515 HPLC pump, Waters 717plus auto-sampler, three columns (Waters Ultrahydrogel-120, -250, -500; 30 cm, 7.8 mm dia.; 6 μm particles; 0-3, 0-50, 2-300 kDa MW ranges), and a Waters 2414 refractive index detector calibrated with narrow disperse poly(ethylene glycol) calibration standards (Waters), ranging from 106 Da to 881 kDa. The mobile phase was 0.3 M $NaNO_3$ with 0.025 M CHES buffer at pH 9 for PMA_6 to PMA_{35}; and 1 M acetate buffer at pH 4.7, for PMA_{52} to PMA_{88}.

2.3.7 Determination of pH(I) of PMA_x by Turbidimetric Titrations

Turbidimetric titrations were carried out at 22 °C on solutions formed by dissolving 10 mg of polymer in 10 mL of distilled water and then diluting 10-fold with distilled water. The final polymer concentration of 0.1 mg/mL was chosen to give significant decreases in transmittance at the pH(I), while minimizing macroscopic precipitation and hysteresis due to slow re-dissolution after the titration has passed the pH(I). A 25 mL aliquot of the

polymer solution was adjusted to pH 2 - 4 with HCl, to ensure the polymer was fully dissolved. Each polymer solution was then titrated manually to pH 9.5 - 10, by adding 25 μL aliquots of 0.01 to 1 M NaOH with a micropipette, while simultaneously monitoring the pH and the turbidity of the solution, using a VWR SympHony pH probe and a Mitsubishi GT-LD photometric detector equipped with an optical fibre turbidity probe (λ >620 nm). The concentration of NaOH was selected to give suitable changes in pH per injection (ΔpH ~0.05 - 0.1).

The same solutions were subsequently titrated from high pH back to low pH, using 25 μL aliquots of 0.01 to 1 M HCl, while monitoring pH and turbidity. The pH(I) was determined as the midpoint between the leading edges of the forward and back titration curves at about the half-maximum turbidity points. To determine the effect of ionic strength on the pH(I), the titrations were repeated in the presence of NaCl (0 - 1 M) obtained by adding solid NaCl.

2.3.8 Optical Microscopy

Microscopy images of the polymer at pH(I) were measured with an Olympus BX51 microscope equipped with a Q-Imaging Retiga EXi camera and Image Pro software.

2.3.9 Temperature Responsive Properties of Aqueous Solutions of PMA_{52}

Cloud point measurements were made using a Varian Cary 3E spectrophotometer fitted with a temperature controlled 12-sample cell holder. The rates of heating and cooling were

both 1 °C/min and the transmittance at 500 nm was measured at 0.5 °C intervals. Solutions containing 2 mg/mL PMA_{52} were used at different pH and salt concentrations. To determine the effect of pH, the salt concentration was fixed at 200 mM NaCl with pH varying from 5.5 to 9. To test the effect of ionic strength, the pH was fixed at 7.5 (near pH(I)) with ionic strengths varied from 200 to 300 mM.

2.4 Result and Discussion

2.4.1 Synthesis of Poly(APM-*co*-AA) by Free Radical Copolymerization

The ratio, type and placement of charged comonomers are key to the properties of polyampholytes. Free radical copolymerization is a convenient route to polyampholytes from a suitable combination of ionizable monomers, though the monomers are almost always consumed at different rates, as governed by their pair-wise reactivity ratios. In batch copolymerizations, this can lead to an offset between comonomer feed ratio and instantaneous copolymer composition, which causes a drift in the ratio of residual comonomers, and thus in the instantaneous copolymer composition. Semi-batch processes, where the more reactive comonomer is judiciously added throughout the copolymerization, can overcome this issue and be used to form constant composition copolymers.[34,35] The decision on whether a semi-batch process is required can hinge on the magnitude of the compositional drifts observed during batch copolymerization.

Following copolymerizations by high-field ^{1}H-NMR permits accurate estimation of the reactivity ratios, by fitting the incremental monomer conversion data to the instantaneous

copolymer composition equation.[33] This approach was used here, as the reactivity ratios of APM and AA have not yet been reported in the literature.

Copolymerizations were carried out in NMR tubes at 55 °C, and the incremental comonomer conversions were analyzed at regular intervals by ^{1}H-NMR at room temperature. The corresponding ^{1}H-NMR spectra obtained during the copolymerization of a 52:48 APM/AA mixture are shown in Figure 2A.1a.

In previous work with the APM-MAA system, MAA was found to be more reactive than APM but the MAA reactivity could be reduced to match that of APM by using MAA/NaMAA mixtures (i.e., raising pH).[32] Since acrylic monomers are usually less reactive than methacrylic ones,[36,37] it was anticipated that a high AA/NaAA ratio (low pH) would be needed to minimize compositional drift during APM-AA copolymerizations. Hence all polymerizations were carried out at initial pH values of 2.4 - 2.5 where APM and most of the AA are in their protonated form.

Figure 2.1 shows the drift in the respective APM mol fractions in the comonomer pools during eight NMR-scale copolymerizations with different initial APM:AA ratios. There was a slight preference for AA consumption in mixtures containing, initially, 75 and 90% APM, while APM was consumed preferentially in mixtures containing, initially, 10 to 50% APM. An azeotropic comonomer feed ratio is evident at 60% APM.

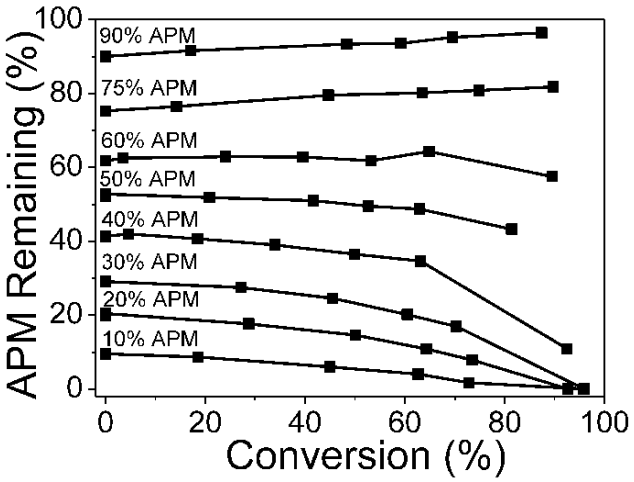

Figure 2.1 The drift of the residual APM mol percentage in the comonomer pool during the copolymerizations with AA in D_2O at 55 °C, as determined by ^{1}H-NMR (200 MHz), for initial APM mol% in comonomer feed, shown above each graph, ranging from 10 to 90 %. Total initial monomer loadings were 10 wt %, and initial pH values were all in the range of 2.4 to 2.5.

No attempt was made to vary AA reactivity by changing pH because the drifts observed were considered to be small, and the AA was already largely in its more reactive acid form. One benefit of using only AA (no NaAA) was that no polymer precipitation was seen for any of the copolymerizations, as the pH was always below pH(I).

Figure 2.2 shows the instantaneous copolymer composition curve (solid line) fitted simultaneously to the incremental conversions for the eight copolymerizations with only r_1 and r_2 as variables, using the non-linear Generalized Reduced Gradient algorithm in the Solver subroutine in Microsoft Excel 2007. Further information about the calculation of r_1 and r_2 is provided in the supporting information (Table 2A.1). Two outlying data points

(solid circles in Figure 2.2) were not used for this fitting procedure. The calculated reactivity ratios are r_1 (APM) = 0.68 and r_2 (AA) = 0.48. These values would not be valid at higher pH, where AA would be significantly ionized and less reactive.

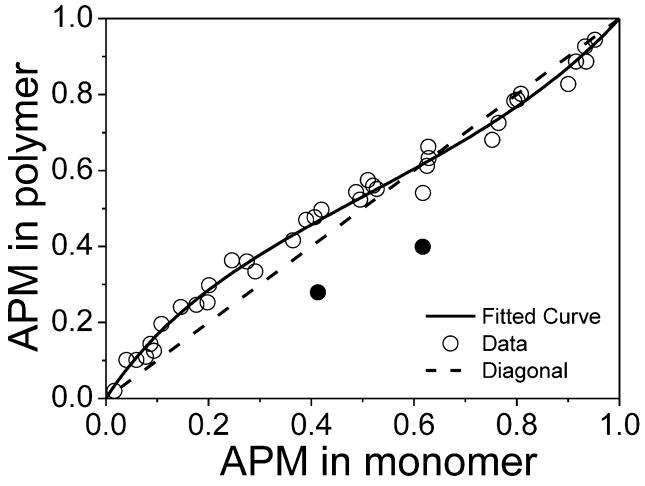

Figure 2.2 Instantaneous copolymer composition graph for copolymerizations of APM and AA in D_2O (pH 2.4-2.5) at 55°C with eight different initial mole ratios. The experimental data from ^{1}H-NMR of comonomer conversion (hollow circles), data excluded from fitting (solid circles) and the curve calculated based on fitting the experimental data to the instantaneous copolymer composition equation (solid line) are shown.

Figure 2.2 confirms the presence of an azeotropic comonomer ratio near 60 mol% APM, and illustrates the offsets between comonomer feed ratios and instantaneous copolymer compositions for different initial comonomer ratios. Copolymer compositions track fairly close to the comonomer feed ratio, including at the 1:1 APM:AA ratio. As a result, we decided to proceed with a series of batch copolymerizations, rather than carrying out semi-

batch processes. These larger-scale copolymerizations covered initial APM ratios from 4% to 90%, and Table 2.1 summarizes the compositional data obtained from elemental analysis and ^{1}H-NMR, as well as the compositions expected based on the reactivity ratios. The ^{1}H NMR spectrum of PMA_{52} is given in Figure 2A.1b.

Conversion in these copolymerizations was kept below 80% in order to limit the compositional drift. The differences between the initial feed ratios and the average copolymer compositions are less than 5% throughout. Table 2A.2 summarizes the composition of copolymer predicted to be formed during the course of the PMA_{12}, PMA_{35} and PMA_{52} copolymerizations, for 10% conversion steps using the actual feed ratios and the reactivity ratios. It shows that for overall conversions of 60%, the instantaneous composition of PMA_{12} drifts from 15% to 9%, PMA_{35} from 37% to 31% and PMA_{52} from 54% to 51%. The comonomer sequences were calculated for different comonomer ratios according to Igarashi,[38] and reflect the tendency towards alternating structure, especially for the compositions close to the stoichiometric ratio (Table 2A.2).

Table 2.1 Summary of PMAx Polymer Composition Analyses

	APM Feed Ratio (mol%)	**Total Comonomer Conversion (%)**	**M_p (kDa)[a]**	**mol% APM in Copolymer**			
				Predicted from reactivity ratios	**Elemental Analysis[c]**	**^{1}H-NMR (600 MHz) of copolymer**	***Average***
PMA_6	5.8	75	830	7	7	5	6
PMA_{10}	8.0	59	800	11	10	8	10

PMA_{12}	8.9	61	672	12	15	10	12
PMA_{35}	29.4	57	544[b]	35	36	34	35
PMA_{52}	50.9	73	342[b]	53	55	50	52
PMA_{61}	61.3	75	262[b]	61	62	60	61
PMA_{69}	69.0	71	269	68	68	71	69
PMA_{88}	86.6	78	230	85	89	91	88

[a] As the polymers contained fractions beyond the upper calibration limits of our GPC columns (881 kDa), only M_P values are given.

[b] The GPC traces of these samples consistently showed two peaks, with the higher MW component attributed to a small amount of crosslinking during polymerization and work-up, the M_p values given is the estimated M_P for the lower MW peak.

[c] Elemental analysis data are shown in supporting information.

GPC analysis of the PMA_x polyampholytes proved challenging due to the strong interactions that limit solubility and the high MW of these particular copolymers. All of the copolymers had high MW fractions that were beyond the exclusion and calibration limits of the GPC system (881 kDa) and, hence, only M_p, the MW associated with the peak maximum, is reported. All of the copolymers are high MW materials with significant fractions above 200 kDa. The GPC curves for some of the copolymers are shown in Figure 2A.2.

Several additional PMA_x copolymers were prepared with APM content between those of PMA_{35} and PMA_{52}. The properties of PMA_{37}, PMA_{43} and PMA_{47}, which were characterized by ^{1}H-NMR but not elemental analysis or GPC, are given in Table 2A.3. These polymers were used in a limited number of the solubility studies described below.

2.4.2 Solubility of PMA_x Polyampholytes

The key solution features of polyampholytes are their pH(I) and the anti-polyelectrolyte effect. Both stem from the interaction between oppositely charged groups on polymer chains, affecting polymer solubility and chain conformation in solution. Phase separation or precipitation is often seen at pH(I) when the net charge of the polyampholytes is zero. Addition of salt at the pH(I) can cause these chains to re-dissolve due to shielding of the electrostatic interactions, an effect known as the anti-polyelectrolyte effect. Accordingly, the influence of copolymer composition, pH, ionic strength and temperature on the solubility of the APM-AA polyampholytes was studied.

2.4.3 Effect of Composition on Turbidimetric pH Titrations

Figure 2.3a shows the pH turbidity titration curves of PMA_x solutions titrated with NaOH (pH increasing). The corresponding titration curves using HCl (pH decreasing) are shown in Figure 2A.3. The titrations were carried out by manually adding small aliquots of NaOH or HCl solutions, increasing the titrant concentrations when passing through the polymer's buffer region to maintain a fairly regular spacing of data points. A typical titration took

about 20 to 30 min. All PMA_x solutions were transparent at both high and low pH, and most showed macroscopic phase separation at intermediate pH. The transmittance minima were at 65-80 %T for PMA_6 through $PAPM_{52}$, and then increased to about 95% at PMA_{61}. The turbidity observed for the 0.1 mg/mL solution of PMA_{61} near pH 9 is weak, but became more pronounced with increasing polymer concentration (Figure 2A.4). Copolymers with >61% APM gave no visible phase separation across the pH range. While many polyampholytes are insoluble at their pH(I),[2,6,8,9,39-41] others remain soluble and the chain collapse near pH(I) must be detected by other means such as viscosity measurements and light scattering.[5,42]

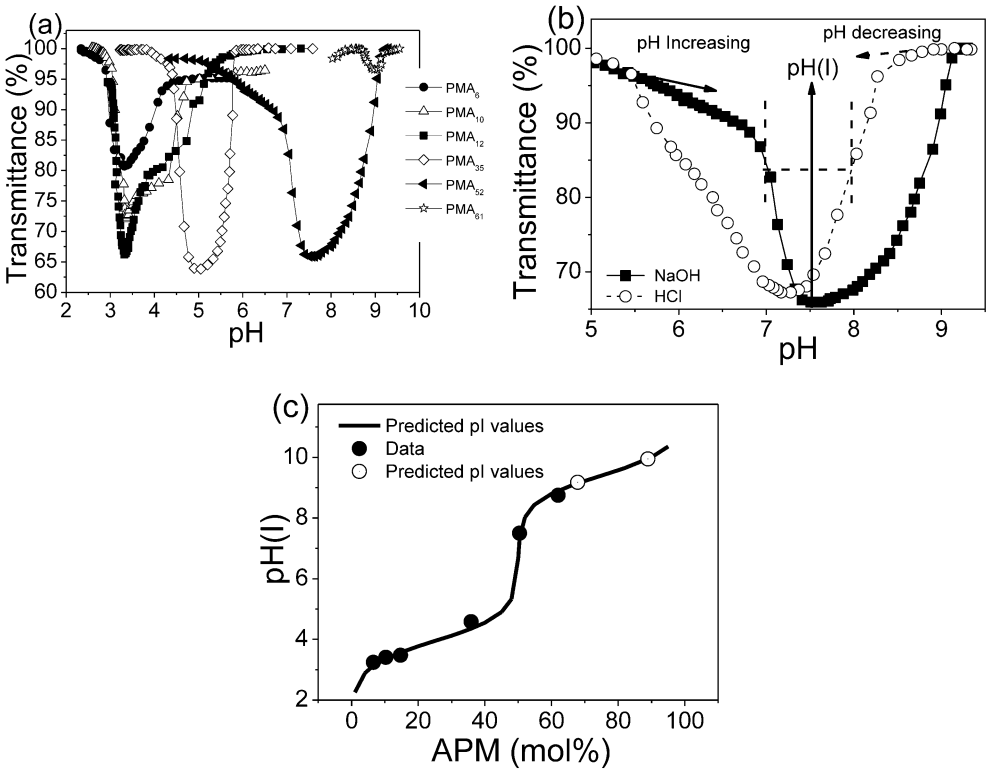

Figure 2.3 (a) Turbidity titrations of PMAx (x = 6 - 61) with NaOH, (b) turbidity titration of PMA_{52} with both NaOH and HCl to find pH(I), and (c) pH(I) of PMAx (x = 6 - 61) as a

function of copolymer composition from turbidity titration and theoretical prediction.[43] Conditions: 0.1 mg/mL polymer in H_2O, no added salt, titrant: 0.01-1 M NaOH or HCl.

The turbidity maxima of the PMA_x solutions occur at increasing pH with increasing APM content in the copolymer, as expected. The turbidity curves shown in Figures 2.3 and 2A.3 are broad, often asymmetric, and show significant hysteresis. While compositional distribution within each copolymer sample may be a contributing factor, slow polymer re-dissolution after passing the pH(I) is likely the main cause. The slow polymer re-dissolution becomes more pronounced with increasing polymer concentration (data not shown), and is more obvious at APM contents close to 10 mol%. Solutions of PMA_{10} and PMA_{12} showed turbidity maxima near pH 3.5 but did not fully clear until nearly pH 7 (Figure 2.3a). These two polymers gave a dense and fibrous precipitate at pH(I) that was more likely to settle, even at very low polymer concentration (0.1 mg/mL), compared to other copolymer compositions (Figure 2.4a).

Because of this hysteresis, the pH(I) values were estimated as the average of the pH values at half-maximum turbidity on the leading edge of the curves measured during titrations with NaOH (Figure 2.3a) and with HCl (Figure 2A.3), as illustrated for PMA_{52} in Figure 2.3b. The pH(I) of all PMA_x determined in this fashion are plotted against APM content in Figure 2.3c, and are found to match well with the pH(I) values predicted for binary weak polyampholytes as described by Patrickios.[43] Only predicted pH(I) values are shown for PMA_{69} and PMA_{88} in Figure 2.3c because these two copolymers did not undergo phase separation, remaining transparent between pH 4 and 11.

The behaviour of these polyampholytes depends on the ratio of the four key groups present, COOH, COO^-, NH_2 and NH_3^+. The relative amounts of these species in PMA_{52}, PMA_{35} and PMA_{12} as a function of pH were calculated from the monomer pKa values of 4.26 for AA,[1] and 9.1 for APM (estimated from the pKa values of the closely-related aminoethyl and aminohexyl analogs).[44] The ratios of the different species are shown in Table 2A.4 and Figure 2A.5. PMA_{52} with an amine/carboxylic ratio close to 1:1 has a predicted pH(I) of 7.5. The net charge distribution as a function of pH is S-shaped with close to zero net charge between pH 5.0 and 8.5, the same region where turbidity is seen during the forward and back titrations (Figure 2.3b). In this pH range, inter- and intrachain ion pairing will cause chain collapse and aggregation. While ion pairing could, in theory, involve nearly every monomer unit on the PMA_{52} chain, in practice this is not likely and there will still be a number of isolated charges, even at pH(I).[21]

In contrast, non-stoichiometric polyampholytes such as PMA_{35} and PMA_{12} have a significant fraction of neutral AA units near pH(I). PMA_{35} has formally about 70% ionized monomer units at pH(I) as well as 30% neutral AA. The net charge on such asymmetric polyampholytes near their pH(I) is predicted to be more sensitive to pH, with net charge changing from +10% to -10% over about one pH unit, compared to over three pH units for PMA_{52}. This matches the narrower regions of insolubility about pH(I) for PMA_{12} and PMA_{35} shown in Figure 2.3 and 2A.3.

A number of theoretical and experimental studies have shown that asymmetrical strong polyampholytes with significant excess charge behave more like polyelectrolytes.[18,20,40] Less is known about the behaviour of asymmetrical weak polyampholytes at their pH(I), where the large number of uncharged units will influence the solubility properties

differently. For AA-rich copolymers, both hydrogen bonding between COOH groups,[45] and electrostatic interactions, may contribute to phase separation at pH(I). In the case of polyampholytes with very low APM content, hydrogen-bonding may dominate the polymer-polymer interactions.

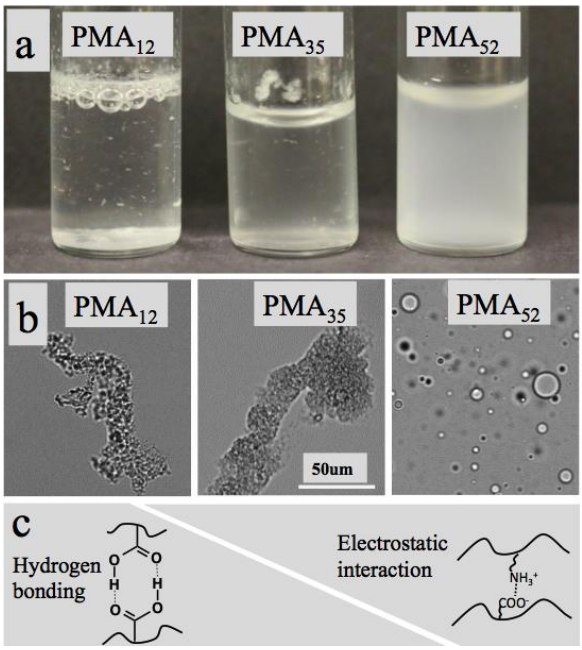

Figure 2.4 (a) photographs of PMA_{12}, PMA_{35} and PMA_{52} at their respective pH(I) of about 3.25, 5, and 7.5, at 1 mg/mL; (b) optical microscope images of PMAx at pH(I) (PMA_{52} at 1 mg/mL, PMA_{35} and PMA_{12} at 0.1 mg/mL); (c) dominant interaction (hydrogen-bonding vs. electrostatic) at pH(I) depends on composition.

Figure 2.4a shows photographs of the turbid aqueous PMA_{12}, PMA_{35} and PMA_{52} dispersions at their respective pH(I) of 3.5, 5 and 7.5, while Figure 2.4b shows the corresponding optical microscopy images of the phase-separated polymers. PMA_{12} phase separates as solid particles and fibres, while PMA_{35} gives hydrogel particles, which are

more rounded and more transparent than those from PMA_{12}. In contrast, PMA_{52} forms a stable suspension of coacervate droplets. At its pH(I), PMA_{52} will have a number of unpaired charges and these isolated charges will still be strongly solvated leading to a liquid upon phase separation. Apparently, the phase-separated material formed by PMA_{35} and PMA_{12} has lower water content indicating stronger polymer-polymer interactions. This may be due to efficient ion pairing, possible for these weak polyampholytes by ionization of carboxylic acids near the ammonium ions, and the onset of H-bonding between carboxylic acid groups. The balance of electrostatic and hydrogen-bonding interactions as function of APM content and pH(I) is illustrated schematically in Figure 2.4c.

Conversely, the APM-rich copolymers showed only marginal (PMA_{61}, Figure 2.3a), or no phase-separation (PMA_{69} and PMA_{88}) across the pH range. At pH(I), these systems have many neutral aminopropyl groups that appear to be well solvated rather than being involved in significant polymer-polymer interactions.

2.4.4 Effect of Salt on PMA_x Phase-Separation

Ionic strength affects polyampholyte conformation and solubility, in particular through shielding of electrostatic interactions. Away from pH(I), the polyampholytes bear significant net charge and behave like polyelectrolytes, with chains shrinking as ionic strength is increased. Near pH(I), increasing ionic strength causes attractive electrostatic interactions to be broken, leading to swelling and dissolution of the polyampholyte chains (anti-polyelectrolyte effect).[19-21] However, the opposite effect, an apparent increase in phase separation, is sometimes seen at low ionic strengths where screening of residual

electrostatic repulsions can cause the chains to further collapse and facilitate chain-chain aggregation (i.e., reduce colloidal stability)[2]

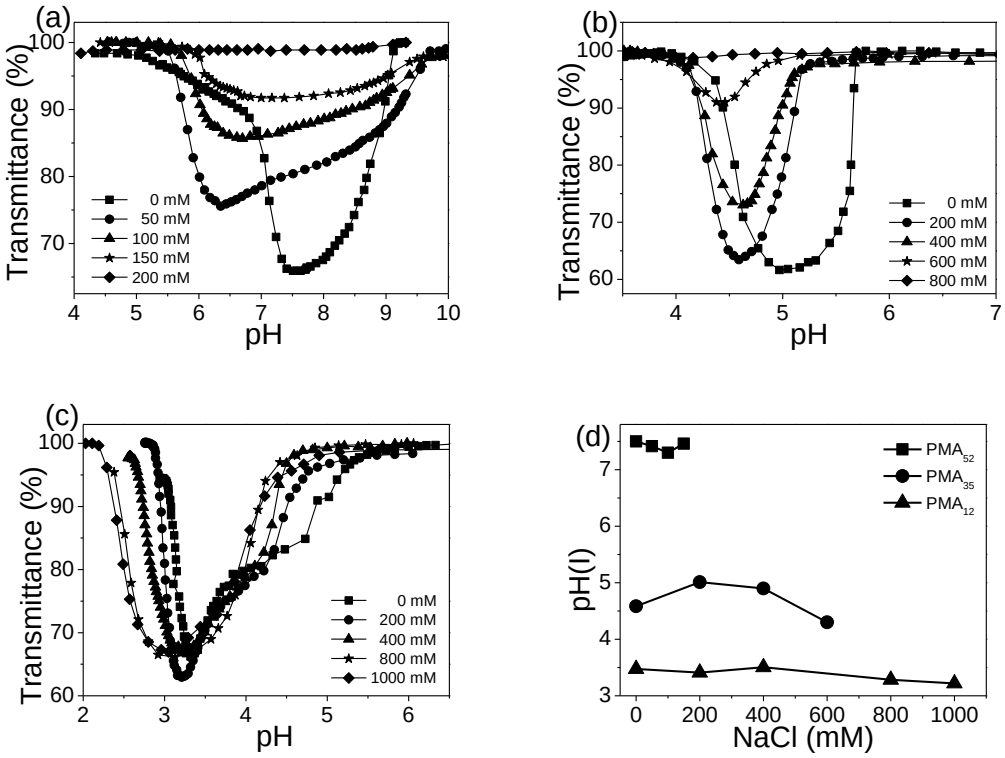

Figure 2.5 Turbidity pH titration curves of PMAx with different salt concentration, (a) PMA_{52}, (b) PMA_{35}, (c) PMA_{12}. Conditions: 0.1 mg/mL polymer in water, titrant: 0.01-1 M NaOH, and (d) pH(I) vs. salt concentration.

The effects of ionic strength on the turbidimetric titrations of PMA_{52}, PMA_{35}, and PMA_{12} are shown in Figures 2.5 and 2A.6. For PMA_{52} titrated with NaOH (Figure 2.5a), the first increase in salt concentration caused the turbidity curve to become shallower but broader, and show a minimum at a lower pH than had been seen in the absence of added salt. As the ionic strength was increased further, the curve became even shallower (increased transmittance), until at 200 mM NaCl the solution remained clear throughout the titration

range. Similar effects were seen during the titration with HCl (Figure 2A.6a) except that the minimum in transmittance moved to higher pH (i.e., also occurred earlier in the titration). PMA_{52} was more easily made soluble than the 50:50 APM-MAA copolymer studied previously,[32] requiring only 200 mM NaCl rather than the 550 mM NaCl, consistent with AA being less hydrophobic than MAA.

In the case of PMA_{35} (Figure 2.5b and 2A.7b), the transmittance minimum also shifted and the solution became clearer as ionic strength increased, but the PMA_{35} solution did not become fully clear until ionic strength was increased to 800 mM NaCl. The addition of up to 1 M NaCl had little effect on PMA_{12} turbidity curves, except that the transmittance minima occurred slightly earlier in the titrations (Figure 2.5c and 2A.6c). Even PMA_6 showed pronounced phase separation at pH 2.5-3.5 (i.e., near its pH(I)), which persists in the presence of up to 400 mM NaCl, the highest ionic strength tested for this polymer (Figure 2A.7). For PMA_{12} and PMA_6, which have high COOH content at pH(I), it appears that salting out of the hydrophobic portions completely offsets any shielding of electrostatic interactions. PAA itself is soluble at low pH, but can be salted out with about 1 M NaCl.[46] Apparently, the ion pairs present in PMA_{12} and PMA_6 at pH(I) cause phase separation at low ionic strength while the high COOH content is responsible for phase separation at high ionic strength.

The trend of lower ionic strength being needed to solubilize the polyampholytes at pH(I) as APM content increased (Figure 2A.6d) continued for polymers with higher APM content as both PMA_{69} and PMA_{88} were soluble with no added salt. At pH(I), APM-rich polyampholytes bear neutral APM groups, which appears to improve water solubility, perhaps because, unlike neutral AA group, they do not efficiently H-bond with each other.

The shift in the position of the transmittance minima seen for all three PMA_x in Figures 2.5 and 2A.6 where the first addition of salt leads to shielding of residual electrostatic repulsions, allowing chains to collapse and aggregate more efficiently such that phase separation occurs earlier than seen in the absence of added salt. Interestingly, Figure 2.5d shows that pH(I) for the three copolymers, taken by averaging the results from NaOH and HCl titrations as described in Figure 2.3b, were not affected by the addition of salt because the forward and back titrations were shifted by similar amounts but in opposite directions.

To summarize, PMA_{52} behaves like a typical polyampholyte with solubility controlled by the electrostatic interactions: aggregation at pH(I), and dissolution by increased salt concentration, in agreement with theoretical prediction[18] and related experiments.[1,5,6] The solubility behaviour of PMA_{12}, a low charge density polyampholyte at pH(I) with nearly 80% neutral carboxylic acid groups, is governed mainly by hydrogen bonding. PMA_{35} represents a middle ground between PMA_{52} and PMA_{12} in that its phase separation is caused by a combination of hydrogen-bonding and electrostatic interactions with near-opposite salt responses, such that adding salt at its pH(I) causes dissolution only at high NaCl concentration.

2.4.5 Effect of Temperature

Some zwitterionic polymers show temperature-sensitive solubility, with examples of both LCST and UCST types.[8-12] The LCST-type is a soluble to insoluble (S-I) transition, which results from breaking of the polymer-solvent interactions upon heating. The UCST-type is an insoluble to soluble (I-S) transition attributed to breaking (melting) of polymer-polymer

interactions, inter/intra chain electrostatic or H-bonding, upon heating. PMA_{52} solutions at pH(I), and in the presence of sufficient NaCl to make the polyampholyte soluble at 20 °C, showed a S-I transition when heated. This indicates that, instead of breaking ion pairs, heating breaks polymer-water interactions, most likely involving hydrophobic portions of the polymer such as the backbone. The LCST behaviour of PMA_{52} as a function of [NaCl], pH and polymer concentration is shown in Figure 2.6 and 2A.8.

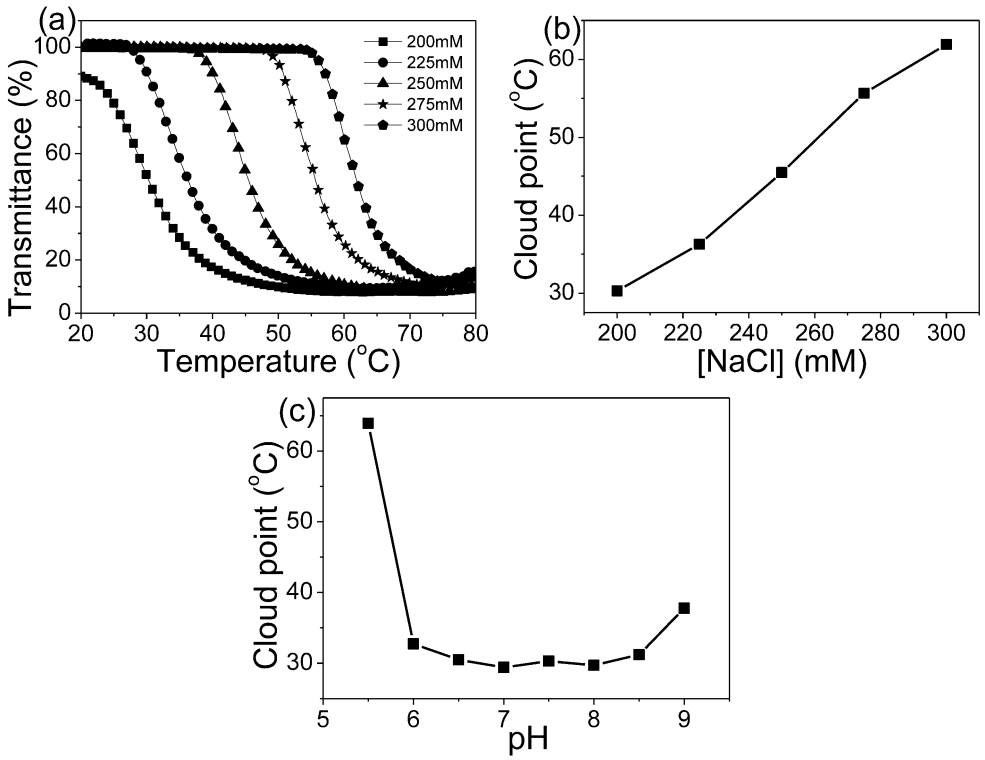

Figure 2.6 The effect of [NaCl] and pH on the cloud point of PMA_{52} at 0.2 wt% in water: (a) Transmittance vs. T (pH 7.5 (pH(I))), (b) Cloud point vs. [NaCl] (pH 7.5), and (c) Cloud point vs. pH (200 mM NaCl).

The cloud point of PMA_{52}, defined here as the temperature at 50% transmittance, shows a strong [NaCl] dependence. The cloud point increased from 30 to 60 °C as [NaCl] increased

from 200 to 300 mM. The onset of phase separation also moves to higher temperature with higher [NaCl]. This increase is caused by shielding of some electrostatic interactions of PMA_{52} (i.e., breaking ion pairs), that make the polymer more hydrophilic even though the net charge remains close to zero, so higher temperature is needed to cause phase separation.

Figures 2.6c and 2A.8a show the effect of pH on the cloud point. The cloud point remained fairly constant between pH 6 and 8.5 (i.e., near pH(I)), but increased at either lower (5.5) or higher (9) pH values. Earlier research has shown that the net charge of polyampholytes is at or very near zero for a certain pH range around the pH(I).[8,15,47] The net charge of PMA_{52} as a function of pH was calculated and found to be close to zero from pH 6 to pH 8.5 (Table 2A.4 and Figure 2A.5), which helps to explain the relative insensitivity of the cloud point to pH in this range. At pH 5.5 and 9, the net charge of PMA_{52} increases making the polymer more hydrophilic, and higher temperature is required to cause phase separation. Another factor that could serve to extend the region of zero or low net charge is that excess ionic groups may promote ionization of complementary groups leading to more ion pairs (lower net charge). This effect has been seen in multilayer systems formed by alternating deposition of a weak polyacid and a weak polybase,[48] where the polymers in the complex can behave as stronger acids (lower pK_a) and bases (higher pK_b) than isolated chains because ammonium ions promoted ionization of nearby carboxylic acids and vice versa.

When the concentration of PMA_{52} was increased, the onset of phase separation did not change much, remaining at about 40 °C, but the curves became steeper, leading to a decrease in cloud point using the definition of temperature at 50% transmission (Figure 2A.8b and 2A.8c). At least part of this phenomenon may be an artifact due to the solutions

with higher polymer concentrations requiring a smaller fraction of the polymer to precipitate to reach 50% transmittance.

PMA_{47}, PMA_{43} and PMA_{37} also showed LCST-type T-responsive behaviour at their pH(I) (Figure 2A.9) but the solutions had to have higher ionic strength than was used with PMA_{52}. APM-rich polymers (>52 mol% APM) did not show a T-response. Interestingly, polyampholytes with high AA content (~90 mol%) showed a T-response but it was of the UCST-type. Solutions of $PMA_{2.5}$, PMA_{6} and $PMA_{8.5}$ at pH 2.9 with no added salt were homogeneous at 50 °C, but became cloudy when cooled (Figure 2.7). For these polymers, heating improved solubility presumably by breaking H-bonds between the free acid groups, as has been seen for the AA homopolymer, PAA.[46] Thus, by varying the polymer composition, PMA samples exhibiting LCST- or UCST-type T-responses may be obtained. It is possible that for certain compositions and solution conditions, a single polyampholyte may show more complex T-responses with both LCST- and UCST-type behaviour, as has been seen for NIPAM-AA copolymers.[46]

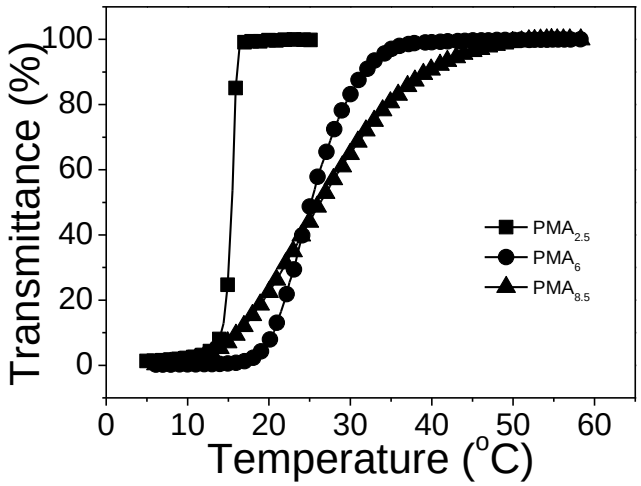

Figure 2.7 The temperature-responsive behaviour of $PMA_{2.5}$, PMA_6 and $PMA_{8.5}$ showing a UCST-type transition. Conditions: 0.5 wt% polymer solution, pH 2.9, no added NaCl; cooling rate: 1 °C/min.

2.5 Conclusion

A series of APM-AA polyampholytes were prepared by free radical copolymerization. The reactivity ratios for copolymerization at pH 2.5 were 0.68 (APM) and 0.48 (AA), determined by following the copolymerization by ^{1}H-NMR.

Polyampholytes comprising 6 to 60 mol% APM showed pH-dependent solubility, and the pH(I) values determined by potentiometric turbidity titrations agreed well with predicted values. The effect of added NaCl on turbidimetric titrations was measured for PMA_{52}, PMA_{35}, and PMA_{12}. The results indicated that the dominant intermolecular force at pH(I) for PMA_{52} are electrostatic interactions, while the solubility of PMA_{35}, and especially PMA_{12}, are increasingly controlled by hydrogen bonding between their carboxylic acid groups.

PMA_{52} showed a LCST-type T-response (cloud point) near pH(I), and the T-response depended on pH, ionic strength and the polymer concentration. Instead of breaking ion pairs, heating caused the ion pairs and other hydrophobic portions of the polymer to be desolvated. The cloud point increased (solubility improved) if the ion pairing was weakened by increasing the ionic strength or changing the pH. The polymer-polymer interactions contributing to the T-response could also be varied by changing the polyampholyte composition. In contrast, AA-rich polyampholytes with ~90 mol% AA

showed UCST-type behaviour near pH(I), likely due to the disruption of H-bonding between the free acid groups.

Overall, the results show that such polyampholytes can be synthesised with little compositional drift, and that they show multi-responsive solution properties controlled by composition, pH, ionic strength, and temperature. The primary amine and carboxylic acid groups on these PMA polyampholytes allow for simple functionalization or crosslinking, and as such these polyampholytes have great potential for use in biomedical fields.

2.6 Acknowledgment

The authors acknowledge funding for this project from the Natural Sciences and Engineering Research Council of Canada through its Discovery Grant and CREATE programs, and from the Ontario Centres of Excellence through the OCE-RE program.

2.7 References:

1. M. Das and E. Kumacheva, *Colloid Polym. Sci.*, 2006, **284**, 1073-1084.

2. A. Ciferri and S. Kudaibergenov, *Macromol. Rapid Commun.*, 2007, **28**, 1953-1968.

3. R. G. Ezell and C. L. McCormick, *J. Appl. Polym. Sci.*, 2007, **104**, 2812-2821.

4. M. J. Fevola, J. K. Bridges, M. G. Kellum, R. D. Hester and C. L. McCormick, *J. Polym. Sci., Part A: Polym. Chem.*, 2004, **42**, 3236-3251.

5. M. J. Fevola, M. G. Kellum, R. D. Hester and C. L. McCormick, *J. Polym. Sci., Part A: Polym. Chem.*, 2004, **42**, 3252-3270.

6. A. B. Lowe and C. L. McCormick, *Chem. Rev.*, 2002, **102**, 4177-4189.

7. B. Bjellqvist, B. Basse, E. Olsen and J. E. Celis, *Electrophoresis*, 1994, **15**, 529-539.

8. X. Zhang, J. Ma, S. Yang and J. Xu, *Soft Mater.*, 2013, **11**, 394-402.

9. Z. Xiong, B. Peng, X. Han, C. Peng, H. Liu and Y. Hu, *J. Colloid Interface Sci.*, 2011, **356**, 557-565.

10. M. Arotcarena, B. Heise, S. Ishaya and A. Laschewsky, *J. Am. Chem. Soc.*, 2002, **124**, 3787-3793.

11. Q. Zhang and R. Hoogenboom, *Chem. Commun.*, 2015, **51**, 70-73.

12. Y. Zhu, J. M. Noy, A. B. Lowe and P. J. Roth, *Polym. Chem.*, 2015. **6**, 5705-5718.

13. Y. Xia, M. Gao, Y. Chen, X. Jia and D. Liang, *Macromol. Chem. Phys.*, 2011, **212**, 2268-2274.

14. S. Boral and H. B. Bohidar, *J. Phys. Chem. B*, 2010, **114**, 12027-12035.

15. S. Ulrich, M. Seijo and S. Stoll, *J. Phys. Chem. B*, 2007, **111**, 8459-8467.

16. Y. Kantor, H. Li and M. Kardar, *Phys. Rev. Lett.*, 1992, **69**, 61-64.

17. S. F. Edwards, P. R. King and P. Pincus, *Ferroelectrics*, 1980, **30**, 3-6.

18. A. Bhattacharjee, P. Kundu and A. Dua, *Macromol. Theory Simul.*, 2011, **20**, 75-84.

19. M. Tanaka and T. Tanaka, *Phys. Rev. E: Stat. Phys., Plasmas, Fluids, Relat. Interdiscip. Top.*, 2000, **62**, 3803-3816.

20. P. G. Higgs and J.-F. Joanny, *J. Chem. Phys.*, 1991, **94**, 1543-1554.

21. A. V. Dobrynin and M. Rubinstein, *J. Phys. II*, 1995, **5**, 677-695.

22. H. Shao, C. Wang, S. Chen and C. Xu, *J. Polym. Sci., Part A: Polym. Chem.*, 2014, **52**, 912-920.

23. J. Song, A. He, Y. Jin and Q. Cheng, *RSC Adv.*, 2013, **3**, 24586-24592.

24. L. Mi and S. Jiang, *Angew. Chem., Int. Ed.*, 2014, **53**, 1746-1754.

25. B. Yu, J. Zheng, Y. Chang, M. Sin, C. Chang, A. Higuchi and Y. Sun, *Langmuir*, 2014, **30**, 7502-7512.

26. K. M. Zurick and M. Bernards, *J. Appl. Polym. Sci.*, 2014, **131**, 1-9**.**

27. M. E. Schroeder, K. M. Zurick, D. E. McGrath and M. T. Bernards, *Biomacromolecules*, 2013, **14**, 3112-3122.

28. Y. Huang, Z. Tang, X. Zhang, H. Yu, H. Sun, X. Pang, and X. Chen, *Biomacromolecules*, 2013, **14**, 2023-2032.

29. R. Rajan, M. Jain and K. Matsumura, *J. Biomater. Sci., Polym. Ed.*, 2013, **24**, 1767-1780.

30. S. Fujii, M. Kido, M. Sato, Y. Higaki, T. Hirai, N. Ohta, K. Kojio and A. Takahara, *Polym. Chem.*, 2015, **6**, 7053-7059.

31. S. Zhai, Y. Ma, Y. Chen, D. Li, J. Cao, Y. Liu, M. Cai, X. Xie, Y. Chen and X. Luo, *Polym. Chem.*, 2014, **5**, 1285-1297.

32. A. Dubey, N. A. D. Burke and H. D. H. Stöver, *J. Polym. Sci., Part A: Polym. Chem.*, 2014, **53**, 353-365.

33. M.R. Aguilar, A. Gallardo, M. D. M. Fernández, and J. San Román, *Macromolecules*, 2002, **35**, 2036-2041.

34. R. Wang, Y. Luo, B. Li and S. Zhu, *AIChE J.*, 2007, **53**, 174-186.

35. X. Sun, Y. Luo, R. Wang, B. Li, B. Liu and S. Zhu, *Macromolecules*, 2007, **40**, 849-859.

36. Y. C. Nho and J. H. Jin, *J. Appl. Polym. Sci.*, 1997, **63**, 1101-1006.

37. S. E. Park, Y. C. Nho, Y. M. Lim and H. I. Kim, *J. Appl. Polym. Sci.*, 2004, **91**, 636-643.

38. S. Igarashi, *J. Polym. Sci., Part B: Polym. Lett.*, 1963, **1**, 359-363.

39. B. S. Ho, B. H. Tan, J. P. K. Tan and K. C. Tam, *Langmuir*, 2008, **24**, 7698-7703.

40. J. M. Corpart and F. Candau, *Macromolecules*, 1993, **26**, 1333-1343.

41. S. E. Kudaibergenov and A. Ciferri, *Macromol. Rapid Commun.*, 2007, **28**, 1969-1986.

42. J. C. Salamone, I. Ahmed, E. L. Rodriguez, L. Quach and A. C. Watterson, *J. Macromol. Sci., Chem.*, 1988, **A25**, 811-837.

43. C. S. Patrickios, *J. Colloid Interface Sci.*, 1995, **175**, 256-260.

44. G. Liu, H. Shi, Y. Cui, J. Tong, Y. Zhao, D. Wang and Y. Cai, *Polym. Chem.*, 2013, **4**, 1176-1182.

45. A. L. P. Fernandes, R. R. Martins, C. G. Da Trindade Neto, M. R. Pereira and J. L. C. Fonseca, *J. Appl.*

Polym. Sci, 2003, **89**, 191-196.

46. G. Bokias, G. Staikos and I. Iliopoulos, *Polymer*, 2000, **41**, 7399-7405.

47. S. Masuda, K. Minagawa, M. Tsuda and M. Tanaka, *Eur. Polym. J.*, 2001, **37**, 705-710.

48. S. E. Burke and C. J. Barrett, *Langmuir*, 2003, **19**, 3297-3303.

2.8 Appendix

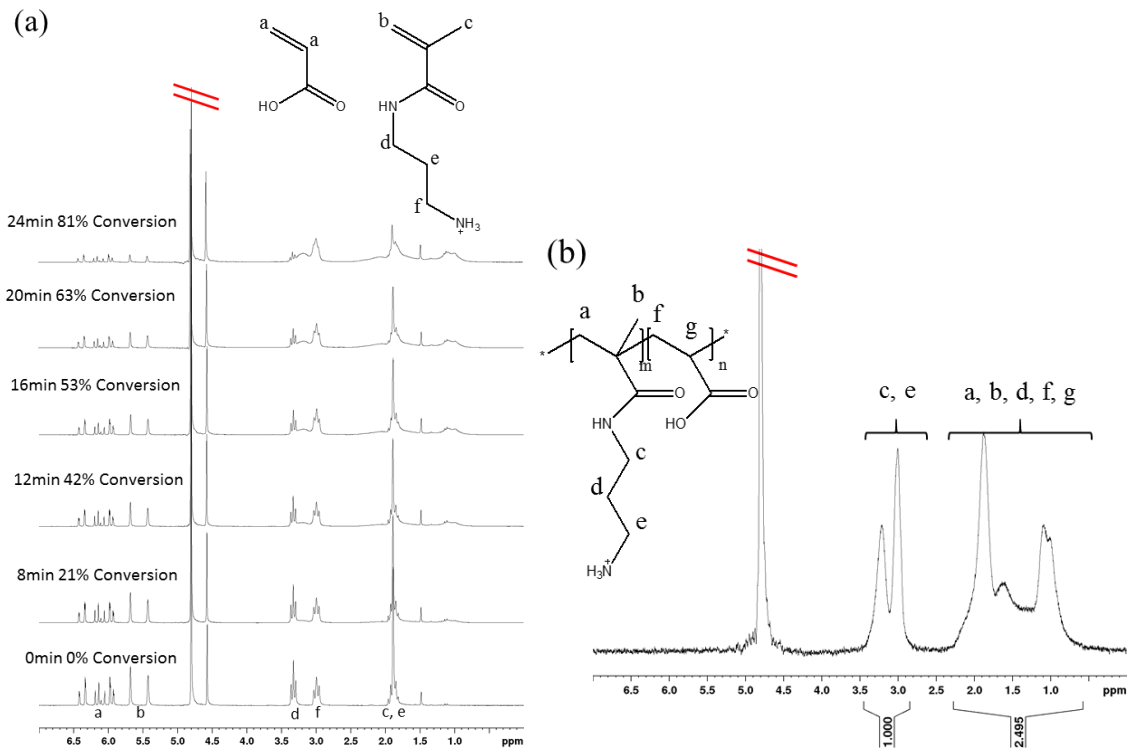

Figure 2A.1 (a) ^{1}H-NMR (200 MHz) spectra taken during copolymerization of a 50:50 APM/AA monomer mixture in D_2O as a function of reaction time at 55 °C. The peak at ~4.6 ppm is from ethylene carbonate, the internal standard. (b) ^{1}H-NMR (600 MHz) spectrum of PMA_{52} copolymer in D_2O.

2.8.1 Calculation of Reactivity Ratios

The reactivity ratios were calculated by fitting the copolymer equation to values of f_1 and F_1, the APM mol fraction in the monomer mixture and the polymer, respectively, as determined by ^{1}H-NMR from eight separate polymerizations. The change in monomer composition with conversion for all of the polymerizations is shown in Figure 2.1 (main

text). These gave 42 individual polymerization steps, of which 5 were excluded in the final fitting. Two steps involved a very small conversion leading to a large uncertainty in F_1 (copolymer composition) while in two others near the end of polymerization, the monomer composition (f_1) changed significantly (>10 mol%) during the step. These changes simply mean that the neighbouring steps or increments become slightly larger, so the relevant conversion data are not lost.

In addition, two of the remaining 39 data points were excluded from the final fitting as they were clear outliers (see Figure 2.2, main text). The copolymer equation (shown below) was fitted to the 37 data points shown in Table 2A.1 with the method of non-linear Generalized Reduced Gradient algorithm in the Solver subroutine of Microsoft Excel 2007 resulting in r_1 (APM) and r_2 (AA) values of 0.68 and 0.48, respectively. The F_1 values calculated using these r_1 and r_2 values are also shown in Table 2A.1.

Copolymerization equation:

$$F_1 = \frac{r_1 f_1^2 + f_1 f_2}{r_1 f_1^2 + f_1 f_2 + r_2 f_2^2}$$

Table 2A.1 f_1 and F_1 values for determination of reactivity ratios.[a]

f_1	F_1 (exp)	F_1(calc)	f_1	F_1(exp)	F_1 (calc)
0.90	0.83	0.87	0.42	0.50	0.47
0.92	0.89	0.89	0.41	0.48	0.46
0.93	0.93	0.91	0.39	0.47	0.45
0.94	0.89	0.91	0.36	0.42	0.43
0.95	0.94	0.93	0.29	0.33	0.37
0.75	0.68	0.72	0.27	0.36	0.36
0.76	0.73	0.73	0.25	0.36	0.33
0.80	0.78	0.76	0.20	0.30	0.29
0.80	0.79	0.77	0.20	0.25	0.28
0.81	0.80	0.77	0.18	0.25	0.26
0.63	0.61	0.62	0.15	0.24	0.23
0.63	0.63	0.62	0.11	0.20	0.18
0.63	0.66	0.62	0.08	0.11	0.14
0.62	0.54	0.62	0.094	0.13	0.16
0.52	0.56	0.55	0.087	0.14	0.15
0.53	0.55	0.55	0.060	0.10	0.11
0.51	0.58	0.53	0.040	0.10	0.08
0.49	0.52	0.53	0.01	0.02	0.03
0.49	0.54	0.52			

a. f_1 is the APM fraction in the monomer mixture at the beginning of a heating segment while F_1 is the APM content of the copolymer formed in that segment as determined by the amount of the two monomers consumed.

Table 2A.2 Predicted drift in composition during preparation of PMAx, starting from 8.8:91.2 (PMA_{12}), 29.4:70.6 (PMA_{35}) and 51:49 (PMA_{52}) APM/AA monomer mixtures, estimated using a series of 10% Conversion Steps. Predicted Comonomer Sequence Distributions calculated by the method of Igarashi.[1]

	% APM in polymer										Blockiness (%)		Alternation (%)
Conversion (%)	**0-10**	**10-20**	**20-30**	**30-40**	**40-50**	**50-60**	**60-70**	**70-80**	**80-90**	**90-100**	**APM**	**AA**	
PMA_{12}	14.8	13.8	12.7	11.5	10.2	8.7	7.1	5.3	3.3	1.0	0.3	82.3	17.1
PMA_{35}	37.0	36.3	35.4	34.3	33.0	31.4	29.3	26.2	21.2	10.2	4.5	45.6	49.9
PMA_{52}	53.7	53.5	53.2	52.9	52.5	52.0	51.3	50.3	48.5	42.3	19.2	17.2	63.6

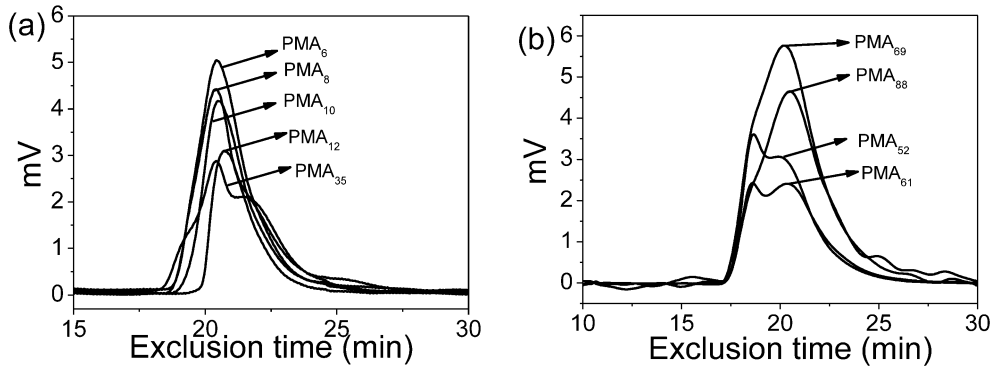

Figure 2A.2 GPC curves of PMAx, (a) pH 9, (b) pH 4.75.

Table 2A.3 The composition of PMA_{37}, PMA_{43} and PMA_{47}.

	APM Feed (mol%)	**Conversion (%)**	**mol% APM in Copolymer**	
			Predicted from reactivity ratios	**^{1}H-NMR (600 MHz) of copolymer**
PMA_{37}	36.5	76	40	37
PMA_{43}	39.3	81	42	43
PMA_{47}	44.3	62	48	47

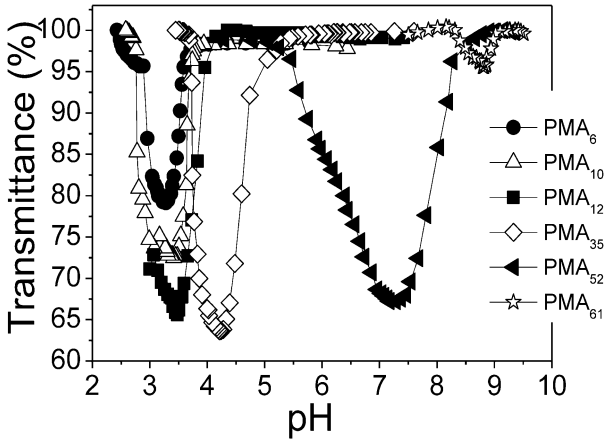

Figure 2A.3 The turbidity titrations of PMAx (x = 6-61). Conditions: 0.1 mg/mL polymer in water, no added salt, titrant: 0.01-1 M HCl. Data collection for PMA_{12} was stopped at pH 3 because the phase-separated material deposited on the pH and optical probes.

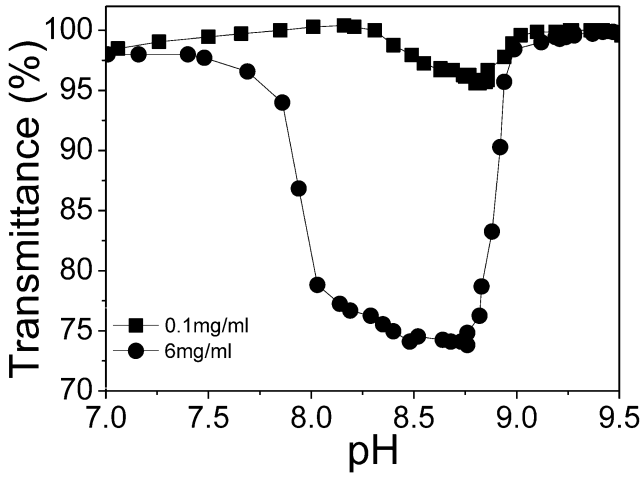

Figure 2A.4 The effect of polymer concentration on the turbidity titration of PMA_{61} titrated with HCl (pH decreasing). Conditions: no added salt, titrant: 0.01-1 M HCl.

2.8.2 Calculation of the Fraction of Charged/Non-charged Monomer Residues on PMA_x at Different pH

The calculation of the fraction of different species (NH_2, NH_3^+, COOH, COO^-, NH_3^+/COO^- ion pair) in the polyampholytes at different pH is based on the Henderson–Hasselbalch equation:

$$pH = pK_a + 1og_{10}\left(\frac{[A^-]}{[HA]}\right).$$

The pKa of monomeric AA is 4.26 and that of APM is close to 9.1, and the ratio of APM and AA in PMA_{12} is 12.7:87.3; in PMA_{35} is 35:65 and in PMA_{52} is 52.3:47.7. For simplicity, it is assumed that the pKa values did not change upon polymerization and do not change with pH, and that the cationic and anionic groups will form ion pairs with 100% efficiency. For example, PMA_{12} is calculated to have 12.7% NH_3^+, 86.8% COOH and 1.22% COO^- at

pH 2.5. If all of the COO^- groups form ion pairs with NH_3^+ ones, it leaves an excess of 11.5% NH_3^+.

Table 2A.4 The calculation of the net charge and the fraction of monomers existing as different species (NH_2, NH_3^+, COOH, COO^-, NH_3^+/COO^- ion pair) on the polyampholyte chain as a function of pH, (a) PMA_{52} (actual composition 52.3:47.7); (b) PMA_{35} (actual composition 35:65), and (c) PMA_{12} (actual composition 12.7:87.3).

(a).

pH	% - NH_2	% -NH_3^+	%-COOH	% - COO^-	Ion Pair	Net charge
3.00	0.00	50.4	47.0	2.58	5.17	47.8
3.50	0.00	50.4	42.3	7.34	14.7	43.1
4.00	0.00	50.4	32.0	17.6	35.2	32.8
4.50	0.00	50.4	18.1	31.5	63.0	18.9
5.00	0.00	50.4	7.64	42.0	83.9	8.43
5.50	0.01	50.4	2.70	46.9	93.8	3.49
6.00	0.04	50.4	0.89	48.7	97.4	1.65
6.50	0.13	50.3	0.28	49.3	98.6	0.96
7.00	0.40	50.0	0.09	49.5	99.0	0.49
7.50	1.23	49.2	0.03	49.6	98.3	-0.41
8.00	3.71	46.7	0.01	49.6	93.4	-2.90
8.50	10.1	40.3	0.00	49.6	80.6	-9.32
9.00	22.3	28.1	0.00	49.6	56.2	-21.5
9.50	36.1	14.4	0.00	49.6	28.7	-35.6
10.00	44.8	5.6	0.00	49.6	11.3	-44.0
10.50	48.5	1.93	0.00	49.6	3.86	-47.7

11.00	49.8	0.63	0.00	49.6	1.25	-49.0

(b).

pH	% -NH_2	% -NH_3^+	%-COOH	% -COO^-	Ion Pair	Net charge
3.00	0.00	35.0	61.6	3.39	6.77	31.6
3.25	0.00	35.0	59.2	5.79	11.6	29.2
3.50	0.00	35.0	55.4	9.62	19.3	25.4
3.75	0.00	35.0	49.7	15.3	30.7	19.7
4.00	0.00	35.0	42.0	23.1	46.1	12.0
4.25	0.00	35.0	32.9	32.1	64.3	2.87
4.50	0.00	35.0	23.7	41.3	70.0	-6.26
4.75	0.00	35.0	15.9	49.1	70.0	-14.1
5.00	0.00	35.0	10.0	55.0	70.0	-20.0
5.25	0.00	35.0	6.03	59.0	70.0	-24.0
5.50	0.01	35.0	3.54	61.5	70.0	-26.5
5.75	0.02	35.0	2.04	63.0	70.0	-28.0
6.00	0.03	35.0	1.16	63.8	69.9	-28.9

(c).

pH	% -NH_2	% -NH_3^+	%-COOH	% -COO^-	Ion Pair	Net charge
2.50	0.00	12.7	85.8	1.49	2.98	11.2
2.75	0.00	12.7	84.7	2.62	5.23	10.1
3.00	0.00	12.7	82.8	4.55	9.10	8.15
3.25	0.00	12.7	79.5	7.77	15.5	4.93
3.50	0.00	12.7	74.4	12.9	25.4	-0.22

3.75	0.00	12.7	66.7	20.6	25.4	-7.91
4.00	0.00	12.7	56.3	31.0	25.4	-18.3
4.25	0.00	12.7	44.2	43.2	25.4	-30.5
4.50	0.00	12.7	31.9	55.4	25.4	-42.7
4.75	0.00	12.7	21.3	66.0	25.4	-53.2
5.00	0.00	12.7	13.4	73.9	25.4	-61.2
5.25	0.00	12.7	8.10	79.2	25.4	-66.5
5.50	0.00	12.7	4.75	82.6	25.4	-69.9
5.75	0.01	12.7	2.74	84.6	25.4	-71.9
6.00	0.01	12.7	1.56	85.7	25.4	-73.1

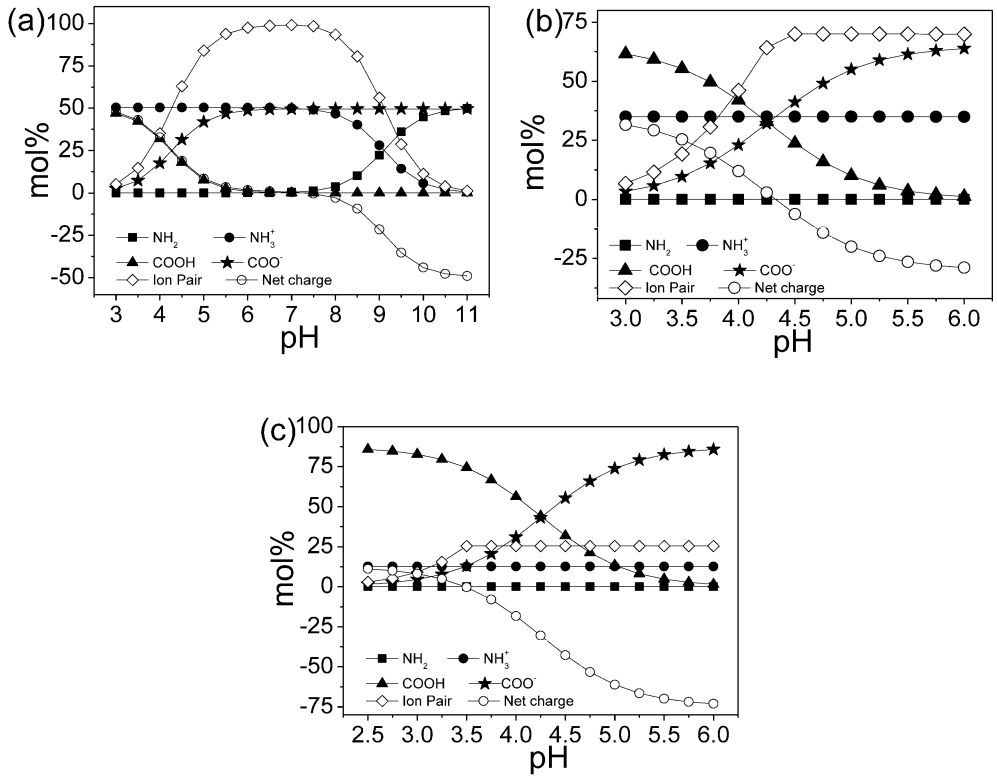

Figure 2A.5 The net charge and the fraction of different species (NH_2, NH_3^+, COOH, COO^-, ion pair) on the polyampholyte chain as a function of pH for: (a), PMA_{52} (actual composition 52.3:47.7); (b) PMA_{35} (actual composition 35:65), and (c) PMA_{12} (actual composition 12.7:87.3).

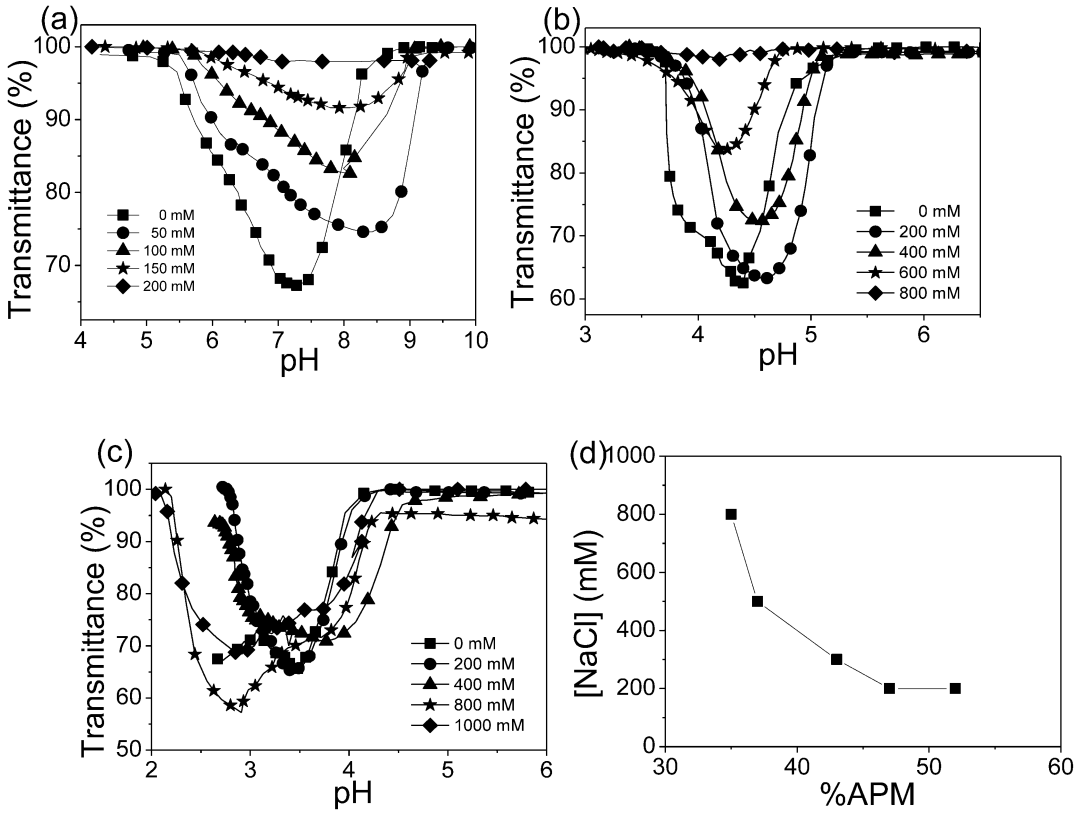

Figure 2A.6 The effect of salt concentration on the turbidity titration curves during titration with HCl (decreasing pH) of (a) PMA_{52}, (b) PMA_{35} and (c) PMA_{12}, and (d) the ionic strength NaCl needed to solubilize the polyampholytes at pH(I). Conditions: 0.1 mg/mL polymer in water, titrant: 0.01-1 M HCl.

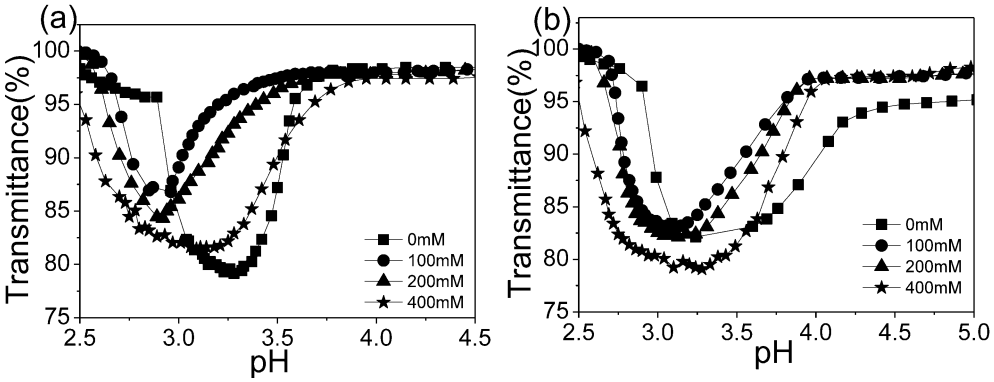

Figure 2A.7 The turbidity titration curves of PMA_6 at different ionic strengths ([NaCl]): (a) decreasing pH, and (b) increasing pH. Conditions: 0.1 mg/mL polymer, titrant: 0.01-1 M HCl and NaOH in (a) and (b), respectively.

3.8.3 Effect of pH and Polymer Concentration on Cloud Point of PMA_x

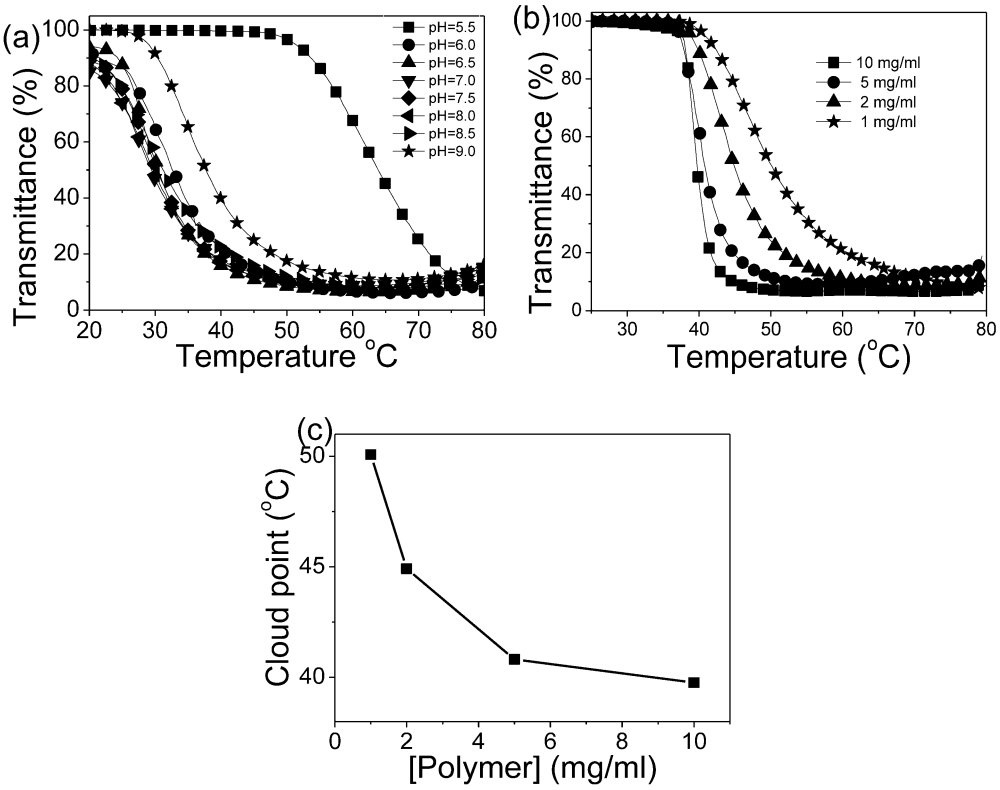

Figure 2A.8 The temperature responsive behaviour of PMA_{52} at (a) various pH (200 mM NaCl, 0.2 wt% polymer) and (b) various polymer concentrations (225 mM NaCl，pH = pH(I) (pH 7.5)); (c) cloud point vs. polymer concentration (225 mM NaCl, pH = pH(I) (pH 7.5)).

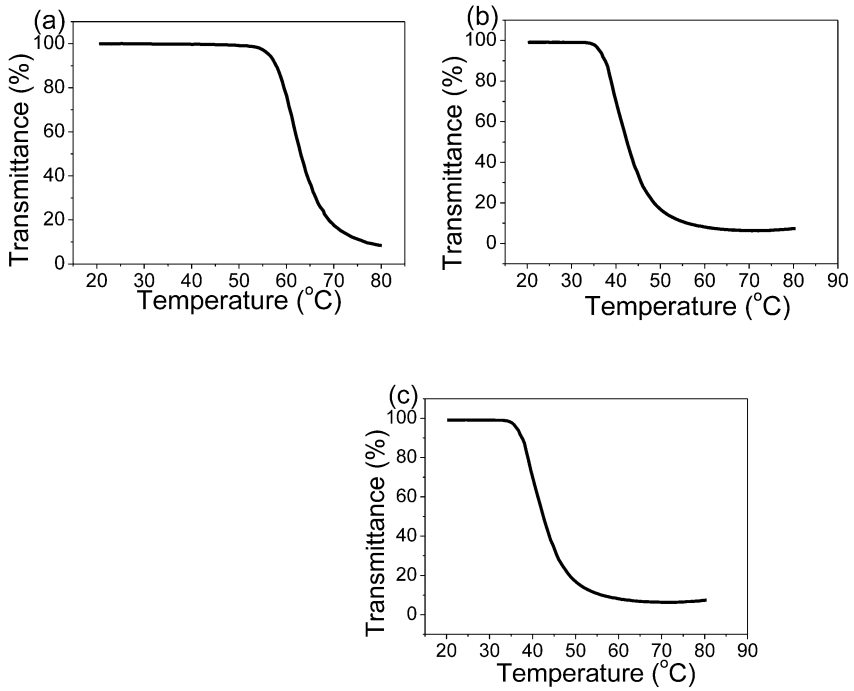

Figure 2A.9 The effect of composition on the temperature-responsive behavior of 0.2 wt% polymer solutions of PMA at pH(I): (a) PMA_{37} at pH 5.0, 600 mM NaCl, (b) PMA_{43} at pH 5.2, 350 mM NaCl and (c) PMA_{47} at pH 5.5, 250 mM NaCl cloud point vs. polymer concentration (225 mM NaCl, pH = pH(I)). Heating rate: 1 °C/min.

2.8.4 References:

1. S. Igarashi, *J. Polym. Sci., Part B: Polym. Lett.*, 1963, **1**, 359-363.

Chapter 3. pH- and Temperature-Induced Phase Separation of Polyampholytes and their use for Dye Binding and Controlled Release

Jing Zhao, Krystle Pinto, Nicholas A.D. Burke, Harald D.H. Stöver

To be submitted.

Contributions: I designed all experiments and performed: ^{1}H-NMR, GPC, fluorescent labelling of copolymers, measurement of phase separation efficiency, cloud points, dye binding and release, and most of coacervate crosslinking, microscopy measurements and some of the polymerizations and titrations. Krystle Pinto carried out most of the polymerizations, purifications, titrations and some of the coacervate crosslinking experiments and microscopy measurements. I also wrote the manuscript, with editorial help and feedback from Dr. Burke and Dr. Stöver.

3.1 Abstract

A series of stoichiometric polyampholytes with molecular weight (MW) ranging from 15 to 460 kDa were prepared by free radical copolymerization of *N*-(3-aminopropyl)methacrylamide hydrochloride (APM) and acrylic acid (AA). Aqueous solutions of these 1:1 copolymers show liquid-liquid phase separation, or simple coacervation, near their pH(I) of 8.0, for M_n of 43 kDa and above. The phase separation efficiencies were determined using FITC-labelled polyampholytes, and found to be constant within $\pm$1 pH units of the pH(I). Lower critical solution behavior was observed

near the pH(I), with cloud points due to thermal phase separation increasing with increasing ionic strength. The cloud points showed a U-shaped dependence on pH centered around pH(I). Coacervate droplets could be covalently crosslinked into hydrogel particles. Finally, the ability of coacervates and covalently crosslinked hydrogel to bind organic model dyes were compared.

3.2 Introduction

In recent years, considerable efforts have focused on multi-responsive, charged polymers, whose solution properties depend strongly on pH, temperature, ionic strength, and light.[1-5] Zwitterionic polymers carry both anionic and cationic charges, are often multi-responsive with composition dependent properties.[6-9] They can have protein-like structure, anti-fouling behaviour and good cell compatibility, leading to potential use as biomaterials.[9-12]

Polyampholytes are a subgroup of synthetic and natural charged polymers that carry cationic and anionic groups on separate monomers units. They typically show anti-polyelectrolyte behaviour, where chain dimension and solubility increase with increasing ionic strength.[8,9,13,14] Polyampholyte solution properties depend on the nature of the charged groups.[7,15,16] Polyampholytes containing weak acids and/or bases will show an isoelectric point, pH(I), where their net charge is zero, and their solubility lowest,[8, 17] while polyampholytes bearing permanent anionic and cationic charges have a fixed, pH-independent net charge, which is zero for a stoichiometric, or 1:1, polyampholyte.[7, 18] The solution properties may also be influenced by their architecture, e.g., random, block, gradient and alternating copolymers,[19-21] and the polymer molecular weight (MW), though

few studies have examined the latter effect.[22] Based on their ability to respond to various stimuli, polyampholytes have been examined for industrial and biomaterial applications including water purification, non-fouling surfaces and cryoprotection.[23-29]

Under certain conditions, aqueous solutions of charged polymers including polyampholytes undergo a liquid-liquid phase separation called coacervation, leading to a polymer-rich and a polymer-poor liquid phase.[30,31] The liquid nature of the polymer-rich coacervate phase has proven useful in, e.g., encapsulation, extraction, and protein purification.[32,33] Similar coacervate formation from natural proteins plays a key role in adhesion by marine organisms.[34-46] Unlike "complex coacervation" of two oppositely charged polyelectrolytes, which involves strictly inter-chain electrostatic interactions,[37-39] polyampholyte coacervation is a "simple coacervation", involving a single macromolecular species that phase-separates due to both inter- and intra-chain interactions. Natural proteins have been shown to undergo simple coacervation, including tropoelastin,[40] histidine-rich proteins involved in reinforcement of squid beaks,[34,41] mussel adhesion proteins[42] and quite recently, inherently disordered proteins responsible for the reversible formation of membrane-free organelles under, e.g., influence of temperature and salinity.[43]

Examples of complex coacervates are more numerous, including anchoring adhesives and construction glue used by marine organisms such as mussels[44] and sandcastle worms.[45]

Both natural and synthetic complex coacervates have been extensively studied with regards to the dependence of the coacervation point on pH, salinity, concentration and temperature as well as with regards to the nature of the phase separation.[46-48] Much less is known about the nature of the phase transitions of simple coacervates, but the increasing reports of

natural[49] and synthetic simple coacervates[50] observation makes them very interesting systems for study.

We recently showed that stoichiometric binary polyampholytes comprising *N*-(3-aminopropyl)methacrylamide (APM) together with either methacrylic acid (MAA)[51] or acrylic acid (AA)[52] undergo simple coacervation near their pH(I). These binary polyampholytes have largely alternating comonomer sequences.[52] There polyampholytes can undergo liquid-solid or liquid-liquid phase separation, to form hydrogel or coacervates dependent on the composition and conditions like pH, [NaCl] and temperature.

The current paper focus on stoichiometric polyampholytes with various MW by APM and AA and employ as the model polymer for exploring the extensive solution properties of polyampholytes. The polyampholytes have liquid to liquid phase separation of coacervates at close to neutral pH in water, with the response to MW, pH, [NaCl] and temperature. This work quantitatively describes the effects of polymer MW, concentration, pH, ionic strength and temperature on coacervate formation the binding and release of model organic dyes by liquid coacervate droplets, and the covalent crosslinking of coacervate droplets into hydrogel particles. This work is showing the general properties of polyampholytes and a simplest polymeric systems able to undergo coacervation, which will promote the following research on new polymer and material design or provide a simple polymer for deeper understating of the phase transitions of simple coacervates.

3.3 Experimental Section

3.3.1 Materials

Acrylic acid (AA, 99%) was obtained from Sigma-Aldrich, and distilled before use. *N*-(3-Aminopropyl)methacrylamide hydrochloride (APM.HCl) from Polysciences, and 2,2'-azobis(2-Methylpropionamidine)dihydrochloride (Vazo-56), L-cysteine hydrochloride monohydrate (98%), tetrakis(hydroxymethyl)phosphonium chloride (THPC) (80%), *N*,*N*-Methylenebisacrylamide (99%), ethylene carbonate (98%), fluorescein isothiocyanate isomer 1 (FITC, ≥90%), *N*,*N*-Dimethylformamide (DMF, reagent grade), rhodamine B, brilliant blue G, methylene blue, from Sigma-Aldrich were used as received. Trypan blue solution (0.4%, Thermo Fisher) was used as received. Deuterium oxide (D_2O) was purchased from Cambridge Isotope Laboratories (Andover, MA). Sodium hydroxide and hydrochloric acid solutions (0.10 and 1.0 M) were obtained from LabChem Inc.

3.3.2 Copolymer Syntheses

Solution copolymerizations were carried out as described previously.[52] Equimolar amounts of APM and AA were dissolved in 10 mL distilled water in 20 mL screw cap glass vials to 10% (w/v) total monomer loading, together with 1 mol% initiator (Vazo-56, relative to total monomer). Chain transfer agent (CTA, L-cysteine hydrochloride monohydrate, 0, 0.2, 0.5, 2 and 5 mol% relative to total monomer) was added to control the MW. The vials were heated at 55 °C in an oven fitted with a set of horizontal steel rollers that rolled the vials at 4 rpm. The progress of the copolymerizations was monitored by removing small aliquots, diluting these with D_2O and determining conversion by ^{1}H-NMR with a Bruker Avance

600 spectrometer. The areas of the vinyl signals of AA at 5.5 ppm and APM at 5.3 ppm relative to the internal standard (ethylene carbonate) were used to determine the conversion of the two monomers. Polymerizations were stopped at 60-80% conversion and the cooled reaction mixtures were dialyzed against distilled water at pH 3 in cellulose tubing (3.5 kDa MW cutoff) for 4 days with daily water changes. The purified polymers were isolated by freeze-drying.

The copolymers are abbreviated as PMA-x, where M, A, and x stand for APM, AA, and the polymer MW in kDa as determined by GPC. The ratio of APM to AA in the polyampholytes discussed in the main paper was found to be 52:48 by ^{1}H-NMR. A series of copolymers with 37, 43, and 47 mol% APM were also prepared, and their solution properties described in the supplemental information.

The PMA hydrogel was prepared analogously to the linear copolymers, with APM and AA in a 1 to 1 molar ratio at 10% (w/v) total monomer loading, 1 mol% initiator and 2 mol% (relative to total monomer) *N*,*N*-methylenebisacrylamide added as crosslinker, dissolved in 10 mL distilled water in 20 mL screw cap glass vials. After mixing, the sample was heated in a water bath at 55 ^{o}C for 2 hrs, then the hydrogel was swelled and extracted in 4 L distilled water for 4 days with daily water changes, during which the hydrogel broke into smaller, millimeter-range pieces. The purified hydrogel pieces were isolated and dried in air in a 70^{o}C oven.

3.3.3 ^{1}H-NMR Analyses

^{1}H-NMR was carried out on a Bruker AV 600 spectrometer, using 10 mg/mL polymer solutions in D_2O. The compositions of the copolymers were calculated by comparing the area of the APM methylene signal (2.5-3.5 ppm, 4H) with the combined area of the backbone signals of APM and AA units at 0.5 to 2.5 ppm (7H for APM and 3H for AA).

3.3.4 GPC Analyses

The molecular weights of the copolymers were measured using an aqueous gel permeation chromatography (GPC) system consisting of a Waters 515 HPLC pump, Waters 717plus auto-sampler, three columns (Waters Ultrahydrogel-120, -250, -500), and a Waters 2414 refractive index detector calibrated with narrow disperse poly(ethylene glycol) standards (Waters). The mobile phase was a 1 M acetate buffer at pH 4.7.

3.3.5 Determination of pH(I)

Turbidimetric titrations were carried out on 0.1 mg/mL solutions, chosen to give significant decreases in transmittance at the pH(I), while minimizing macroscopic precipitation, and hysteresis due to slow re-dissolution, after the titration has passed the pH(I). The solutions, which had an initial pH near 5, were titrated manually to pH 9-10, by adding 25 µL aliquots of 0.01 to 1 M NaOH with a micropipette at 22 °C, while simultaneously monitoring the pH and the turbidity of the solution, using a VWR SympHony pH probe and a Mitsubishi GT-LD photometric detector equipped with an optical fiber turbidity probe (λ >620 nm).

The concentration of NaOH was selected to give suitable changes in pH per injection (ΔpH ~0.05-0.1).

The same solutions were subsequently titrated back from high to low pH, using 25 µL aliquots of 0.01 to 1 M HCl, while monitoring pH and turbidity. The pH(I) was determined as the midpoint between the leading edges of the forward and back titration curves at about the half-maximum turbidity points. To determine the effect of ionic strength on the pH(I), the titrations were repeated in the presence of different concentrations of NaCl achieved by adding solid NaCl.

3.3.6 Fluorescent Labelling of Copolymers

In a 20 mL screw cap glass vial, 100 mg of the PMA-x (0.41 mmol amine) was dissolved in 10 mL of a 0.1M $NaHCO_3$ buffer at pH 9 and then the pH was adjusted back to pH 9 by addition of 1 M NaOH. FITC as a 5 mg/mL solution in DMF (318 µL; 0.0041 mmol; 1 mol% amines) was added to the stirred polymer solution. The solution was protected from light and left stirring for 2 hours before being dialyzed using cellulose tubing (Spectrum Laboratories; 3.5 kDa MW cutoff) against distilled water maintained at pH 9-10 to prevent pH(I)-related precipitation in the dialysis tubing. The dialysis water was changed daily and after 4 days the FITC-labelled polymer was isolated by freeze drying.

3.3.7 Measurement of Phase Separation Efficiency

In a glass screw cap vial, FITC-labelled PMA-x copolymers were dissolved in water and the pH adjusted to 9.7. The initial polymer concentration was determined by measuring the fluorescein concentration with a UV-visible spectrometer (Varian Cary 50 Bio UV-Vis Spectrophotometer; λ_{max} 493-495 nm). Then the pH was adjusted to pH(I) (7.7), the cloudy polymer solution transferred to a centrifuge tube and then centrifuged at 4000 rpm (~3000 g) for 40 min. The supernatant was removed, adjusted back to pH 9.7, and analyzed by UV-visible spectroscopy to determine the concentration of polymer remaining in the supernatant.

$$\text{Phase Separation Efficiency} = \frac{A\,(initial) - \text{A}\,(pH(I))}{A\,(\text{initial})} \times 100\%$$

The effect of polymer concentration was measured for PMA-460, PMA-87 and PMA-32, using 0.1, 0.2, 0.5, 1 and 2 mg/mL solutions for each of these MW. After centrifugation, the supernatants of the 0.1 and 0.2 mg/mL samples were directly measured, while the supernatants of the 0.5, 1 and 2 mg/mL samples were diluted 5-, 10- and 20-fold, respectively, before analysis. The effect of salt concentration was examined for PMA-460 using a 0.2 mg/mL polymer solution, and [NaCl] of 50, 100, 150, 200, 250 and 300 mM. The effect of pH on PMA-460 phase separation efficiency was measured using a 0.2 mg/mL solution without added NaCl, and pH of 9.50, 8.98, 8.28, 7.75, 7.11, 6.82, 6.36 and 5.73. To measure the effect of MW, PMA-460, PMA-180, PMA-87, PMA-32 and PMA-15 were tested at 0.2 mg/mL polymer without added NaCl.

3.3.8 Cloud Point Measurements

Cloud point measurements were made using a Varian Cary 3E spectrophotometer fitted with a temperature controlled 12-sample cell holder. The rates of heating and cooling were both 1 °C/min and the transmittance at 500 nm was measured at 0.5 °C intervals. Solutions containing 2 mg/mL PMA-x were used at different pH and salt concentration. To determine the effect of pH, the salt concentration was fixed at the lowest concentration to keep the solution clear, with pH varying from 5.5 to 10. To test the effect of ionic strength, the pH was fixed near pH(I) and ionic strength was varied from 25 to 250 mM. The cloud point was defined as the temperature at which the transmittance had fallen to 50%.

3.3.9 Coacervation and Crosslinking

Polymer coacervates were made from 1 mg/mL polymer solutions without NaCl, and the pH was adjusted to pH(I). The coacervates were crosslinked with THPC. A 1% solution of THPC was adjusted to pH 7.5-8 before being added to the coacervate suspension to give the desired THPC arm : NH_2 mol ratio, ranging from 1.25% to 50%.

3.3.10 Characterization of Polyampholyte Coacervates by Microscopy

PMA-x with or without FITC label were dissolved in distilled water to make 1 mg/ml solutions and then adjusted to pH(I), where phase separation occurred. The samples were characterized on a Nikon ECLIPSE LV100ND optical microscope fitted with an ANDOR ZYLA-5.5-CL10 digital camera and NIS-Elements AR 4.30.02 software.

3.3.11 Dye Binding and Release

To individual 3 ml aliquots of PMA-460 coacervate suspension (1 mg/mL, pH 7.7) in 15 mL centrifuge tubes were added 30 µL of dye solutions containing: Rhodamine B (1 mg/mL, 2.1 umol/ml), Brilliant Blue G (1 mg/mL, 1.3 umol/ml), or Methylene Blue (1 mg/mL, 3.1 umol/ml), or Trypan Blue (4 mg/mL, 4.2 umol/ml). The samples were centrifuged immediately after mixing at 4000 rpm (~3000g) for 5 min and the dye concentrations in the reference and supernatant solutions were measured by visible light spectrophotometry in 1 cm square quartz cuvettes on a Cary 50 Bio UV-Visible Spectrophotometer, using absorption at Brilliant Blue G 590 nm, Trypan blue 592 nm, Methylene Blue 665 nm, Rhodamine B 555 nm wavelength. Samples containing 30 µL of the respective dye solutions diluted in 3 mL water, were used as reference. For the hydrogel dye binding, individual dry gel particles weighing about 3 mg were placed into separate UV/Vis cuvettes and covered with 3 ml water at different pH containing 30 µL of a 1 mg/ml BB aq. solution.

For the hydrogel dye binding and release, fresh single pieces of about 3 mg dry gel were immersed each in 1 ml of 1 mg/ml BB solution for 12 hrs, then briefly dried using a Kimwipe® before transferring them into a UV/Vis cuvette containing 3 ml of water with different pH. Both the binding and release of dye was followed in *situ* by UV-Vis spectroscopy.

3.4 Results and Discussion

3.4.1 Preparation of PMA-x

A series of APM-AA copolymers with composition close to 50:50 but with varying MW were prepared by free-radical copolymerization using a CTA. Based on the reactivity ratios found in previous work,[52] copolymerizations were stopped at 60-70% conversion to minimize the drift in copolymer composition.

Table 3.1 summarizes the composition and MW data for the PMA-x copolymers obtained from ^{1}H-NMR and GPC analyses. GPC curves are shown in Figure 3A.1. For simplicity, we chose to prepare copolymers using 1:1 molar feed ratios. In each case the copolymer had a 52:48 APM/AA composition, consistent with that expected on the basis of the reactivity ratios and monomer conversions of about 70%.[52] This copolymer will have a slight net cationic charge given the small molar excess of APM, but we believe this effect is too small to significantly affect its polyampholyte character. The MW decreased as the CTA concentration used during polymerization was increased (Figure 3A.1b), resulting in PMA-x samples with M_w ranging from 460 to 15 kDa. Normally, the MW dispersity ($Đ_M$) increases with CTA concentration, but the opposite behavior was seen here, likely because low MW fractions of the samples were lost during dialysis.

Table 3.1 Summary of PMA-x polymer composition analyses.

CTA (mol%)	Conversion (%)	APM:AA (NMR)	M_n (kDa)	M_w (kDa)	$Đ_M$
0	67	52:48	161[a]	460	2.3
0.2	66	52:48	80	180	2.2
0.5	85	52:48	42	87	2.1
2	67	52:48	19	32	1.7
5	68	52:48	11	15	1.4

a. The high MW sample (0% CTA) contained chains beyond the upper calibration limit of the GPC system (881k), and hence the M_n and M_w values reported were estimated values, obtained by extrapolating the calibration to allow analysis of the entire peak. MW calibration were carried out using narrow-disperse PEG standards.

3.4.2 Solution Properties and Liquid-Liquid Phase Separation

Polyampholytes will often undergo electrostatically induced phase separation at their pH(I), where their net charge is zero. When salts are added at pH(I), polyampholytes can re-dissolve due to shielding of the electrostatic interactions. In previous work, the solubility of related PMA polyampholytes was found to depend on the copolymer composition, pH, ionic strength and temperature.[52] The current work expands these studies to cover a range of polyampholyte MW, quantifies coacervation efficiency as function of pH, [polymer], MW and [NaCl], and explores binding of model organic dyes to both coacervate and crosslinked polyampholyte.

3.4.2.1 Effect of MW on Potentiometric Turbidity Measurements

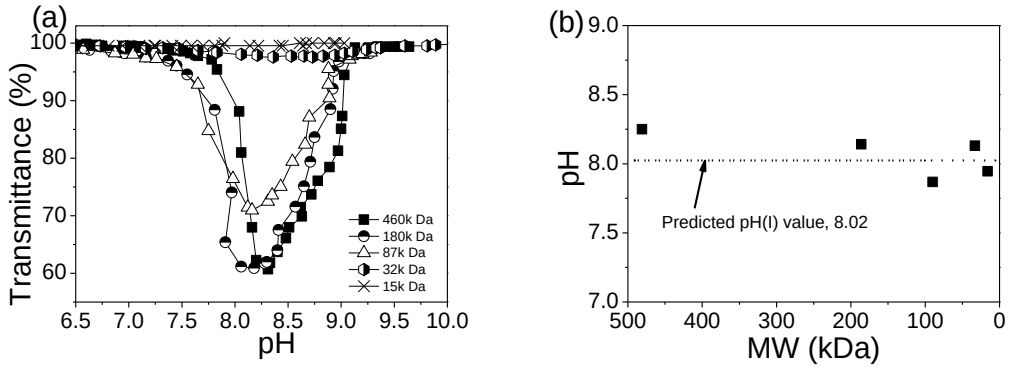

Figure 3.1 (a) Turbidity titration curves for PMA-x with MW ranging from 460 to 15 kDa. (b) pH(I) vs. MW (Mw) for PMA-x. Conditions: 0.1 mg/mL polymer, no added salt, titrant: 0.01-1 M NaOH. pH(I) for PMA-32 and PMA-15 were estimated from titration curves obtained with 1 mg/mL polymer concentrations (Figure 3A.3). The lines in (a) are drawn to guide the eye, not to imply physical meaning.

Figure 3.1a shows the turbidity titration curves of PMA-x solutions with different MW, titrated with NaOH. The corresponding HCl titration curves are shown in Figure 3A.2. The midpoint between half-max turbidity values for HCl and NaOH-based titrations were used as approximation for the actual, thermodynamic pH(I). All PMA-x solutions were fully transparent at high and low pH but showed cloudiness at pH(I), especially for the higher MW samples. In the case of PMA-32, the turbidity at pH(I) of the 0.1 mg/mL solution was weak while the PMA-15 solution remained transparent. However, phase separation for these two polymers at pH(I) was readily detected when the polymer concentration was increased to 1 mg/mL (Figure 3A.3). High MW samples show a gradual onset of turbidity prior to the pH(I), which may be attributed to forming of soluble complexes similar to those

seen in complex coacervation,[47, 48] or to coacervation of a portion of the chains having a higher acrylic acid content and hence a pH(I) shifted to lower pH values.

As shown in Figure 3.1b, polymer MW had little effect on pH(I), which fell between 7.8 and 8.2 for all MW, in good agreement with the value of 8.02 predicted for a 52:48 APM/AA composition.[53] This is not surprising since the pK_a of the acid and base groups on the side chains, which determine pH(I), should be independent of MW. The small variation in the experimental pH(I) values observed is attributed to the uncertainty of estimating pH(I) from titration curves of phase-separating systems.

Figure 3.2 shows optical microscopy images of phase-separated PMA-x solutions at pH(I), while corresponding fluorescence microscopy images are shown in Figure 3A.4. All of the PMA-x polymers phase-separate as liquid coacervates, apparent as clear, round droplets in the low micrometer diameter range. As the polymer MW decreased, the amount of coacervate decreased, consistent with the observations during the turbidity titrations (Figure 3.1a). Fluorescence microscopy of coacervates from FITC-labelled PMA-x revealed bright droplets (Figure 3A.4) confirming that the polymer is concentrated in the coacervate. The fluorescence of the coacervate droplets decreased as MW decreased (Figures 3A.4) suggesting that the coacervate has decreasing polymer concentration (higher water content). The fluorescence microscopy images also show few coacervate droplets for the PMA-32 and PMA-15 solutions. The results of the turbidity titration and microscopy experiments suggest that the efficiency of phase separation decreases as the MW of PMA decreases. The effect of MW on polyampholytes separation agrees with the theoretical prediction of polyelectrolytes that the coacervation requires a minimum molecular weight of 10,000 Da, and a minimum concentration of 0.01%.[54]

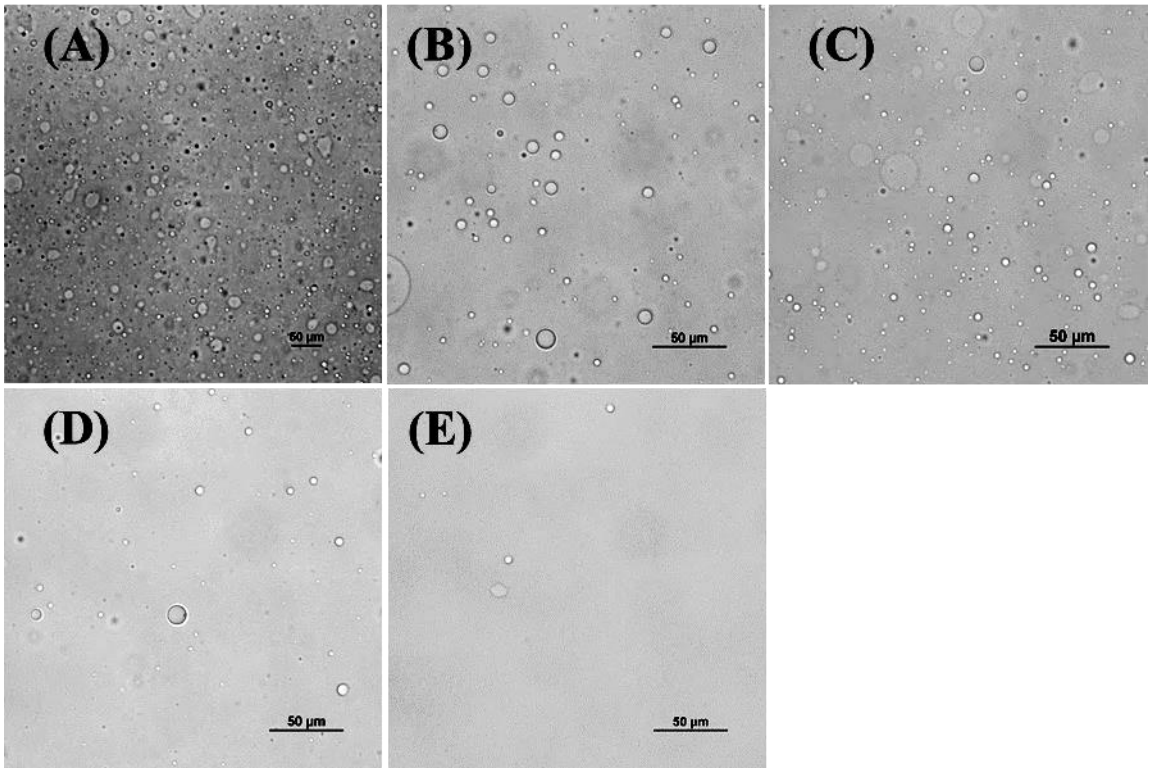

Figure 3.2 Optical microscopy images of phase separated material formed from 1 mg/ml solutions of PMA-x at pH(I) for polymers with MW of (A) 460 kDa at pH 8.34, (B) 180 kDa at pH 8.40; (C) 87 kDa at pH 8.31, (D) 32 kDa at pH 8.31and (E) 15 kDa at pH 8.34.

3.4.2.2 Effect of Ionic Strength

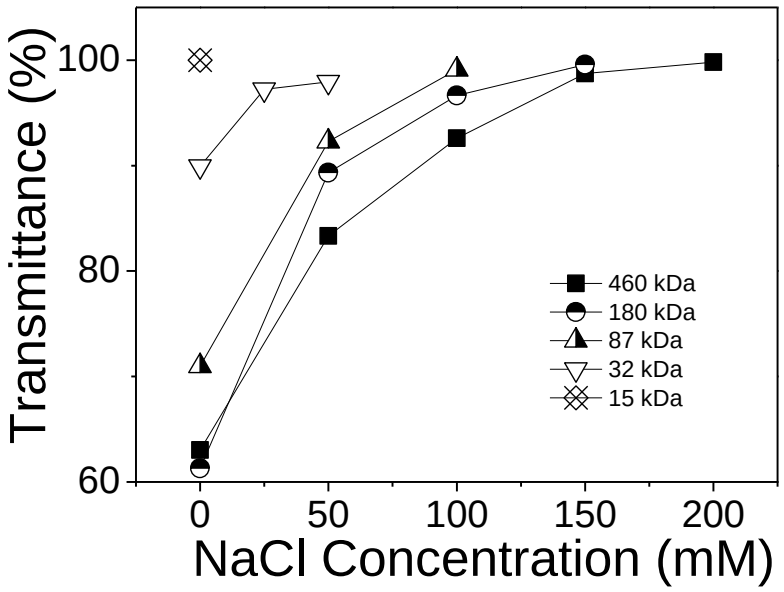

Figure 3.3 The effect of ionic strength on the transmittance at pH(I) observed during titration of 0.1 mg/mL solutions of PMA-x of varying MWs.

Ionic strength affects polyampholyte conformation and solubility through shielding of the electrostatic interactions.[15, 21, 55, 56] Near pH(I), adding salt promotes polymer solubility by shielding inter- and intra-chain electrostatic interactions. Titration curves were measured at different ionic strengths for each PMA-x polymer (Figure 3A.5), and Figure 3.3 shows the transmittance minima near pH(I) as function of [NaCl], which serve as a qualitative indicator of the degree of phase separation. The salt concentration required to prevent phase separation falls from 200 mM NaCl for PMA-460 to 0 mM for PMA-15. Coacervation involves multiple weak, intra- and inter-chain interactions. The polyampholyte solutions with different MW all have the same pKa values, pH(I), polymer concentration and

polymer composition, so the decrease of MW should not change the strength of the electrostatic interactions per monomer unit. However, as the shorter chains have higher mobility, they show less efficient phase separation. Hence, in addition to pH and ionic strength, polymer MW can have a profound effect on polyampholyte solubility near their pH(I).

3.4.2.3 Phase Separation Efficiency as Function of MW, [polymer], pH and [NaCl]

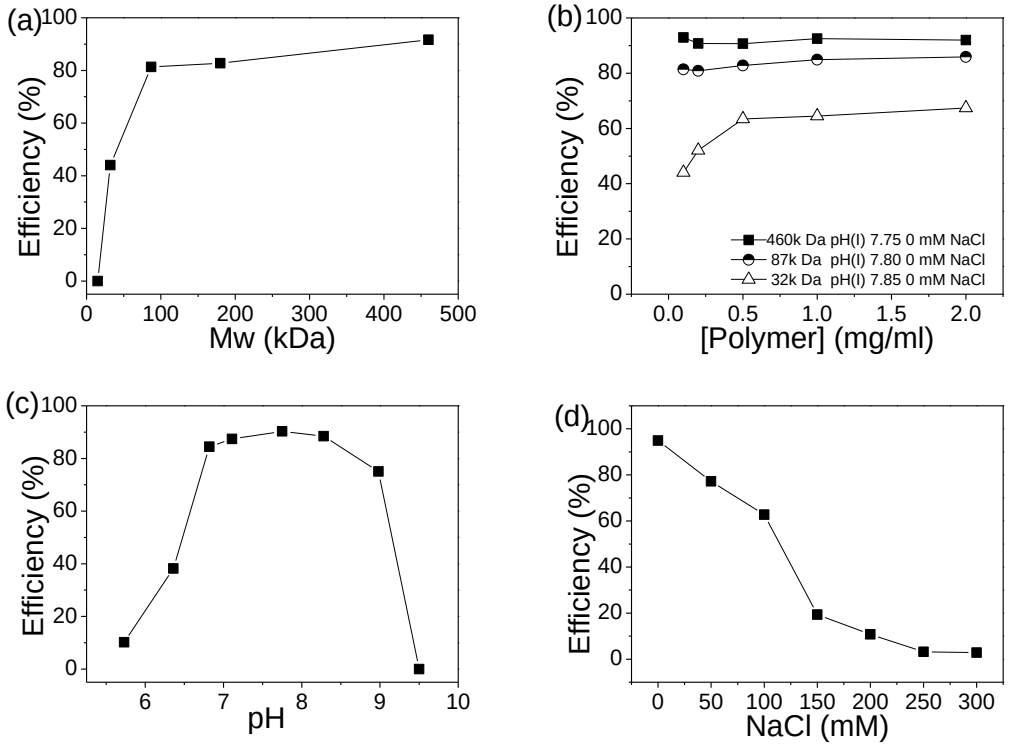

Figure 3.4 The phase separation efficiency of PMA-*f* solutions as a function of: (a) MW (at pH(I) 7.75, 0.2 mg/mL, 0 mM NaCl), (b) polymer concentration for 460, 87 and 32 kDa samples (at pH(I) 7.75-7.8, 0 mM NaCl) , (c) pH for 460 kDa sample (0.2 mg/mL, 0 mM NaCl) and (d) ionic strength ([NaCl]) for 460 kDa sample (at pH(I) 7.75, 0.2 mg/mL).

Phase separation efficiency in this work is the fraction of total polymer found in the coacervate, is an important issue, and depends on multiple parameters, including polymer MW, like Kawar et al.[57] carried out calculations suggesting that in complex coacervations and Bohidar et al.[54] predicted the for simple coacervation, MWs have to be above 10,000 to achieve phase separation. Phase separation efficiency was determined quantitatively using absorbance spectroscopy to measure the fraction of fluorescein-labeled polymers remaining in the supernatant polymer-poor phase at pH(I). The phase separation efficiency decreased from 90% for PMA-460 to 0% for PMA-15, all in 0.2 mg/mL solutions (Figure 3.4a). Increasing the polymer concentration ten-fold led to little further gain for PMA-460 phase separation, remaining at 90 - 95% efficiency, while the phase separation efficiency of PMA-32 increased from 45% - 65%.

As the phase separation efficiency of PMA-460 was independent of [polymer], this polymer was used to further probe the effect of pH and ionic strength on phase separation efficiency. Figure 3.4c shows that pH has little effect on the phase separation efficiency of PMA-460 across several pH units (7 to 9) near pH(I), but the efficiency drops dramatically at higher or lower pH values. The net charge is often at or very close to zero for a certain pH range around the pH(I) for polyampholytes,[20,58] including PMA.[52] In addition, it is known that anionic or cationic groups can promote the ionization of neighboring amines or acids, respectively, leading to reduced net charge and improved ability to resist changes of ionization status.[59]

While increasing ionic strength generally improves polyampholyte solubility, some systems show low phase separation efficiency at 0 mM ionic strength, and then higher

efficiency once salts are first added, and colloidal stability is decreased.[51] PMA-x showed high phase separation efficiency in the absence of added salts and the efficiency steadily decreased as ionic strength was increased (Figure 3.4d). The high phase separation efficiency of PMA-x in the absence of added salt may be due to the nature of the polymer or perhaps the solutions have >0 mM ionic strength due to the presence of low levels of small ion impurities in the polymer sample. Microscopy images taken as ionic strength was increased revealed that the size of the coacervate droplets increased (colloidal stability decreased) and the number of coacervate droplets decreased, until the coacervate finally disappeared due to shielding of the attractive electrostatic interactions (Figure 3A.6).

3.4.2.4 Effect of Molecular Weight and [NaCl] on Cloud Point Temperature

Temperature-sensitive solubility has been observed for some zwitterionic polymers, with both lower and upper critical solution temperatures (LCST and UCST) reported.[19, 60-62] Previous work found that PMA polyampholytes with close to 50:50 APM/AA showed LCST-type behaviour.[52] Interactions between the polyampholyte and small ions, as well as between polyampholyte and water, may be broken upon heating, leading to increased inter- and intra-chain interactions and phase separation. In the case of zwitterionic polymers that show UCSTs, heating is believed to break inter- and intra-chain electrostatic interactions.[60]

The LCST behavior of PMA-x was investigated by measuring transmittance vs. temperature curves (Figure 3A.7). The effects of pH, ionic strength and MW on the cloud point are summarized in Figures 3.5 and 3.6.

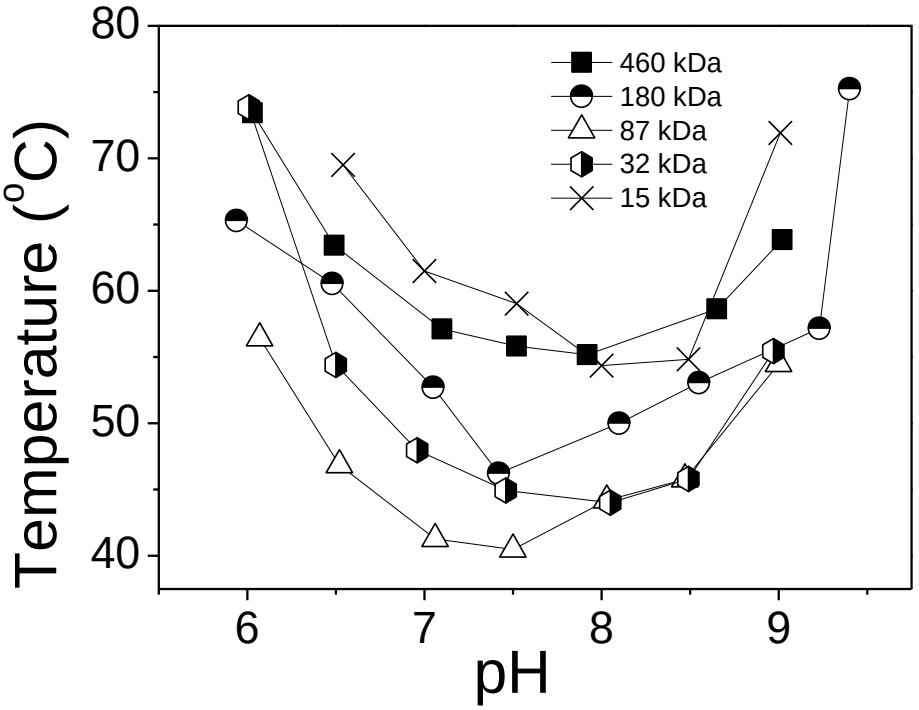

Figure 3.5 The cloud points vs. pH for 2 mg /ml of PMA-460 (225 mM NaCl), PMA-180 (175 mM NaCl), PMA-87 (150 mM NaCl), PMA-32 (50 mM NaCl) and PMA-15 (25 mM NaCl). [NaCl] was adjusted to give LCSTs above room temperature.

All of the PMA-x showed a similar U-shaped dependence of the cloud point on pH, with a minimum near pH(I), and increasing at either lower or higher pH values (Figure 3.5). The solutions did not show a cloud point for pH <6 or >9. Analogous behavior has been seen for poly(DMAEMA-*b*-AA) block copolymers, which showed a minimum in cloud point temperature at pH 9.5, close to the pH(I) of 9.[19] The relative insensitivity of the cloud point to pH near pH(I) is consistent with the phase separation efficiency results (Figure 3.4c), and again results from these stoichiometric polyampholytes having near zero charge over several pH units around pH(I).[20, 58] Figure 3A.8 shows that the cloud point of PMA_{47}, a

copolymer quite similar to the stoichiometric copolymers studied here, remains fairly constant in the pH range of 5.5 to 7, while the cloud points of both PMA_{43} and PMA_{37} are quite sensitive to pH. The effect of pH to the cloud point derives mainly from the resulting net charge. At zero net charge, the polymer chain is hydrophobic, and the cloud point temperature at its minimum. When pH deviates from pH(I), the polymer chains start to have net charges, become more hydrophilic, and the cloud point temperature increases.

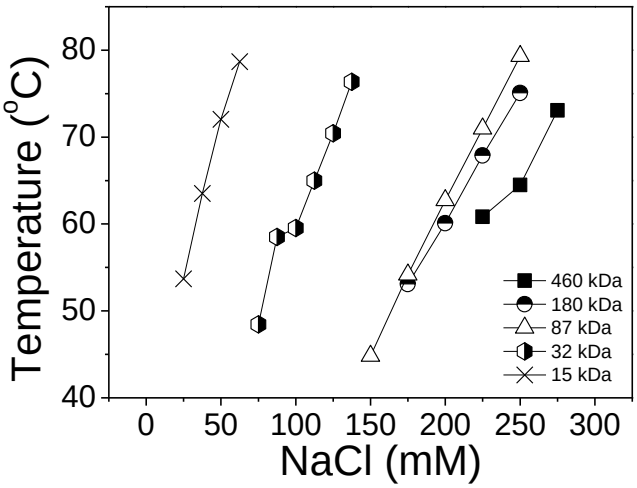

Figure 3.6 The cloud points vs. [NaCl] for PMA-x at their respective pH(I). Conditions: 2 mg/ml polymer solutions; pH 8.25 (460 kDa), pH 7.58 (180 kDa), pH 7.52 (87 kDa), pH 7.58 (32 kDa) and pH 8.30 (15 kDa).

The cloud point temperatures of PMA-x are strongly dependent on ionic strength, increasing linearly with NaCl concentration (Figure 3.6). Increased ionic strength shields the attractive electrostatic interactions, causing the polymer chains to become more hydrophilic such that higher temperatures are needed to effect phase separation. As MW

increases, the higher NaCl concentration is needed to achieve the same cloud point temperatures.

The LCST of polyampholytes is believed to involve reforming of electrostatic interaction between polyampholyte, since the heating will break the shielding electrostatic interaction between polyampholytes and small ions.[8, 51, 52] As well, increasing the temperature will also increase any hydrophobic associations analogous to those that cause the LCST phase transition of neutral polymers like PNIPAM.[63-65]

3.4.3 Covalently Crosslinked Hydrogel Microspheres

The liquid nature of coacervates is convenient for handling and the formation of a desired shape or coating, but it is often desirable to further stabilize the material by physical or chemical crosslinking. The primary amines on the APM units allow ready functionalization or crosslinking reactions. In this work, THPC, an amine-reactive crosslinker, was used to convert the coacervates into covalently crosslinked hydrogels (Scheme 3A.1). THPC has been used previously to crosslink proteins[66] and APM-containing polymers.[51]

The coacervate formed from 1 mg/ml PMA-460 (pH 8, no added NaCl) was treated with varying amounts of THPC (1.25 to 50 mol% relative to amine groups), followed by addition of 1 M HCl, which would cause any non-crosslinked coacervate to dissolve. Coacervate treated with 1.25 or 5 mol% THPC dissolved after exposure to HCl (Figure 3.7A/a and B/b), however, when 25 or 50 mol% THPC was used the hydrogels survived showing that they are crosslinked (Figure 3.7C/c and D/d). Each THPC molecule has four

reactive arms such that in theory all of the NH_2 groups could be reacted with as little as 25 mol% THPC.

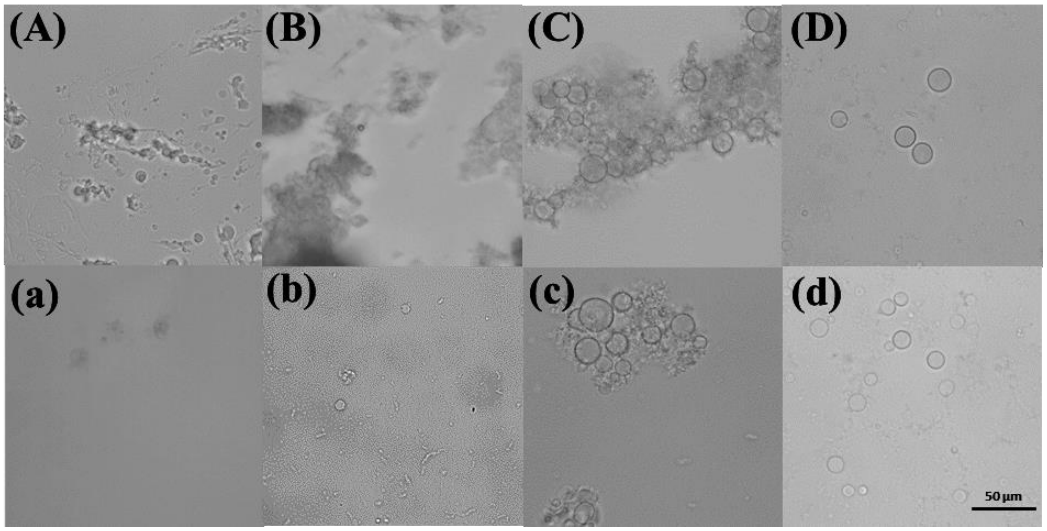

Figure 3.7 Optical microscopy images of coacervate formed from 1 mg/ml PMA-460 at pH 8.0 after addition of THPC (top row) and after subsequent addition of a drop of 1 M HCl (bottom row): (A, a) 1.25 mol% THPC; (B, b) 5 mol% THPC; (C, c) 25 mol%; (D, d) 50 mol% THPC.

While low levels of THPC (1.25 or 5 mol%) did not result in crosslinked material, they did change the nature of the coacervate. Rather than forming individual droplets (Figure 3.2a), the coacervate aggregated into viscous, partially crosslinked material that was not sufficiently crosslinked to withstand low pH. Lower MW PMA also led to less crosslinked material that was less able to withstand low pH (Figure 3A.9).

3.4.4 Dye Removal from Water

The ability of the PMA polyampholytes to act as capture/release agents was examined using several organic dyes as model compounds. The net charges of the dyes near pH 7 varied from negative (Brilliant Blue G, BB), (Trypan Blue, TB) to neutral (Rhodamine B, RB) and positive (Methylene Blue, MB). Aqueous solutions of the dyes were added to a PMA-460 coacervate suspension, which were then centrifuged to isolate the coacervate before analysis of the supernatant for residual dye content. Reference samples were made by adding the dye solution to water.

The degree of dye removal is shown visually in Figure 3.8 with images of the reference solutions as well as coacervate/dye suspensions before and after centrifugation. The coacervate/dye mixture was cloudy before centrifugation (middle vial in each set) but cleared after centrifugation. It is apparent that the coacervate has captured significant fractions of both BB (Figure 3.8a) and TB (Figure 3.8b) but not the other dyes. Spectrophotometry of the supernatants at 590 nm (Brilliant Blue), 592 nm (Trypan Blue), 665 nm (Methylene Blue), 555 nm (Rhodamine B) revealed that ≥90% of TB and BB and about 5-10% of MB and RB had been removed from solution (Figure 3.9).

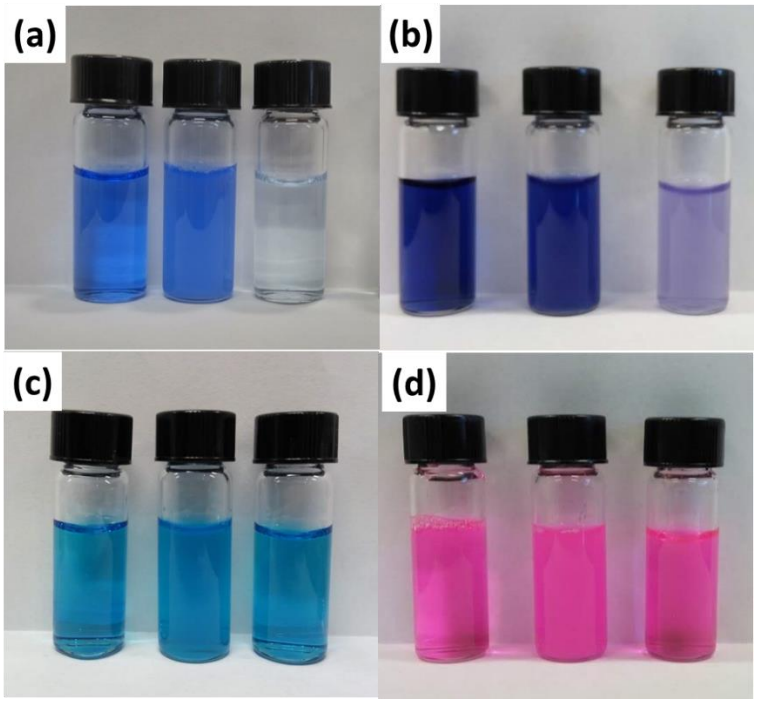

Figure 3.8 Solutions of (a) Brilliant Blue G, (b), Trypan Blue (c) Methylene Blue and (d) Rhodamine B, in water (left), and in 1 mg/mL of PMA-460 at pH 7.7 before (middle) and after (right) centrifugation.

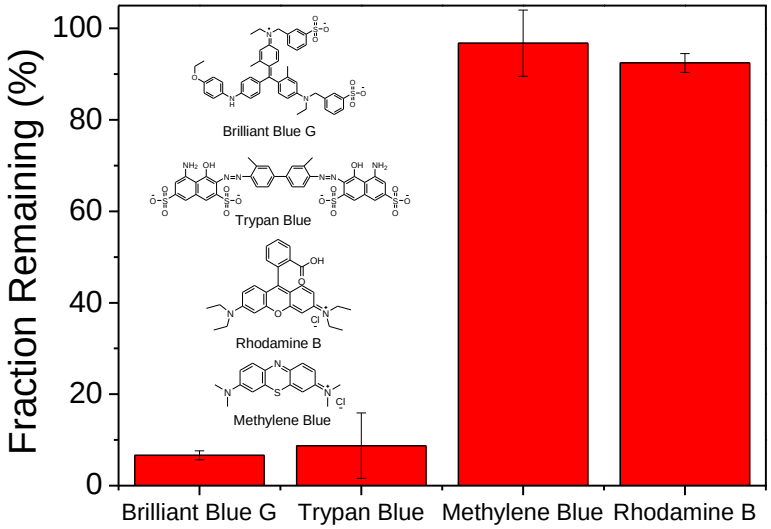

Figure 3.9 The fraction of dye remaining in supernatant after treatment with PMA-460 coacervate and centrifugation.

Dye capture may involve both electrostatic and hydrophobic interactions. PMA-460 has both anionic and cationic groups at pH(I), so it may form attractive interactions with charged groups on any of the dyes. However, only BB and TB, the two negatively charged dyes, were efficiently captured, while cationic or neutral dyes were not removed. The polyampholytes studied here have a slight excess of cationic comonomer (APM, 52 mol%) over anionic comonomer (AA, 48 mol%). Future experiment will be needed to assess if and to what extent this small charge potential imbalance may affect dye binding and selectivity.

While some microgels appear to bind dyes slowly,[67] the present coacervates showed rapid dye binding, with centrifugation carried out within seconds after mixing at neutral pH and ambient temperature. Even without centrifuging the polyampholyte coacervates will slowly settle at room temperature after a few days, as shown in Figure 3A.10.

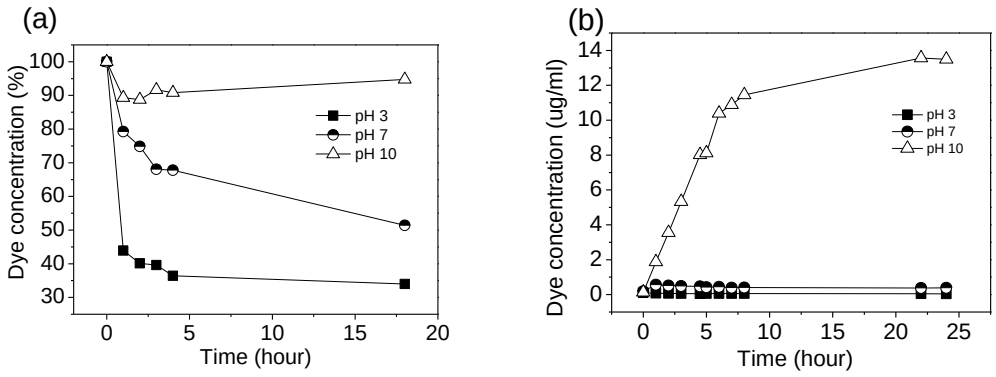

Figure 3.10 The curves of PMA hydrogels with Brilliant Blue G (a) absorption and (b) releases at pH 3, 7 and 10.

For comparison, conventional hydrogel were prepared by addition of 2 mol% *N*,*N*-methylenebisacrylamide during copolymerization, followed by mechanical break-up of the resulting covalently crosslinked gel into 5 to 10 mm size pieces and extensive washing and drying. Figure 3.10 shows the absorption and release profiles of BB with these PMA hydrogel particles at pH 3, 7 and 10. The absorption rate at pH 7 is much slower than for the liquid coacervates, in agreement with literature results for dye absorption by such relatively large microgel particles.[67] The absorption efficiency decreases with increasing pH, which suggests the absorption is strongly affected by electrostatic interaction between the PMA hydrogel and BB. The release curves support this assumption as release only happens at pH 10. The strong binding at pH 7 corresponds to the behavior seen with coacervates.

This indicates that PMA polyampholytes may be used to absorb toxic molecules such as trypan blue from cell suspensions, involving the PMA polyampholytes as either coacervates or crosslinked hydrogel, where the coacervates offer higher rates of adsorption while the hydrogel can work over broader pH ranges.

The phase transition of PMA polyampholytes is summarized in Scheme 3.1: the electrostatic interaction makes the polyampholyte chains collapse into coacervates. In coacervates, the anionic and cationic groups on polymer chains can adopt three states: they can participate in inter- and intra-chain electrostatic association, and exist as free charged

groups. The addition of NaCl will shield the electrostatic interaction, causing PMA polyampholytes to dissolve at pH(I). Heating the resulting solution interferes with shielding and can promote hydrophobic interactions, causing the coacervate to form again.

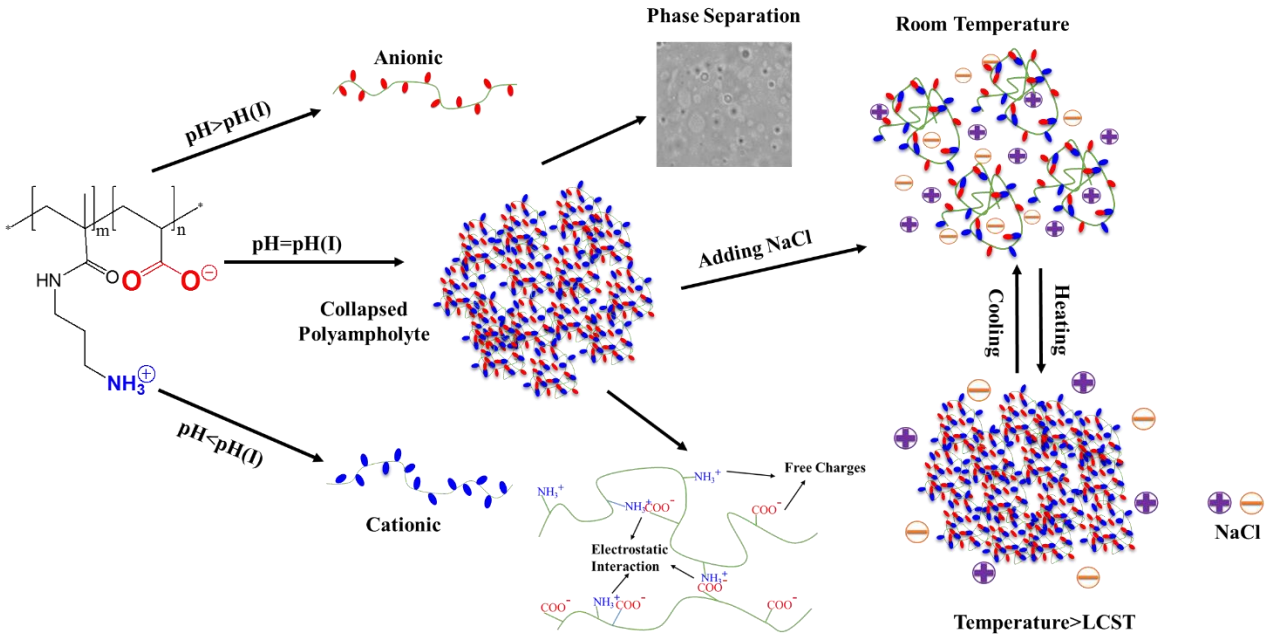

Scheme 3.1 Mapping the PMA-x phase transitions at pH(I), and the effects of NaCl and heating.

3.5 Conclusion

In this work, a series of stoichiometric APM and AA polyampholytes with different MW were prepared by controlled use of chain transfer agent. These polyampholytes were employed as the model to explore the stoichiometric polyampholytes' properties. The series of polyampholytes have pH and temperature responsive phase separation in water. For pH response, the polyampholytes have simple coacervates at the pH(I). The phase

separation efficiency is not only affected by polymer concentration, pH and ionic strength but strongly increases with MW, however, the pH(I) is MW independent. The coacervation of polyampholytes are agreement with the theoretical and experimental results of simple and complex coacervation of synthetic and natural macromolecules.

The polyampholytes also show thermally induced cloud points (LCST behaviour) when the pH is near pH(I). The cloud point temperatures are sensitive to ionic strength and polymer MW as well as to pH. Furthermore, the PMA-x polyampholyte could be crosslinked in their coacervate state, leading to stable hydrogel particles or coatings. In either coacervate or crosslinked state, these polyampholytes can selectively remove organic dyes from water. Finally, the possible mechanism of phase transition of stoichiometric APM and AA polyampholyte in aqueous solution is described. This work provides extensive properties of stoichiometric polyampholytes including the pH introduced coacervation, LCST, the further crosslinking of coacervates and potential applications. This work also reveals more interesting questions on the single polymer coacervation which will provide many useful information of the complex coacervates of synthesized or natural macromolecules and open a new method of microgel synthesis and the application of polyampholytes.

3.6 Acknowledgements

The authors would like to acknowledge funding for this research from NSERC through its Discovery Grant and CREATE programs.

3.7 References

1. Woodfield, P. A.; Zhu, Y.; Pei, Y.; Roth, P. J. *Macromolecules* **2014**, *47*, 750-762.

2. Käfer, F.; Liu, F.; Stahlschmidt, U.; Jérôme, V.; Freitag, R.; Karg, M.; Agarwal, S. *Langmuir* **2015**, *31*, 8940-8946.

3. Dai, S.; Ravi, P.; Tam, K. C. *Soft Matter* **2008**, *4*, 435-449.

4. Zhao, B.; Moore, J. S. *Langmuir* **2001**, *17*, 4758-4763.

5. Hribar, K. C.; Lee, M. H.; Lee, D.; Burdick, J. A. *ACS Nano* **2011**, *5*, 2948-2956.

6. Shao, Q.; Jiang, S. *Adv. Mater.* **2014**, *27*, 15-26.

7. Zurick, K. M.; Bernards, M. *J. Appl. Polym. Sci.* **2014**, *131*, 40069 (1-9).

8. Dubey, A.; Burke, N. A. D.; Stöver, H. D. H. *J. Polym. Sci., Part A: Polym. Chem.* **2015**, *53*, 353-365.

9. Lowe, A. B.; McCormick, C. L. *Chem. Rev.* **2002**, *102*, 4177-4189.

10. Brzozowska, A. M.; Parra-Velandia, F. J.; Quintana, R.; Zhu, X.; Lee, S. S. C.; Lim, C.; Jańczewski, D.; Teo, S. L. M.; Vancso, J. G. *Langmuir* **2014**, *30*, 9165-9175.

11. Liu, P.; Emmons, E.; Song, J. A. *J. Mater. Chem. B* **2014**, *2*, 7524-7533.

12.Xia, Y.; Gao, M.; Chen, Y.; Jia, X.; Liang, D. *Macromol. Chem. Phys.* **2011**, *212*, 2268-2274.

13. Das, M.; Kumacheva, E. *Colloid Polym. Sci.* **2006**, *284*, 1073-1084.

14. Ciferri, A.; Kudaibergenov, S. *Macromol. Rapid Commun.* **2007**, *28*, 1953-1968.

15. Bhattacharjee, A.; Kundu, P.; Dua, A. *Macromol. Theory Simul.* **2011**, *20*, 75-84.

16. Fevola, M. J.; Bridges, J. K.; Kellum, M. G.; Hester, R. D.; Mccormick, C. L. *J. Polym. Sci., Part A: Polym. Chem.* **2004**, *42*, 3236-3251.

17. Ogawa, K.; Nakayama, A.; Kokufuta, E. *Langmuir* **2003**, *19*, 3178-3184.

18. Sun, T.; Kurokawa, T.; Kuroda, S.; Ihsan, A. B.; Akasaki, T.; Sato, K.; Haque, Md. A.; Nakajima, T.; Gong, J. *Nat. Mater.* **2013**, *12*, 932-937.

19. Xiong, Z.; Peng, B.; Han, X.; Peng, C.; Liu, H.; Hu, Y. *J. Colloid Interface Sci.* **2011**, *356*, 557-565.

20. Ulrich, S.; Seijo, M.; Stoll, S. *J. Phys. Chem. B* **2007**, *111*, 8459-8467.

21. Tanaka, M.; Tanaka, T. *Phys. Rev. E* **2000**, *62*, 3803-3816.

22. Mahltig, B.; Gohy, J.; Jérôme, R.; Stamm, M. *J. Polym. Sci., Part B: Polym. Phys.* **2001**, *39*, 709-718.

23. Kudaibergenov, S. E.; Didukh, A. G.; Ibraeva, Z. E.; Bimendina, L. A.; Rullens, F.; Devillers, M.;

Laschewsky, A. *J. Appl Polym. Sci.* **2005**, *98*, 2101-2108.

24. Song, J.; He, A.; Jin, Y.; Cheng, Q. *RSC. Adv.* **2013**, *3*, 24586-24592.

25. Yu, B.; Zheng, J.; Chang, Y.; Sin, M.; Chang, C.; Higuchi, A.; Sun, Y. *Langmuir* **2014**, *30*, 7502-7512.

26. Schroeder, M. E.; Zurick, K. M.; McGrath, D. E.; Bernards, M. T. *Biomacromolecules* **2013**, *14*, 3112-3122.

27. Huang, Y.; Tang, Z.; Zhang, X.; Yu, H.; Sun, H.; Pang, X.; Chen, X. *Biomacromolecules* **2013**, *14*, 2023-2032.

28. Rajan, R.; Matsumura, K. *J. Mater. Chem. B* **2015**, *3*, 5683-5689.

29. Liu, E. J.; Sinclair, A.; Keefe, A. J.; Nannenga, B. L.; Coyle, B. L.; Baneyx, F.; Jiang, S. *Biomacromolecules* **2015**, *16*, 3357-3361.

30. Wang, Q.; Schlenoff, J. B. *Macromolecules* **2014**, *47*, 3108-3116.

31. Perry, S. L.; Sing, C. E. *Macromolecules* **2015**, *48*, 5040-5053.

32. Xu, Y.; Mazzawi, M.; Chen, K.; Sun, L.; Dubin, P. L. *Biomacromolecules* **2011**, *12*, 1512-1522.

33. Martin, N.; Li, M.; Mann, S. *Langmuir* **2016**, *32*, 5881-5889.

34. Tan, Y.; Hoon, S.; Guerette, P. A.; Wei, W.; Ghadban, A.; Hao, C.; Miserez, A.; Waite, J. H. *Nat. Chem. Biol.* **2015**, *11*, 488-495.

35. Stewart, R. J.; Weaver, J. C.; Morse, D. E.; Waite, J. H. *J. Exp. Biol.* **2004**, *207*, 4727-4734.

36. Wei, W.; Tan, Y.; Martinez Rodriguez, N. R.; Yu, J.; Israelachvili, J. N.; Waite, J. H. *Acta Biomater.* **2014**, *10*, 1663-1670.

37. Hwang, D. S.; Zeng, H.; Srivastava, A.; Krogstad, D. V.; Tirrell, M.; Israelachvili, J. N.; Waite, J. H. *Soft Matter* **2010**, *6*, 3232-3236.

38. Overbeek, J. T. G.; Voorn, M. J. *J. Cell. Physiol.* **1957**, *49*, 7-26.

39. Yin, X.; Stöver, H. D. H. *Macromolecules* **2003**, *36*, 8773-8779.

40. Vrhovski, B.; Jensen, S.; Weiss, A.S. *Eur. J. Biochem*. **1997**, *250*, 92-98.

41. Cai, H.; Gabryelczyk, B.; Manimekalai, M.S.S.; Gruber, G.; Salentinig, S.; Miserez, A. *Soft Matter* **2017**, *13*, 7740-7752.

42. Wei, W.; Tan, Y.; Martinez Rodriguez, N. R.; Yu, J.; Israelachvili, J. N.; Waite, J. H. *Acta Biomater*. **2014**,

10, 1663-1670.

43. Nott, T. J.; Petsalaki, E.; Farber, P.; Jervis, D.; Fussner, E.; Plochowietz, A.; Craggs, T. D.; Bazett-Jones, D.P.; Pawson, T.; Forman-Kay, J. D.; Baldwin, A. J. *Mol. Cell.*, **2015**, *57*, 936-947.

44. Miller, D. R.; Das, S.; Huang, K.-Y.; Han, S.; Israelachvili, J. N; Waite, J. H. *ACS Biomater. Sci. Eng*. **2015**, *1*, 1121-1128.

45. Zhao, Q. Lee, D. W.; Ahn, B. K.; Seo, S.; Kaufman, Y.; Israelachvili, J. N.; Waite, J. H. *Nat. Mater*. **2016**, *15*, 407-412.

46. van der Gucht, J., Spruijt, E., Lemmers, M.; Stuart, M. A. C. *J. Colloid Interface Sci.* **2011**, *361*, 407-422.

47. Kaibara, K.; Okazaki, T.; Bohidar, H. B.; and Dubin, P. L. *Biomacromolecules* **2000**, *1*, 100-107.

48. Pathaka, J.; Rawat, K.; Bohidara, H. B. *Int. J. Biol. Macromol.* **2014**, *63*, 29-37.

49. Muthuselvi, L.; Dhathathreyan, A. *Colloids Surf. B Biointerfaces* **2006**, *51*, 39-43.

50. Seo, S.; Das, S.; Zalicki, P. J.; Mirshafian, R.; Eisenbach, C. D.; Israelachvili, J. N.; Waite, J. H.; Ahn, B. K. *J. Am. Chem. Soc*. **2015**, *137*, 9214-9217.

51. Abdilla, A.; Shi, S.; Burke, N. A. D.; Stöver, H. D. H. *J. Polym. Sci., Part A: Polym. Chem.* **2016**, *54*, 2109-2118.

52. Zhao, J.; Burke, N. A. D.; Stöver, H. D. H. *RSC Adv.* **2016**, *6*, 41522-41531.

53. Patrickios, C. S. *J. Colloid Interface Sci.* **1995**, *175*, 256-260.

54. Gupta, A; Bohidar, H. B. *Phys. Rev. E* **2005**, *72*, 011507.

55. Higgs, P. G.; Joanny, J. F. *J. Chem. Phys.* **1991**, *94*, 1543-1554.

56. Dobrynin, A.; Rubinstein, M. *J. Phys. II* **1995**, *5*, 677-695.

57. Pawar, N.; Bohidar, H. B. *Phys. Rev*. *E* **2010**, *82*, 036107.

58. Masuda, S.; Minagawa, K.; Tsuda, M.; Tanaka, M. *Eur. Polym. J.* **2001**, *37*, 705-710.

59. Burke, S. E.; Barrett, C. J. *Langmuir* **2003**, *19,* 3297-3303.

60. Zhang, Q.; Hoogenboom, R. *Chem. Commun*. **2015**, *51*, 70-73.

61. Shih, Y.; Chang, Y. *Langmuir* **2010**, *26*, 17286-17294.

62. Maji, T.; Banerjee, S.; Biswas, Y.; Mandal, T. K. *Macromolecules* **2015**, 48, 4957-4966.

63. Xia, Y.; Yin, X.; Burke, N. A. D.; Stöver, H. D. H. *Macromolecules* **2005**, *38*, 5937-5943.

64. Zhao, J.; Wang, H. *J. Polym. Sci., Part B: Polym. Phys.* **2016**, *54*, 1869-1877.

65. Wang, X.; Qiu, X.; Wu, C. *Macromolecules* **1998**, *31*, 2972-2976.

66. Chung, C.; Lampe, K. J.; Heilshorn, S. C. *Biomacromolecules* **2012**, *13*, 3912-3916.

67. Parasuraman, D.; Serpe, M. J. *ACS Appl. Mater. Interfaces* **2011**, *3*, 4714-4721.

3.8 Appendix

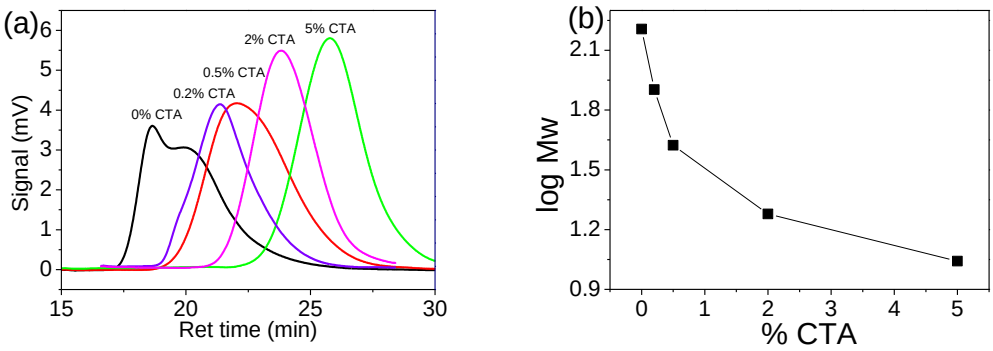

Figure 3A.1 (a) the GPC curves (b) and Log Mw of PMA-x made with different amounts of chain transfer agent.

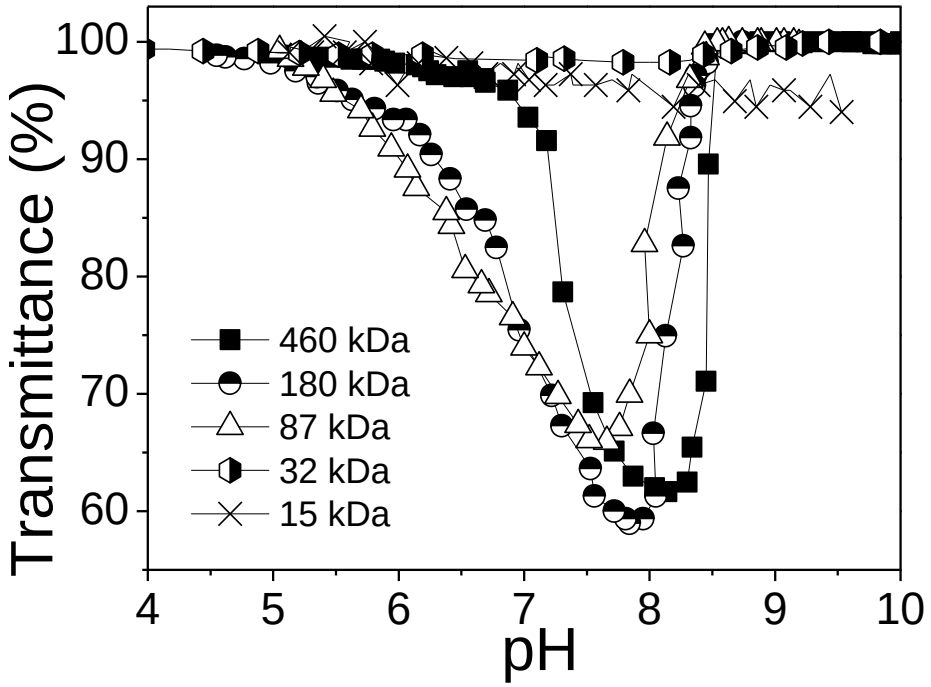

Figure 3A.2 Turbidity titration curves for PMA-x of various MWs. Conditions: 0.1 mg/mL polymer, no added salt, titrant: 0.01-1 M HCl.

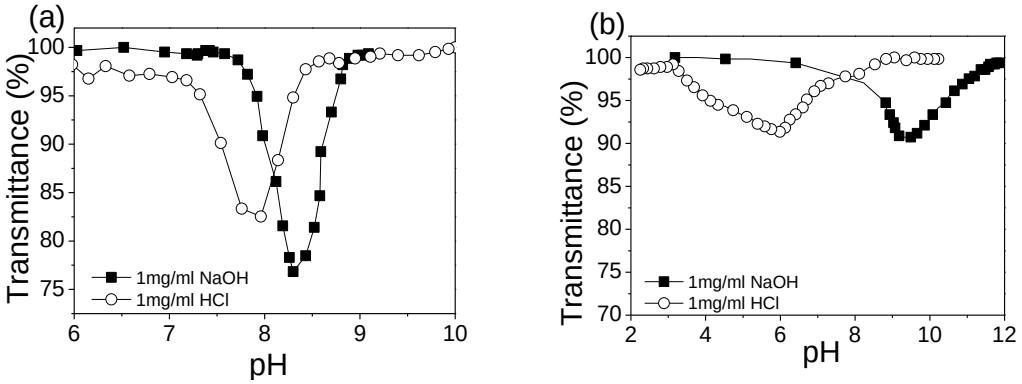

Figure 3A.3 Turbidity titrations of (a) PMA-32 and (b) PMA-15 at 1 mg/mL polymer concentration. Conditions: no added salt, titrants: 0.01-1 M HCl and NaOH.

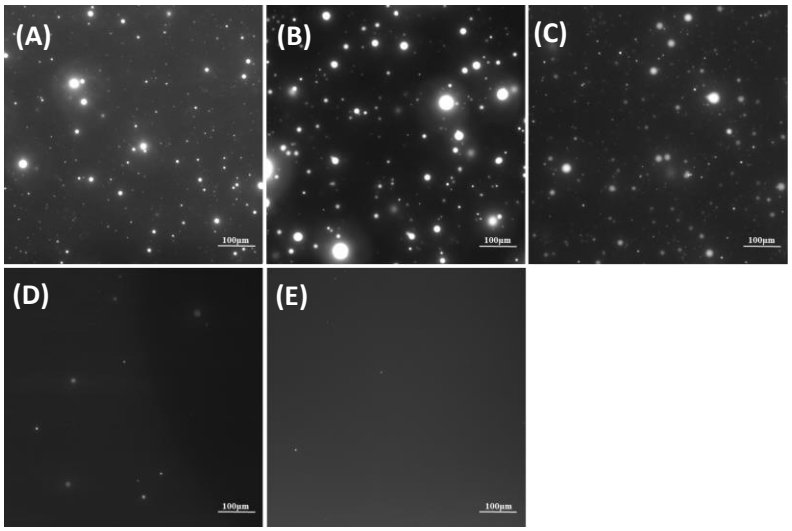

Figure 3A.4 The fluorescence microscopy images of phase separated material from 1 mg/ml PMA at pH(I) (pH 8.3-8.4): (A) 460 kDa, (B) 180 kDa; (C) 87 kDa, (D) 32 kDa and (E) 15 kDa.

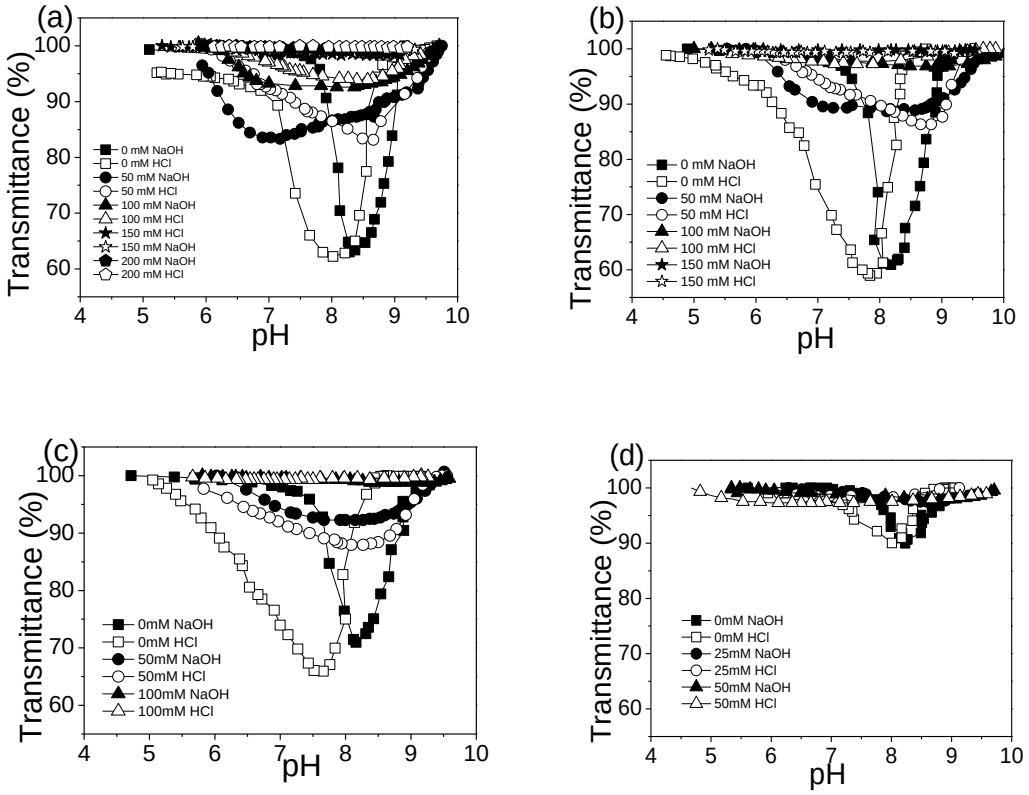

Figure 3A.5 Turbidity titrations curves of PMA-x as a function of NaCl concentration. (a) PMA-460; (b) PMA-180; (c) PMA-87 and (d) PMA-32. Conditions: 0.1 mg/mL of PMA-x, titrant: 0.01-1 M HCl and NaOH.

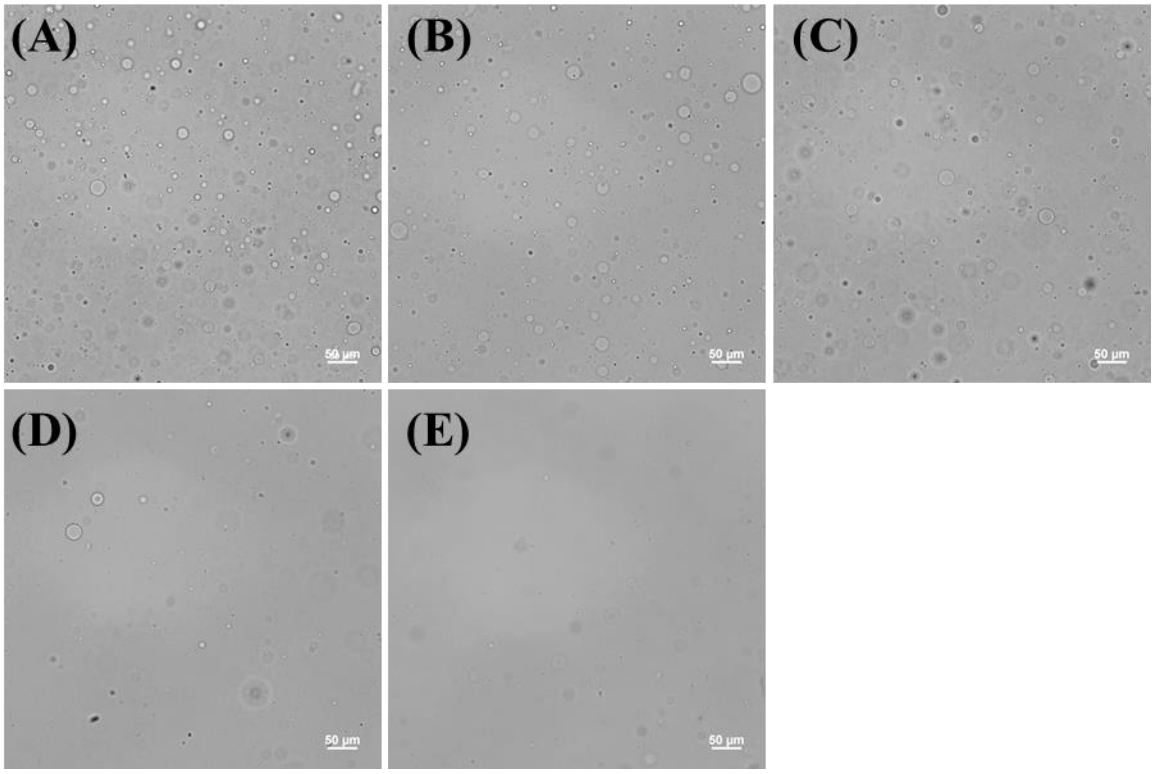

Figure 3A.6 The optical micrograph of 1 mg/ml PMA-460 at pH 7.5 in the presence of salt: (A) 0 mM; (B) 50 mM; (C) 100 mM; (D) 150 mM and (E) 200 mM.

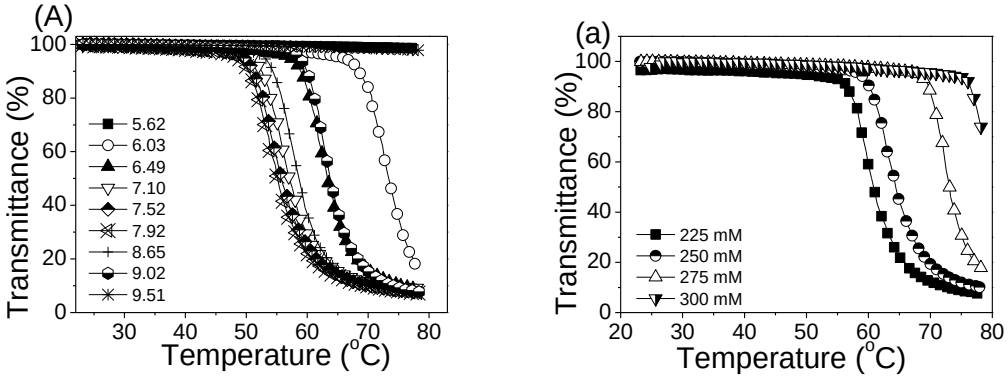

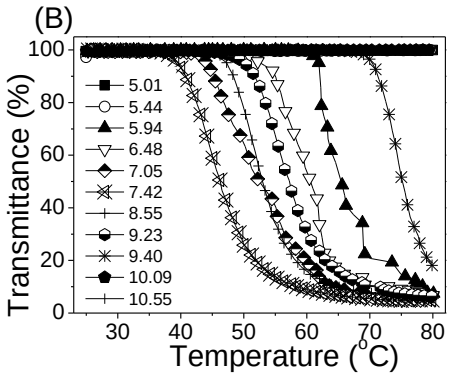
(B)
Transmittance (%)
Temperature (°C)
5.01
5.44
5.94
6.48
7.05
7.42
8.55
9.23
9.40
10.09
10.55

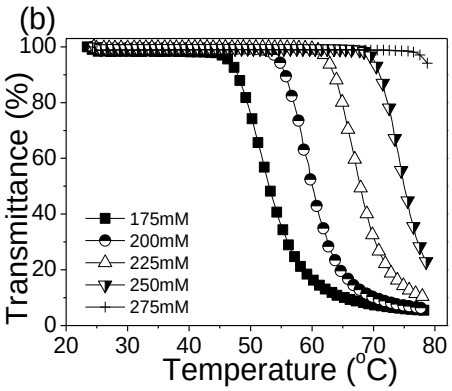
(b)
Transmittance (%)
Temperature (°C)
175mM
200mM
225mM
250mM
275mM

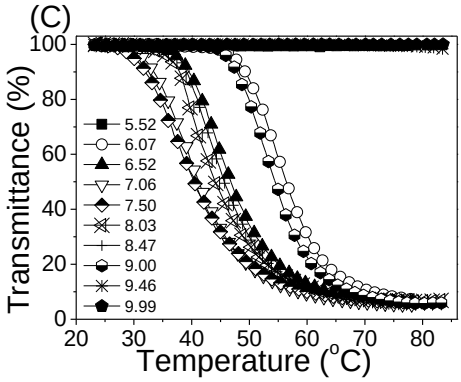
(C)
Transmittance (%)
Temperature (°C)
5.52
6.07
6.52
7.06
7.50
8.03
8.47
9.00
9.46
9.99

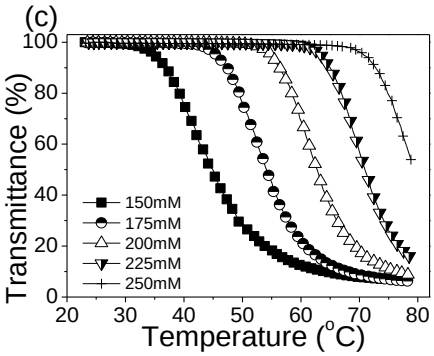
(c)
Transmittance (%)
Temperature (°C)
150mM
175mM
200mM
225mM
250mM

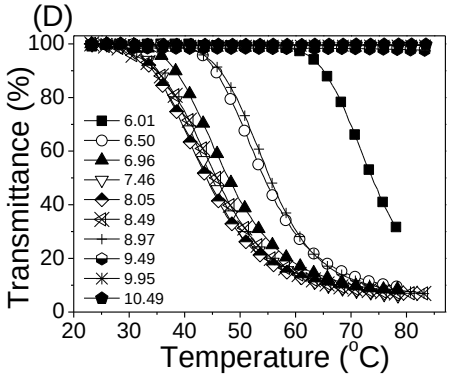
(D)
Transmittance (%)
Temperature (°C)
6.01
6.50
6.96
7.46
8.05
8.49
8.97
9.49
9.95
10.49

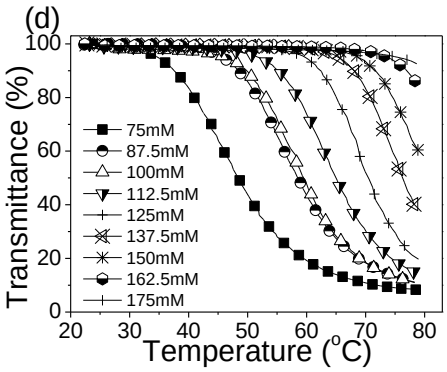
(d)
Transmittance (%)
Temperature (°C)
75mM
87.5mM
100mM
112.5mM
125mM
137.5mM
150mM
162.5mM
175mM

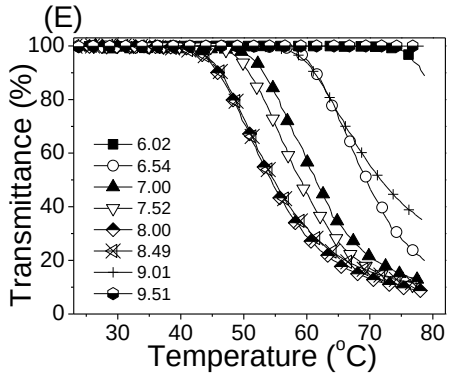
(E)
Transmittance (%)
Temperature (°C)
6.02
6.54
7.00
7.52
8.00
8.49
9.01
9.51

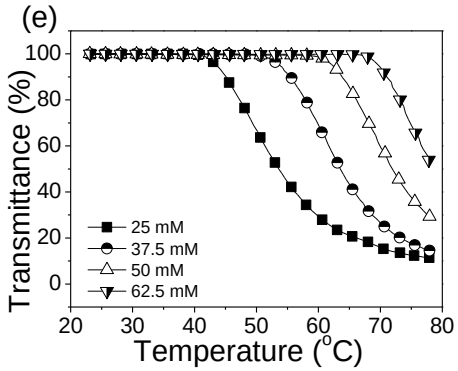
(e)
Transmittance (%)
Temperature (°C)
25 mM
37.5 mM
50 mM
62.5 mM

Figure 3A.7 Transmittance vs. temperature for 2 mg/ml solutions of PMA as a function of MW, pH (A - E) and ionic strength (a - e): (A) 460 kDa, 225 mM NaCl; (B) 180 kDa, 175 mM NaCl; (C) 87 kDa, 150 mM NaCl; (D) 32 kDa, 50 mM NaCl; and (E) 15 kDa, 25 mM NaCl and (a) 460 kDa, pH 8.25; (b) 180 kDa, pH 7.58; (c) 87 kDa, pH 7.52; (d) 32 kDa, pH 7.58 and (e) 15 kDa, pH 8.30.

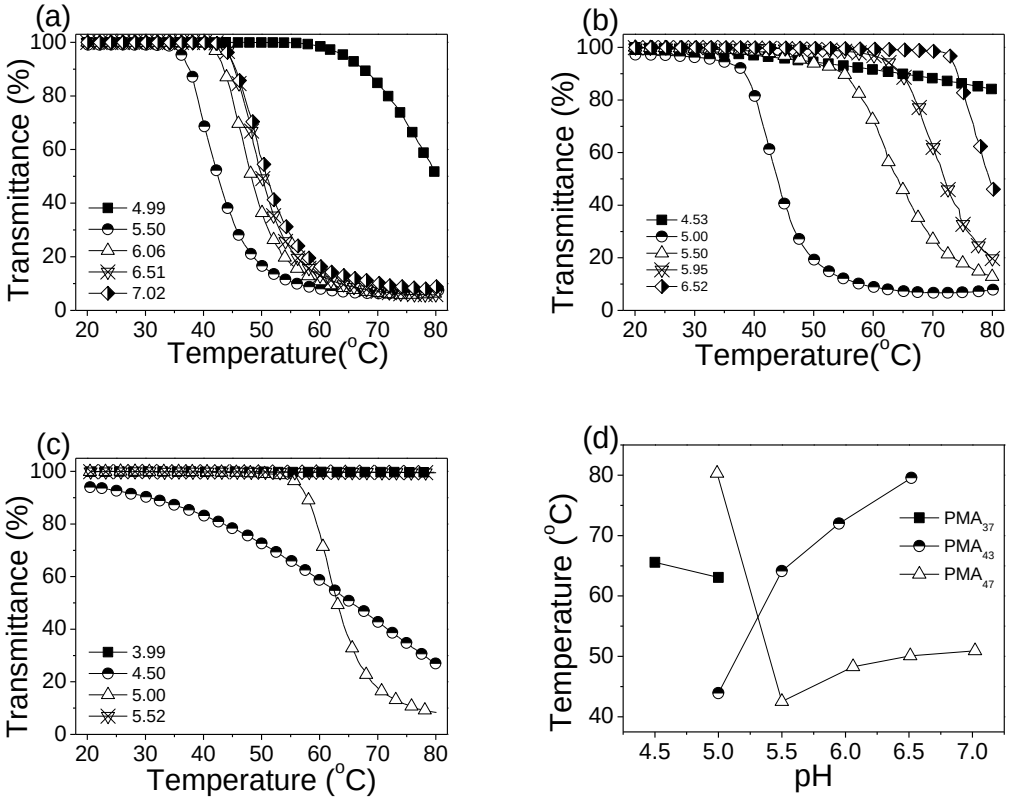

Figure 3A.8 Transmittance vs. temperature for 2 mg/ml solutions of PMAx polyampholytes: (a) PMA47, 250 mM NaCl; (b), PMA43, 350 mM NaCl; and (c) PMA37, 600 mM NaCl. (d) Cloud point vs. pH for PMA37 (600 mM NaCl), PMA43 (350 mM NaCl) and PMA47 (250 mM NaCl). The subscript means the %APM in copolymer.

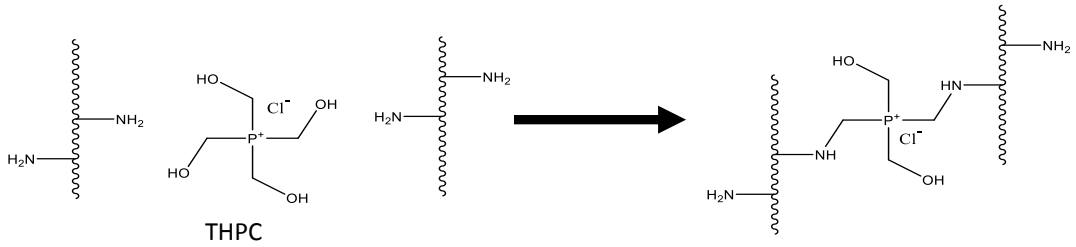

Scheme 3A.1 The crosslinking of PMA with THPC.

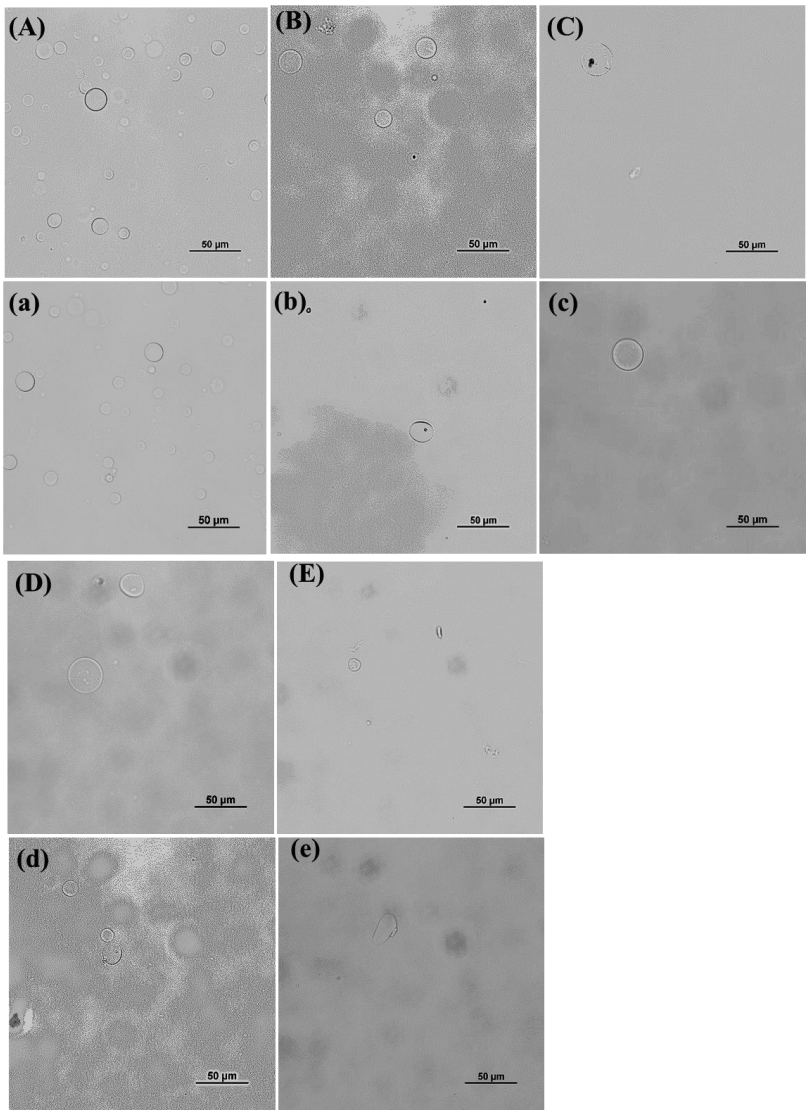

Figure 3A.9. The optical microscopy images of 1 mg/ml PMA at pH(I) 50 mol% THPC after addition of THPC (top row) and after subsequent addition of a drop of 1 M HCl (bottom row) (A, a) 460 kDa at pH 8.30 (B, b) 180 kDa at pH 8.30 and (C, c) 87 kDa at pH 8.31; (D, d) 32 kDa at pH 8.34 and (E, e) 15 kDa at pH 8.31.

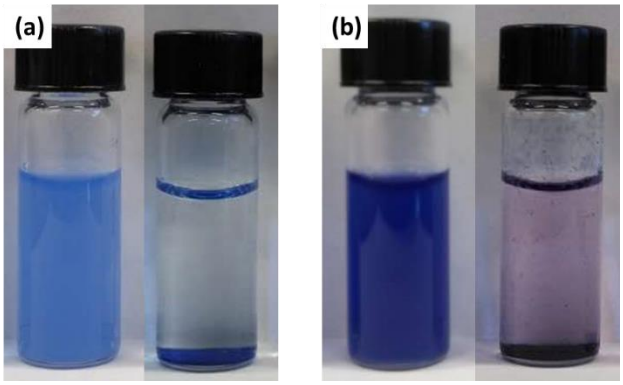

Figure 3A.10 The solutions of (a) Brilliant Blue G and (b) Trypan Blue with 1 mg/mL of PMA-460 at pH 7.7, after mixing (left), and after being stored at room temperature for 1 week (right).

Chapter 4: The Influence of Monomer Side Chain Hydrophobicity and Ionic Groups on the Phase Separation of Stoichiometric Polyampholytes

Jing Zhao, Nicholas A. D. Burke, Harald D.H. Stöver

To be submitted.

Contributions: I designed all experiments, performed all measurements and synthesized most of polymers. Dr. Burke synthesized three of the polymers: PMAs49, PMcAs54 and PAPM. I also wrote the manuscript, with editorial help and feedback from Dr. Stöver.

4.1 Abstract

This work investigates the effect of hydrophobicity and ion type on the thermal phase transitions of polyampholytes in aqueous solutions. Nine stoichiometric polyampholytes were prepared by radical binary copolymerizations of anionic and cationic monomers with different degrees of hydrophobicity. The reactivity ratios of different monomer pairs were measured by ^{1}H-NMR and stoichiometric (50±5% cationic groups) polyampholytes were prepared with little compositional drift. Depending on comonomer choice, liquid to liquid (coacervate) and liquid to solid (hydrogel) and no macroscopic phase separation (clear solution) were observed upon heating the polyampholyte solutions at their pH(I). The pH response, anti-polyelectrolyte effect, and temperature responsive solubilities were measured by turbidity titration, and the morphology of phase separated polymer was assessed by optical microscopy. The results show that both electrostatic interaction and

polymer hydrophobicity affect the polyampholyte phase separations. The polyampholytes having either strong electrostatic interaction, or weak electrostatic interaction together with higher hydrophobicity, can have visible, macroscopic, phase separation from aqueous solutions, including both liquid-liquid and liquid-solid transitions. Polyampholyte behavior was compared with the corresponding polyelectrolyte complexes formed by cationic and anionic homopolymers. Finally, polyampholyte binding of organic dyes from aqueous solution were used to study the effects of electrostatic and hydrophobic interaction on dye binding.

4.2 Introduction

Polyampholytes are copolymers with both cationic and anionic charges located on different monomer units. Based on the type of ionic groups, polyampholytes are separated into four groups with different combinations of strong and weak acidic and basic groups.[1-4] The polyampholytes with weak acids and bases have the pH(I), the pH at which the net charge of polyampholytes is zero. Other polyampholytes with one weak acid/base or both strong acids and bases do not have pH(I), but can have zero net charge at the stoichiometric charge ratio. At zero net charge, the electrostatic interactions cause polyampholyte chains to shrink or collapse, as the result, polyampholyte solutions at pH(I) will show the change of viscosity , lower transparency or precipitation. However, increasing the solution ionic strength will shield the electrostatic interactions between polyampholytes chains and increase their solubility, a phenomenon called the anti-polyelectrolyte effect.[5,6] With these

properties, polyampholytes have many industrial[7-10] and biomedical applications,[11-16] including being used to mimic proteins.[17]

Theoretical research successfully predicted many of the properties of polyampholytes. For charge symmetric polyampholytes with zero net charge, the polymer chain will collapse, but redissolve with the addition of salts.[18-21] Low charge density non-neutral polyampholytes are calculated to behave similar to neutral polyampholytes, however, high charge asymmetry polyampholytes should behave like polyelectrolytes.[20,21] The effect of salt can go in two directions, with the addition of small amounts of salt leading to a decrease in polyampholyte solubility by screening the electrostatic repulsion due to their net charge; but subsequent addition of more salt will increase the polyampholyte solubility by disrupting the electrostatic attraction. Simulation was used to study the effect of primary structures[22,23] such as block, alternate, random copolymers, and showed that these structures play an important role in the polyampholyte properties.

The theoretical results have been confirmed by experimental results. In the early studies McCormick, Candau and others prepared random polyampholytes with pH nonresponsive ionic monomers, and found salt concentration and pH to affect viscosity and turbidity, with neutral polyampholyte showing mainly anti-electrolytes properties, and non-neutral polyampholytes behaving like polyelectrolytes.[24-28] The pH(I) of polyampholytes with pH responsiveness depends on the polymer composition, and the anti-polyelectrolyte behavior appears at pH(I).[29-31] Recently, many polyampholyte block copolymers were prepared with interesting properties based on their amphiphilic nature.[32] The block copolymers can form complexes at the pH around pH(I), and micelles at higher or lower pH.[33,34]

Both theoretical and experimental results show that polyampholytes have anti-polyelectrolyte properties and pH(I), and that the charge ratios and chain primary structures strongly affect the properties. However, there has not been much discussion about the effect of ionic group type and monomer hydrophobicity on polyampholyte properties, aside from brief comments that increasing the monomer hydrophobicity will increase the polyampholyte polymer-polymer interaction.[6,35] In comparison, polybetaine and polyelectrolyte complex films have been much more thoroughly studied. Jiang etc. found the charge type and the number of carbon atoms between charged groups to have significant effects on polybetaine properties,[36,37] for example where polysulfobetaines have temperature responsiveness but the corresponding polycarboxybetaines do not. Increasing the hydrophobicity of polybetaines will increase the UCST.[38] For the polyelectrolyte complexes, it was found that strong electrostatic interactions produce strong polymer-polymer interactions,[39-41] but the electrostatic interaction is not the only factor, as the hydrophobicity also plays an important role in polyelectrolytes interactions.[32,42-44]

Hence it is reasonable to assume that polyampholyte properties will be affected not only by electrostatic interaction but also by hydrophobic effects and ion type. In our previous work, we found the APM/AA (acrylic acid, *N*-(3-aminopropyl)methacrylamide hydrochloride) polyampholytes with different composition can have no phase separation, liquid-liquid or liquid-solid phase separation at pH(I).[45] The electrostatic interaction produces liquid coacervates for the stoichiometric polyampholytes, however, the extra amine groups or hydrogen bonding on non-stoichiometric polyampholytes can prevent phase separation or cause liquid-solid hydrogel. When focused on the stoichiometric polyampholytes, polyampholytes with MAA/APM[30] have more methyl groups on the

backbone than AA/APM polyampholytes, and as a result the minimum [NaCl] needed to dissolve MAA/APM polyampholyte at pH(I) is twice that needed for the corresponding AA/APM polyampholyte, reflecting the stronger hydrophobic interaction. With increasing the hydrophilicity by incorporating HEA (2-hydroxyethyl acrylate) in MAA-APM polyampholyte, the [NaCl] needed for dissolution at pH(I) drops.[31] Hence, other factors like hydrogen bonding and hydrophobicity combine with electrostatic interaction to control polyampholyte solution properties.

The other similar example includes polyampholytes made by different monomers with quaternary ammonium cations and AMPS (sodium 2-(acrylamido)-2-methylpropanesulfonate).[27,28] AMPS copolymers with [2-(acrylamido)-2-methylpropyl] trimethylammonium chloride are water soluble and show viscosity changes, however, AMPS copolymer with [2-(methacryloyloxy)ethyl]trimethylammonium chloride shows phase separation with [NaCl]. Further increasing the hydrophobicity by introducing aromatic rings, the polyampholyte made by NaSS (sodium styrene sulfonate) and MAPTAc ([3-(methacryloylamino) propyl] trimethyl ammonium chloride) form a strong physical hydrogel in water without any crosslinker. When MAPTAc is replaced with more hydrophilic monomers MAETAc (2-(methacryloyloxy)ethyltrimethylammonium) or TMA (2-(acryloyloxy)ethyl)trimethylammonium chloride), the Young's modulus drops by factors of 6 and 12, respectively.[46,47] These five polyampholytes all have quaternary ammonium cations and sulfonate groups, but their behavior changes from soluble polymer, liquid coacervate, to physical hydrogel, so again the electrostatic interaction is not the single factor affecting polyampholyte properties.

This work aims to study the effect of the side chain electrostatic interaction and hydrophobicity on the macroscopic phase separation of stoichiometric polyampholytes. In particular, we are searching for the factors responsible for the formation of soluble polyampholytes, polyampholyte coacervates and polyampholytes hydrogel at pH(I). The soluble polyampholytes at pH(I) have great potential for preparing non-fouling[11,12] and blood compatible materials,[15,16] and understanding polyampholyte coacervates and hydrogels can provide a lot of information on natural macromolecule interactions[48-50] and also be helpful to prepare new marine biofouling,[51] drug delivery,[13] emulsion stabilization[52] materials and physically crosslinked high mechanical strength hydrogels.[46,47]

Nine binary polyampholytes were prepared with close to neutral ratios of selected monomers (Scheme 4.1) selected to contain different side chains and ionic groups on similar backbones. Turbidimetric titration and optical microscopy were employed to identify the phase separation of these polyampholytes as function of pH, [NaCl], and temperature,[48-52] and UV-vis spectroscopy was used to study their ability to bind organic dyes from water.

4.3 Experimental Section

4.3.1 Materials:

Acrylic acid (AA, 99%) was obtained from Sigma-Aldrich, and distilled before use. *N*,*N*-[(Dimethylamino)propyl]acrylamide (DMAPAM, 99%) from Sigma-Aldrich was neutralized by concentrated HCl with stirring in an ice bath, with the concentration measured by ^{1}H-NMR. *N*-(3-aminopropyl)methacrylamide hydrochloride (APM HCl,

99%), [3-(methacryloylamino) propyl]trimethyl ammonium chloride solution (MAPTAc 50 wt % in H_2O), 2-acrylamido-2-methyl-1-propanesulfonic acid (APMS, 99%), sodium styrene sulfonate (NaSS, >90%, the real ratio was measured by ^{1}H-NMR), ethylene carbonate (98%), 2,2'-azobis(2-methylpropionamidine)dihydrochloride (Vazo-56), rhodamine B, brilliant blue G, methylene blue, acriflavine from Sigma-Aldrich were used as received. Trypan blue solution (0.4%, Thermo Fisher) was used as received. Poly(acrylic acid) 50 kDa (25% wt in water) from Polysciences, Inc., poly(sodium 4-stylenesulfonate) 70 kDa (30% wt in water) from Aldrich were precipitated in acetone and freeze dried before use. Deuterium oxide (D_2O) was purchased from Cambridge Isotope Laboratories (Andover, MA). Sodium hydroxide and hydrochloric acid solutions (0.10 and 1.0 M) were obtained from LabChem Inc.

4.3.2 Synthesis of Polyampholytes

Solution copolymerization was carried out at 55 °C on a set of horizontal steel rollers fitted with an enclosure and a thermostatted heater pad, with 10% (w/v) total monomer loading, 1 mol% initiator (Vazo-56, relative to total monomer). The feed ratios were varied based on the different reactivity ratios of different monomer pairs. The progress of the copolymerizations was monitored by removing small aliquots, diluting by D_2O, and determining conversion by ^{1}H-NMR on a Bruker Avance 600, and polymerizations were stopped at 40-70% conversion. After polymerization, acetone was added to the cooled mixture (1:4.5 v:v) to precipitate the polymer, then the mixture was centrifuged at 4000 rpm for 5 min, and the supernatant was removed. Then the polymer was re-dissolved in

water, the precipitation repeated a total of 3 times. Finally, the purified polymers were isolated by freeze-drying from water. After freeze drying, 10 mg of purified polymer was dissolved in 1 mL of D_2O, and the ^{1}H-NMR spectrum obtained using a Bruker AV 600 spectrometer to measure the polymer composition. The detailed process is shown in the appendix.

Nomenclature for monomers are M = APM, D = DMAPMA, Mc = MAPTAc, A = AA, As = AMPS and N = NaSS, consequently, polymers are named as PMA50, PDA49, PMcA52, PMAs49, PDAs50, PMcAs54, PMN45, PDN50, PMcN48, where the number represents the %mol of cationic comonomer in the copolymer.

4.3.3 GPC Analysis

The molecular weights (MWs) of polymers were measured using an aqueous gel permeation chromatography (GPC) system consisting of a Waters 515 HPLC pump, Waters 717plus auto-sampler, three columns (Waters Ultrahydrogel-120, -250, -500; 30 cm, 7.8 mm dia.; 6 μm particles; 0-3, 0-50, 2-300 kDa MW ranges), and a Waters 2414 refractive index detector calibrated with narrow disperse poly(ethylene glycol) standards (Waters). The mobile phase was either a 1 M sodium acetate/acetic acid buffer adjusted to pH 4.7 or 0.025 M CHES buffer adjusted to pH 10 and containing 0.5 M $NaNO_3$.

4.3.4 Turbidimetric Titrations

Turbidimetric titrations were carried out at 22 °C on solutions with 1 mg/mL polymer solution. The PMcN48 formed a gel in water at room temperature, in order to do the titration, the PMcN48 was stirred at 90 ^{o}C for 1 h, to form a cloudy solution. A 25 mL aliquot of the polymer solution was adjusted to various pH to ensure the polymer was fully dissolved. Each polymer solution was then titrated manually by adding 10 µL aliquots of 0.01 to 5 M NaOH or 0.01 to 6 M HCl with a micropipette, while simultaneously monitoring the pH and the turbidity of the solution, using a VWR SympHony pH probe and a Mitsubishi GT-LD photometric detector equipped with an optical fiber turbidity probe (λ >620 nm). The concentration of NaOH was selected to give suitable changes in pH per injection.

To determine the effect of ionic strength on polyampholytes at zero net charge, the pH of the polymer solutions were adjusted to pH(I) (shown in Table 4A.2) or pH 7, then the titrations were measured by adding 0.3 g/ml NaCl solution (5.17 M) (with 1 mg/ml corresponding polyampholyte to avoid diluting the solution). Exceptionally, PMN45, PDN50 and PMcN48 and PAA/PAPM were titrated by 0.3g/ml NaCl to 50 mM, and then 74 mg solid NaCl was added to increase the NaCl concentration in steps of 50 mM per addition.

4.3.5 Optical Microscopy

Microscopy images of the polyampholytes were measured with Nikon ECLIPSE LV100ND optical microscope fitted with an ANDOR ZYLA-5.5-CL10 digital camera and

NIS-Elements AR 4.30.02 software. The pH values of the polyampholyte solutions were adjusted to pH(I) or pH 7, different polymer concentrations were used to give clear results. Different NaCl concentration were used for PMN45 and different pH were used for PDN50.

4.3.6 Temperature Responsive Properties of Polyampholytes Solutions

Cloud point measurements were made using a Varian Cary 3E spectrophotometer fitted with a temperature controlled 12-sample cell holder. The rates of heating and cooling were both 1 °C/min and the transmittance at 500 nm was measured at 0.5 °C intervals. Polyampholytes showing phase separation were measured at pH(I) or pH 7 without added NaCl to test for UCST. To the cloudy solutions was added enough NaCl to make clear solutions, and then the clear solutions were heated to test for LCST. Polyampholytes without phase separation were only measured at pH 7 without NaCl to test for LCSTs.

4.3.7 Dye Absorption

30 µL of 1 mg/mL of dye were added to individual 3 ml aliquots of 1 mg/mL polyampholytes of PMA50 (pH 7.09), PDA49 (pH 6.92), PMAs49 (pH 7.20), PDAs50 (pH 6.02), PMN45 (pH 7.06 with 200 mM NaCl), PDN50 (pH 6.49), PMcN48 (pH 6.98) suspension in 15 mL centrifuge tubes. The samples were mixed for 30 min and then centrifuged immediately after mixing at 4000 rpm (~3000 g) for 30 min. Samples containing 30 µL of the respective dye solutions diluted in 3 mL water were used as reference. Finally, the dye concentrations in the reference and supernatant solutions were measured by UV-Vis spectroscopy.

4.4 Results and Discussion

4.4.1 Preparation of Polyampholytes

Nine binary stoichiometric polyampholytes were prepared from the monomers shown in Scheme 4.1, using free radical copolymerization. From APM to MAPTAc and AA to NaSS the charge density decreases,[37,40] the ability to form electrostatic interaction decreases but hydrophobicity increases. The reactivity ratios of different monomer pairs were measured by NMR and are summarized in Table 4.1. The reactivity ratio of APM to AA and DMAPMA to AA have been reported before,[45,53] and are close to those of MAPTAc and AA. Because APM, DMAPMA and MAPTAc have similar structures and the amine of APM and DMAPMA are protonated during polymerization, their reactivity ratios should be similar, for copolymerizations with the same comonomer. Therefore, only the reactivity ratios of APM-APMS and APM-NaSS are calculated and used to guide polymerization of other polymers, the monomer ratio drift and instantaneous copolymer composition during polymerization are shown in Figure 4A.1.

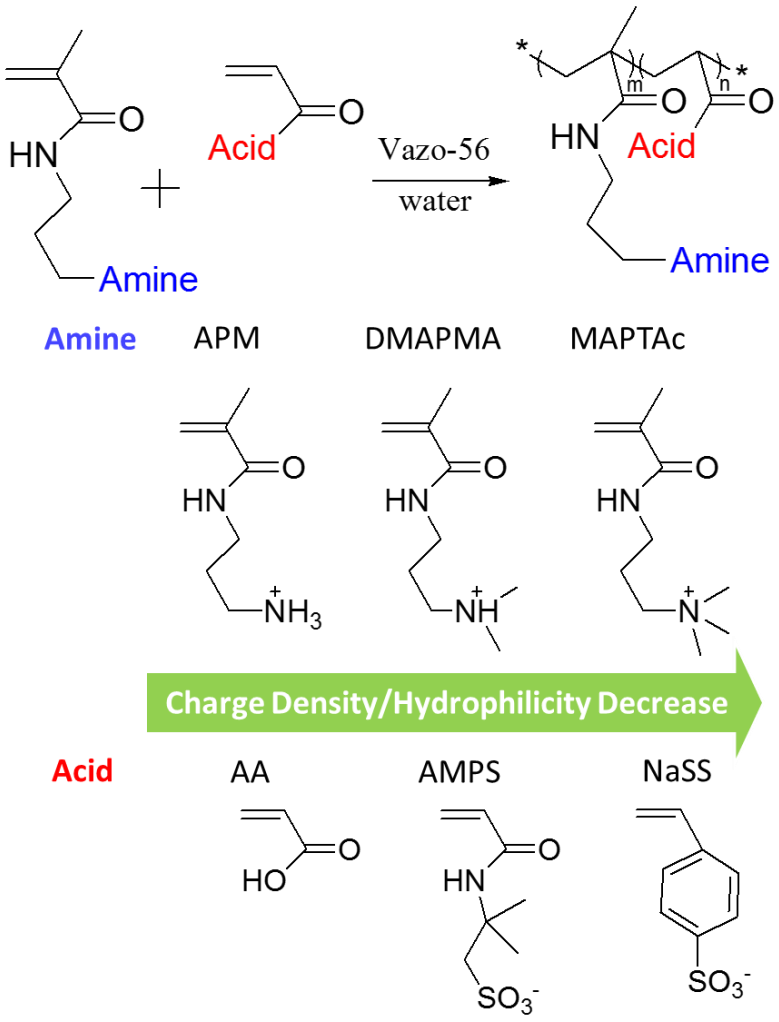

Scheme 4.1 The synthesis of polyampholytes, and monomers used.

Table 4.1. The experimental determined reactivity ratios of different monomer pairs, the first number corresponds to the cationic monomers, r_1.

	APM	DMAPMA	MAPTAc
AA	0.68; 0.48	0.59; 0.42	0.68; 0.50
AMPS	0.24; 0.10	-	-
NaSS	0.006; 0.21	-	-

Based on the reactivity ratios, to have stoichiometric polyampholytes, the feed ratio of AA and AMPS with cationic monomers should be 50:50, and feed ratio of the cationic monomers with NaSS should be 70:30. The predicted ratio drift of every 10% conversion is shown in the Table 4A.1 with selected feed ratio and indicates the selected feed ratios will give stoichiometric polyampholytes. The polymer information is summarized in Table 4.2. With the feed ratios selected depending on reactivity ratio, all nine polyampholytes have 50±5% cationic group, and can be thought of as stoichiometric polyampholytes. The polymer composition and molecular weight are measured by ^{1}H-NMR and GPC. PMN45 and PMcN48 did not dissolve in the GPC buffer at room temperature, but we except them to have similar molecular weight as PDN50.

Table 4.2 Polyampholyte Composition and Molecular Weight.

	Feed ratio (Amine/Acid)	**Conv (%)**	**Amine (%) (NMR)**	**Mn**	**Mw**	**PDI**
PMA50	49:51	70	50	76	226	2.9
PDA49	53:47	66	49	144	269	1.9
PMcA52	48:52	66	52	76	199	2.6
PMAs49	45:55	60	49	46	106	2.3
PDAs50	43:57	74	50	52	125	2.4
PMcAs54	50:50	63	54	66	140	2.1

PMN45[1]	72:28	63	45	N/A	N/A	N/A
PDN50	72:28	54	50	67	157	2.3
PMcN48[1]	69:31	54	48	N/A	N/A	N/A

1. These copolymers have no GPC results as they are insoluble in GPC buffer.

4.4.2 Solution Properties

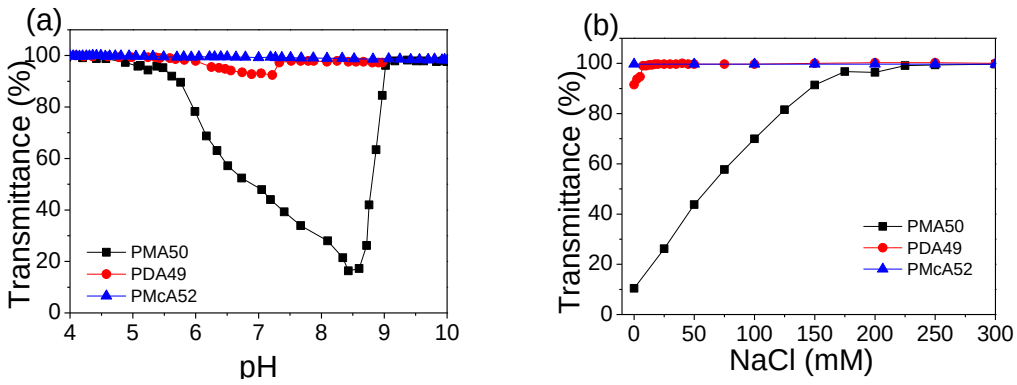

Figure 4.1 The titration curves titrated by (a) HCl and (b) NaCl of 1 mg/ml polyampholytes comprised of AA and different cationic monomers.

A key feature of polyampholytes is the pH driven phase separation due to interaction between oppositely charged groups. Turbidimetric titration is a simple and useful method to measure the phase separation of polyampholytes. Polyampholytes are separated into 3 groups by different anionic monomers, because the difference between cationic monomers is smaller compared with the anionic monomers.

The titration curves of polyampholytes composed of AA with different cationic comonomers using HCl are shown in Figure 4.1a and the corresponding reverse (NaOH) titrations are shown in Figure 4A.2a. Their pH(I), calculated as the midpoint between the pH of the half-maximum turbidity points on the leading edges of the forward (HCl) and reverse (NaOH) titration curves, are shown in Table 4A.2. The PMA50 has obvious transmittance changes from 100% to 10% and the solution stays cloudy over a broad pH range, which is believed to be due to the zero net charge at a broad pH around pH(I).[29,45] PDA49 only becomes slightly cloudy at pH(I) close to 90% transmittance, and the pH range of cloudy region is much narrower. However, the PMcA52 stays transparent from pH 4 to 10, and does not show any phase separation. The effect on turbidity of adding NaCl to solutions of the above copolymers at their pH(I) is shown in Figure 4.1b. Both PMA50 and PDA49 show anti-polyelectrolyte effect, with the minimum NaCl needed to make the solutions clear being 250 mM and 10 mM respectively. The PMcA52 solution keeps clear and does not show any visible phase separation even when NaCl reaches 1 M, shown in Figure 4A.2b.

The photographs and optical microscope images of these polyampholytes at pH values close to their pH(I), are shown in Figure 4.2. The PMA50 is milky, the PDA49 is a little bit cloudy and the PDA49 is transparent. Optical microscopy shows that PMA50 and PDA49 form coacervate droplets, indicating liquid-liquid phase separation. The phase separation of PDA49 is weak, and in order to obtain images of the coacervates, the concentration was increased to 5 mg/mL.

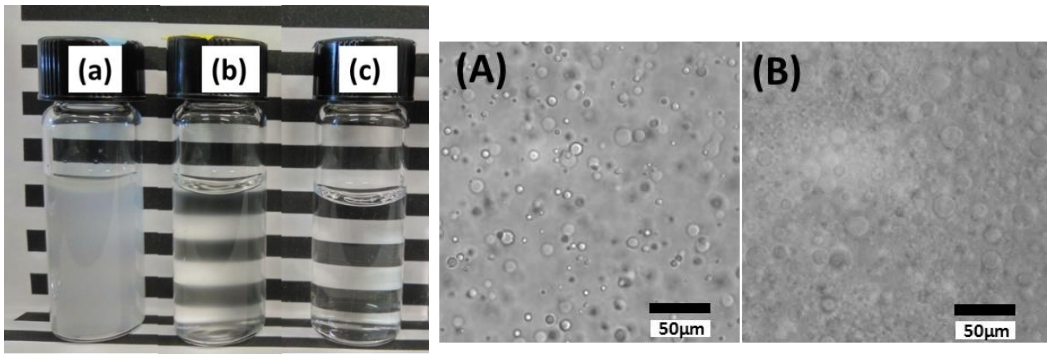

Figure 4.2 The photographs of (a) PMA50 at pH 7.11 (b) PDA49 at pH 6.63 and PMcA52 at pH 7.06, 1 mg/mL; and optical microscope images of (A) PMA50 at pH 7.35, 1 mg/ml (B) PDA49 at pH 7.01, 5 mg/ml.

The turbidity and morphology of coacervates indicate that with the charge density on the amine decreasing, the phase separation of polyampholytes becomes weaker, and increasing the hydrophobicity by introducing more methyl groups on the amine does not increase the phase separation, in contrast to adding a methyl on the backbone.[29.45] The [NaCl] titration in Figure. 4.1 also shows the electrostatic interaction grows weaker from APM to MAPTAc. We can conclude that the phase separation of these three polyampholytes at pH(I) were largely controlled by electrostatic interactions. With the charge density of amine decreasing, the phase separation becomes weaker and finally disappears.

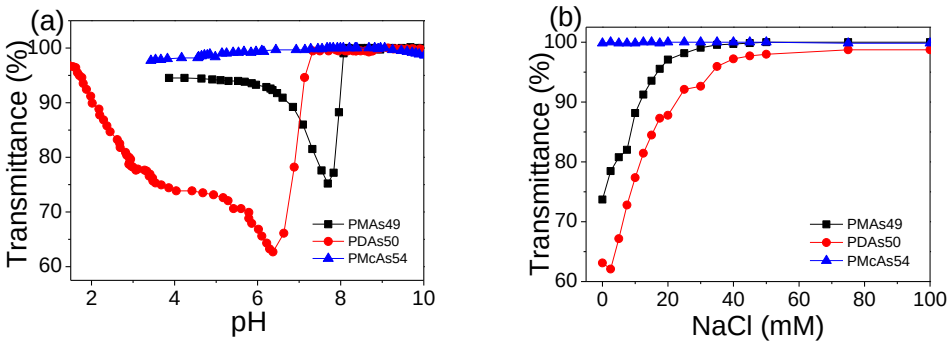

Figure 4.3 The titration curves titrated by (a) HCl and (b) NaCl of 1 mg/ml polyampholytes with AMPS and different cationic monomers.

When we replace the anionic monomer AA with AMPS, the electrostatic interaction between cationic and anionic groups becomes weaker, but the hydrophobicity of the polyampholytes increases. In Figure 4.3 and 4.4, the PMAs49 and PDAs50 have similar behaviors in that both of them have a liquid to liquid phase separation to form coacervate, and have comparable cloudiness; around 30 to 50 mM NaCl can cause the polyampholyte solutions to become clear.

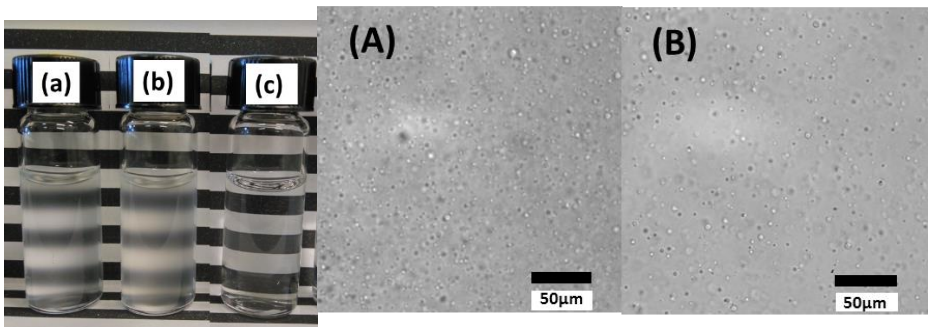

Figure 4.4. The photographs of (a) PMAs49 at pH 7.53 (b) PDA50 at pH 6.32 and PMcA54 at pH 6.98, 1 mg/mL; and optical microscope images of (A) PMAs50 at pH 7.21, 5 mg/ml (B) PDAs49 at pH 6.10, 5 mg/ml.

Comparing Figure 4.1 and Figure 4.3, the transmittance minima at pH(I) of PMAs49 and PDAs50 (60 to 80%) are between those for PMA50 (10%) and PDA49 (90%). Similarly, the clearance [NaCl] is 30 to 50 mM for PMAs49 and PDAs50, compared with 250 mM

for PMA50 and 10 mM for PDA49. The results show the polymer-polymer interaction decreases in the order PMA50>PMAs49≈PDAs50>PDA49. As mentioned above, using AMPS to replace of AA will decrease the electrostatic interaction but increase the hydrophobicity. The decrease of electrostatic interaction will cause weaker polymer-polymer interaction, so the PMAs49, PDAs49 should have weaker phase separation than PMA50, PDA50. However, the ranking of phase separation is PMA50>PMAs49≈PDAs50>PDA49, which means the increase of hydrophobicity promotes the phase separation. The phase separation of PMAs49 is weaker than PMA50 because of the decrease of electrostatic interaction, but stronger than in PDA49 due to the increase of hydrophobicity. Hence, the results show both the electrostatic interaction and the polymer hydrophobicity contribute to the polyampholyte phase separation. However, neither PMcAs54 nor PMcA52 have phase separation, indicating the electrostatic interaction is the primary factor for phase separation of these polyampholytes.

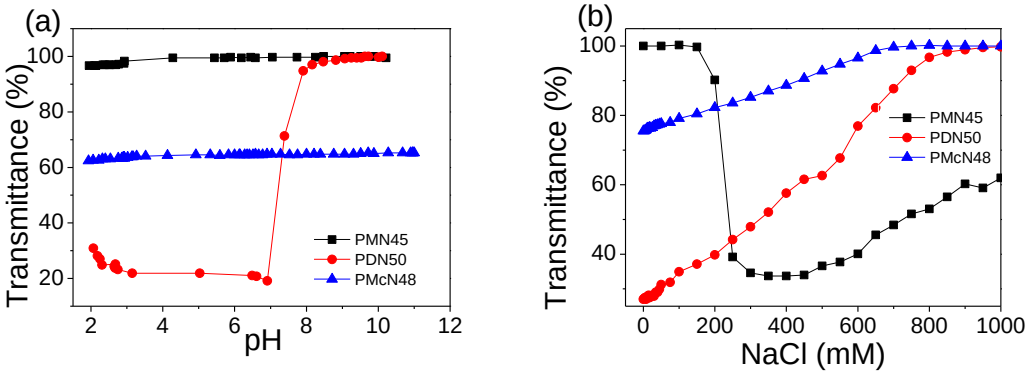

Figure 4.5. The titration curves titrated by (a) HCl and (b) NaCl titration of 1 mg/ml polyampholytes with NaSS and different cationic monomers.

a.

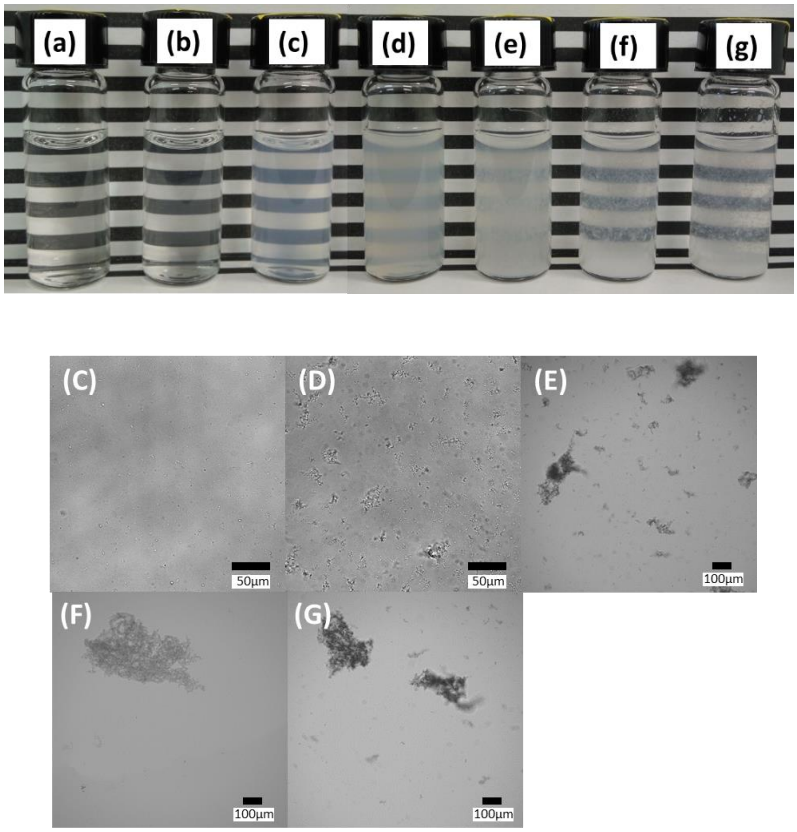

b.

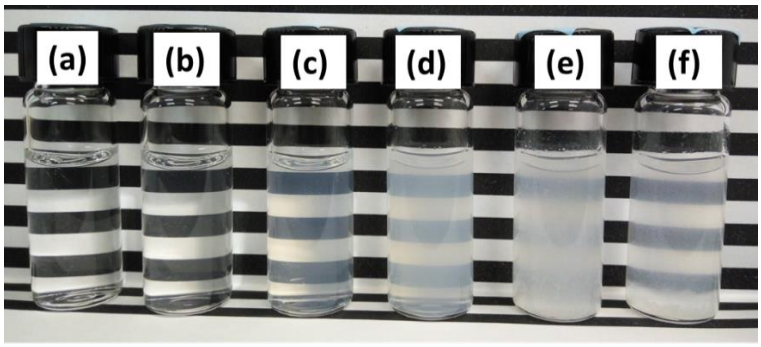

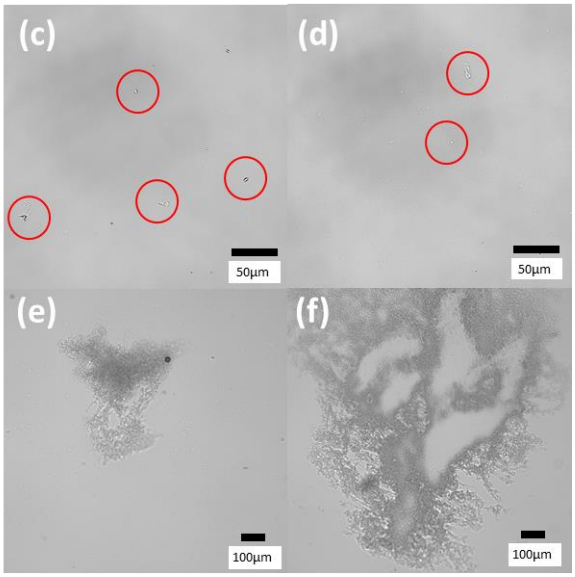

c.

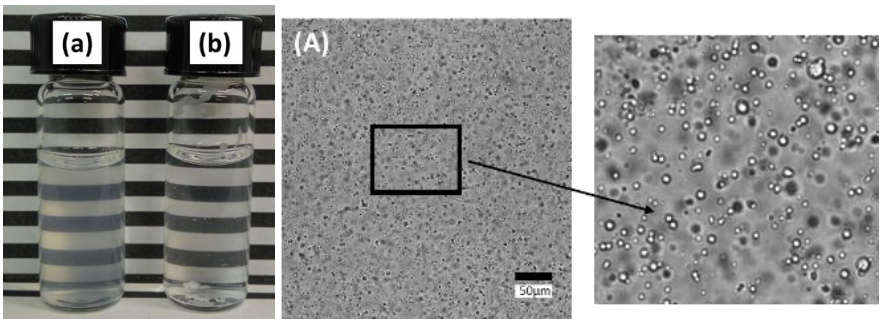

Figure 4.6 The optical microscope images of polyampholytes with NaSS and different cationic monomers. a. PMN45 with different [NaCl] at 1 mg/ml, (a) to (g) [NaCl] = 0, 50, 100, 150, 200, 300 and 500 mM, at pH 7±0.1, (C) to (G) corresponding microscope images; b. PDN50 with different pH at 1 mg/ml, (a) to (f) pH 8.98, 8.05, 7.45, 7.01, 6.03 and 5.01, (C) to (F) corresponding microscope images; c. PMcN48 (a) 1 mg/ml, pH 7.05, (b) at room temperature, at 1 mg/ml, pH 7.13 and (A) PMcN50 after heating at 90 ^{o}C for 60 min at pH 6.98, 5 mg/ml.

When NaSS is used as the anionic monomer, the hydrophobicity of polymer is further increased, however, the electrostatic interaction is now weaker. The pH titration results (Figure 4.5a) are significantly different from those of the previous polyampholytes. The PMN45 solution is transparent across the whole pH range, PDN50 phase separates when the pH is below about 7, close to the pKa of DMAPMA. PMcN48 solutions remain constantly cloudy over the whole pH range in this work.

In NaCl titrations, at pH 7 PMN45 phase separates around 200 mM NaCl, with the transmittance going back up above 500 mM NaCl owing to precipitation of solid polymer. Decreasing the polyampholyte concentration will suppress this precipitation and result in cloudy solution at [NaCl] as high as 1.5 M, as shown in Figure 4A.2d. The behavior of PMN45 is more characteristic of polyelectrolytes than of polyampholytes. The PDN50 and PMcN48 show the typical anti-polyelectrolyte properties as both become clear at 900 mM NaCl.

The appearance of polyampholyte solutions is shown in Figure 4.6. For PMN45, with increasing [NaCl], the solution becomes cloudy and finally forms visible precipitates above 200 mM NaCl. The microscopic pictures in Figure 4.6 a show PMN45 forming irregular particles at low [NaCl] with particle size increasing at higher [NaCl]. Similar results are seen for PDN50 in Figure 4.6b. With decreasing pH, the solution turns cloudy and the PDN50 forms irregular particles that grow at even lower pH. This liquid to solid phase transitions contrasts with the liquid-liquid phase separation or no phase separation seen for other polyampholyte.

The PMcN48 is again different, because of its pH non-response. The PMcN48 forms a hydrogel in water, but after heating at 90 ^{o}C with stirring for 2 hrs, the hydrogel disperses

to small particles in Figure 4.6 c. The particles are small, dark and have regular margins, so after heating, the PMcN48 forms small particles with lower water content.

The phase separation of the nine polyampholytes is summarized in Table 4.3. There are liquid to liquid, liquid to solid, and no phase separation. With the hydrophilic anionic comonomers AA and AMPS, polyampholyte phase separation is weak, and the electrostatic interaction plays the dominant role. As the charge density of the cationic monomer decreases from APM to MAPTAc, the phase separation changes from coacervate to no phase separation. The results are consistent with previous results that polyampholytes with weak acid and weak base groups[3,30,31] have phase separation and the ones with strong acid and strong bases[24,28] do not show phase separation but viscosity change. There are indications that the polymer hydrophobicity also contributes to the phase separation, as the phase separation of PMAs49 is weaker than PMA50 but stronger than that of PDA49. The polyampholytes with NaSS have strong phase separation into hydrogel due to their strong hydrophobic interaction.[28,35,40,46] Because the electrostatic interaction between NaSS and amines are weaker than the interactions of AA or AMPS with amine, the hydrophobicity plays a more important role in phase separation, especially for the polyampholytes with quaternary ammonium cations that only show phase separation with NaSS.

The response to [NaCl] is also affected by both electrostatic interaction and hydrophobicity. As typical polyampholytes, the anti-polyelectrolyte properties are well studied by both theoretical[20,21] and experimental research,[5,6,26] showing that increasing [NaCl] will shield the polymer-polymer interaction and lead to polyampholyte dissolution, with higher [NaCl] needed for polyampholytes with stronger electrostatic interactions.[26] However, the minimum NaCl needed to make the polyampholytes solutions clear in this work does not

follow the strength of electrostatic interaction. In Table 4.3, from left to right and top to bottom, the electrostatic interactions decreases. So the minimum [NaCl] from left to right, and from top to bottom should decrease, and the highest and lowest [NaCl] should be at the top left and bottom right, respectively. However, the systems in the shaded section do not follow this role and need higher [NaCl], presumably due to stronger net polymer-polymer interaction with contributions from both electrostatic interaction and polymer hydrophobicity. So far, results show the phase separation of polyampholytes are decided by both electrostatic interaction and polymer hydrophobicity, strong electrostatic interaction can form coacervates, and strong hydrophobicity will lead to precipitate and increase the [NaCl] resistance of anti-polyelectrolytes.

Table 4.3 The summary of the morphology of polyampholytes after phase separation and the minimum [NaCl] for redissolution.

Ionic groups	**APM**	**DMAPMA**	**MAPTAc**
AA	Coacervate (250 mM)	Coacervate (10 mM)	No phase separation
AMPS	Coacervate (30-50 mM)	Coacervate (30-50 mM)	No phase separation
NaSS	Hydrogel (with NaCl)	Hydrogel (900 mM)	Hydrogel (900 mM)

When thinking more about the effect of NaCl on the nine polyampholytes, there are a few more questions. The first issue is that PMN45 does not show anti-polyelectrolyte effects, but behaves more like a polyelectrolyte. This may be because of small net charges from unbalanced charge ratio. These net charges may make the polyampholyte stable in water,

but [NaCl] will shield this electrostatic repulsion, and further increasing [NaCl] will increase the solubility.[6,20,21,27] However, PMN45 does not show the solubility increasing up to 1.5 M NaCl in Figure 4A.1d. Comparing with PDN50 and PMcN48 which turn clear at 900 mM NaCl, the behavior of PMN45 is abnormal, which could be because PMN45 has both relatively strong electrostatic and hydrophobic interactions. Further comparison with the three polyampholytes of each line in Table 4.3, from top to bottom, the electrostatic interactions become weaker, but the minimum [NaCl] for clarification increases. To explain this observation, the assumption is only some of the electrostatic interactions are shielded by NaCl. The polyampholyte solution becoming clear does not mean the chains are fully dissolved, they can be "soluble primary complexes" which are implicated in the early state of protein and polymer complexation before the macroscopic coacervate formation.[54] The detail of the information and behavior of the soluble complex is beyond the scope of this work. The soluble complexes could still keep electrostatic interactions, but some free ionic groups will keep them soluble in water. So for polyampholytes with more hydrophobic groups, to overcome the hydrophobicity interaction, more NaCl is needed to break more electrostatic interactions.

If this assumption is right, there should have been different and weaker electrostatic interactions as shown in Scheme 4.2. Because of the random distribution of charges on polymer chains, there are strong and weaker electrostatic interaction, the one between small block fragments are stronger and the others between single or multi-ionic pairs are weaker.[47] There should be some unpaired ionic groups as shown in Scheme 4.2 too, so the phase separation of polyampholytes should be weaker than polyelectrolyte complex.

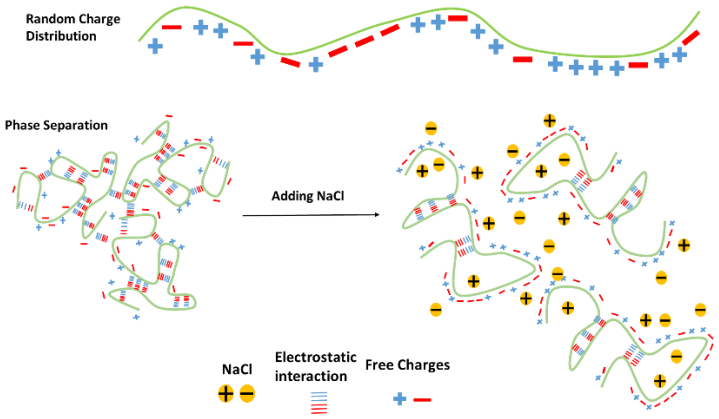

Scheme 4.2 The diagram of electrostatic interaction along polyampholyte chains.

The phase separation of polyelectrolyte complexes is shown in Figure 4.7, the information of polyelectrolytes are summarized in Table 4A.3. As expected, the polyelectrolyte complexes have stronger phase separation than polyampholytes, as shown in Figure 4.7a, all the polyelectrolyte complexes are cloudy with lower transmittance (<5% in Table 4A.4), especially for the PAA-PMAPTAc, PAMPS-PMAPTAc and PAPM-PNaSS, where the solution of the corresponding polyampholytes made by same monomers are transparent. The microscope images show the morphology of polyelectrolyte complexes are similar to those of the polyampholytes: with the hydrophilic PAA and PAMPS there are liquid to liquid phase separation (droplets), and with the hydrophobic PNaSS, there are liquid to solid phase separation (gel particles). The polyelectrolyte complexes have stronger phase separation than polyampholytes because they have stronger electrostatic interaction, but the stronger interaction does not change the morphology of phase separation.

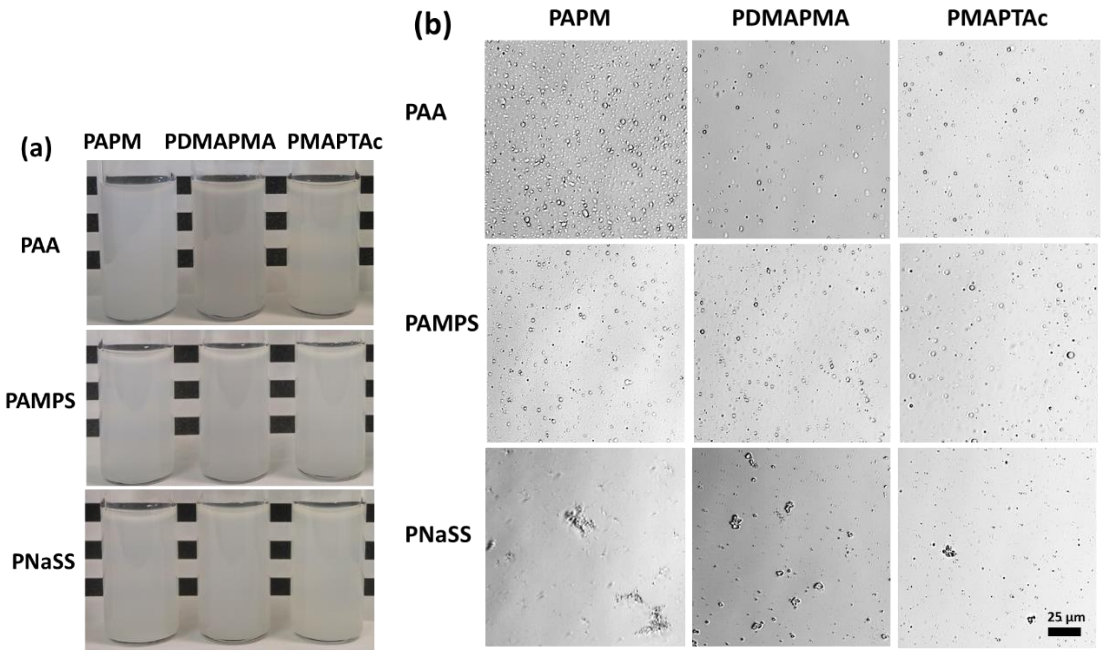

Figure 4.7 The photographs (a) and optical microscope images (b) of polyelectrolyte complex. The mole ratio is 1 to 1, total concentration is 1 mg/ml at pH 7±0.3.

To learn more about the difference between polyampholytes and polyelectrolyte complex, the PAA and PAPM 1:1 complex was selected as an example. The pH and [NaCl] titrations are shown in Figure 4.8. The PAA-PAPM complex behaves similarly with PMA49 which keeps cloudy at a broad pH range. The PAA-PAPM complex have stronger phase separation compared with PMA49. The asymmetry in the titration may be attributed to a little bit excess of PAPM. When increasing pH, the polyelectrolyte complex contains a little bit of free cationic charge, which results in the higher transmittance (70% to 80% between pH 5 to 8), and at pH 10, there is zero net charge, so the transmittance decreases to 10%. When pH decreases, the polyelectrolyte complex reaches to zero net charge first, the electrostatic interaction causes the phase separation first, then the little bit of free

cationic charge between pH 8 to 5 only slightly increases the solubility until at lower pH when PAA starts to be protonated.

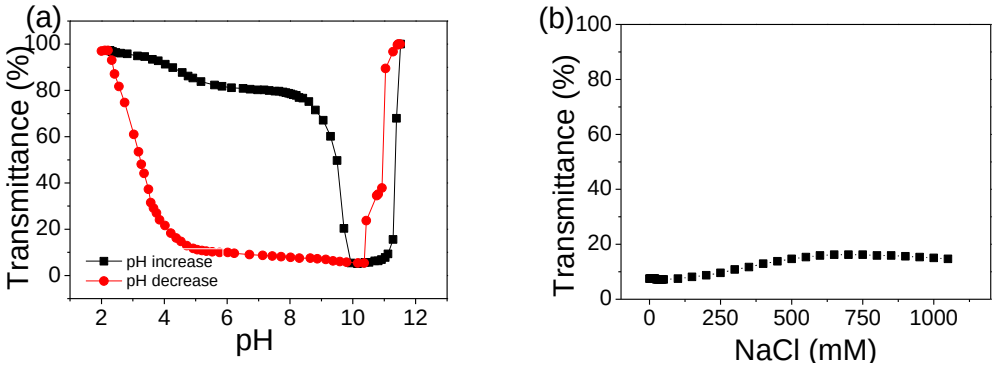

Figure 4.8. The pH titration curves (a) and NaCl titration (b) of PAPM and PAA complex, total 1 mg/ml.

The effects of [NaCl] are different with the polyampholytes, shown in Figure 4.8b. 1 M NaCl only slightly increases the transmittance of PAA-PAPM complex, and for PMA50 the critical NaCl is 250 mM. It suggests 1 M NaCl can partly shield polymer-polymer electrostatic interaction, so the promotion of solubility is limited. The comparison of the PAA/PAPM complex and PMA49 show the polyelectrolyte complexes have stronger electrostatic interaction compared with polyampholytes made by the same monomers, increasing the NaCl concentration has limited ability to increase the polyelectrolyte solubility. Similar titration curves of the PAA/PAPM in Figure 4A.3 show increasing NaCl first decreasing the solubility of the complex and then the transmittance only slightly increases up to 1M.

4.4.3 Temperature Response

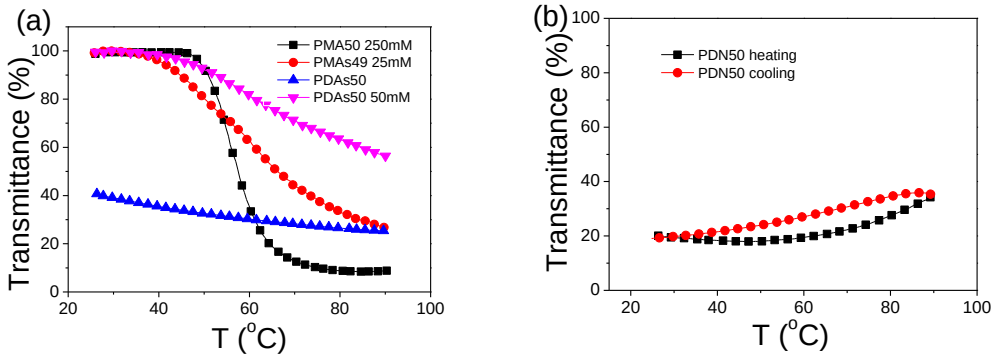

Figure 4.9 The transmittance vs temperature curves of polyampholytes (a) heating of PMA50, pH 7.16, 250 mM NaCl; PMAs49 pH 7.13, 25 mM NaCl; PDAs50 pH 6.07, 0 or 25 mM NaCl, (b) heating and cooling of PDN50 pH 7.1 without NaCl.

Besides the pH driven phase separation, the temperature driven phase separation is another important property of polyampholytes. In our previous work we reported polyampholytes having LCST in presence of sufficient NaCl to make the polyampholyte soluble at room temperature.[30,31,45] Because heating breaks polymer-water interactions, it can cause enhanced polymer-polymer electrostatic and hydrophobic interactions leading to phase separation. Increasing [NaCl] leads to higher LCST because of shielding of electrostatic polymer-polymer interactions. However, polyampholytes are predicted to have UCST[20] by weakening the electrostatic interaction with heating, and the similar polybetaines are well known polymer with UCST by breaking electrostatic interaction with heating.[36,38] Therefore, the polyampholytes may show both LCST and UCST. However, polyampholytes only have been reported to have UCST in water/ethanol solution mixture.[35,55] In order to study this question the temperature responses of the nine

polyampholytes were measured. Figure 4.9 only shows the polyampholytes with temperature responses. Only a limited number of polyampholytes have temperature responses, with three polymers showing LCST type phase separation, with enough NaCl to keep the solution clear at room temperature, the PMA50 250 mM NaCl, PMAs49 25 mmol NaCl, and PDAs50 at 50 mmol NaCl. Curiously, PDAs50 without NaCl also show weak LCST type phase separation instead of UCST. Only PDN50 polyampholyte show weak UCST type phase separation in water.

The effect of temperature on polyampholytes is complex. For one way, heating could break the polymer-water interaction and promote polymer-polymer interaction by rebuilding the polymer-polymer electrostatic interaction or making the hydrophobicity parts aggregation. On the other way, heating will break the polymer-polymer interaction and promote polymer soluble. To have LCST, polyampholytes should have the ability to form electrostatic interactions and some degree of hydrophobicity, which can come from the hydrophobic backbone or side chain and also from ion pairs formed by electrostatic interaction, which was found to decrease the number of water bonding on the charge groups[56] and believed to increase the hydrophobicity.[57] Polyampholyte with weaker electrostatic interaction, hydrophilic side groups or at high NaCl concentration cannot have LCST. To have UCST, polyampholytes should have appropriate electrostatic interaction and hydrophobicity. The electrostatic interaction should be strong enough to make polyampholytes phase separate but also weak enough to be broken at high temperature; the hydrophobicity should be enough to promote polymer phase separation, but cannot encourage hydrophobic (LCST-type) phase separation at high temperature. Because of these exacting conditions, as far as we know, there is no polyampholyte that shows UCST in water without any additive, and

even PDN50 only shows weak UCST type phase separation. Even for the well-known polybetaine, the UCST is structure dependent.[36]

4.4.4 Dye Removal from Water

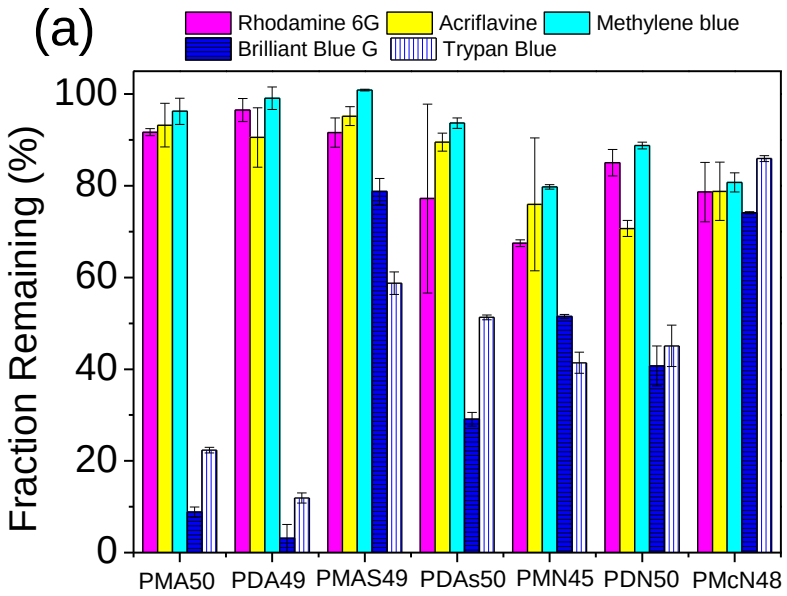

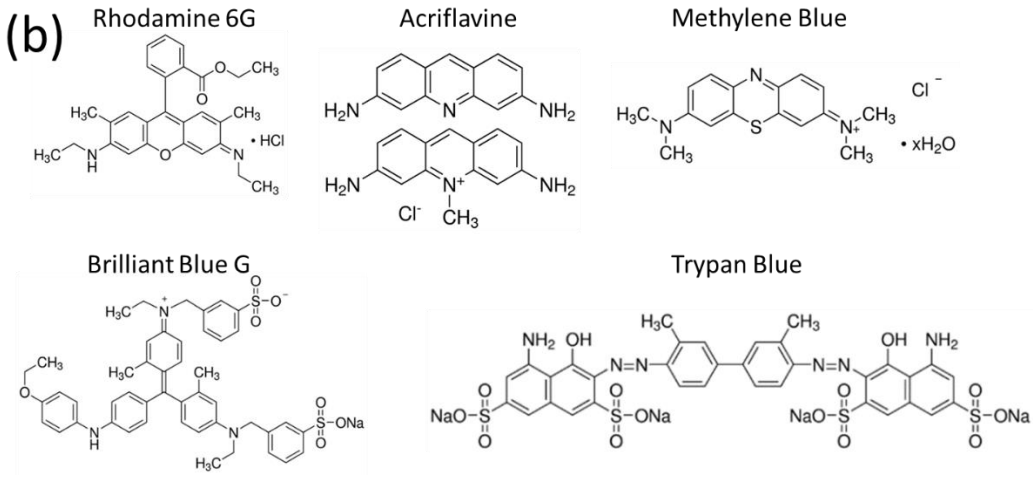

Figure 4.10 Fraction of dye remaining in supernatant after treatment with polyampholytes and centrifugation (a) and dye structures (b).

As mentioned in Scheme 4.2, after phase separation, there are free charges on polyampholyte chain, and polyampholytes also have hydrophobicity coming from the backbone.[57] So the polyampholyte droplets or gels should have an ability to bind ionic amphiphiles from water. To further explore this, dye capture properties by polyampholytes were measured by mixing polyampholyte coacervates or gels with different organic dyes in aqueous solution. Dye capture likely occurs by a combination of electrostatic and hydrophobic interactions[58] so different polyampholytes should have different ability to capture dyes.

The dye capture results are shown in Figure 4.10a, with the dye structures shown in Figure 4.10b. In Figure 4.10a from left to right, the polyampholytes have less electrostatic interaction but higher hydrophobicity, and the first three dyes Rhodamine 6G, Acriflavine and Methylene Blue all have one charge group and Brilliant Blue G and Trypan Blue have multiple charges. The general trend is from left to right, the binding ability of Brilliant Blue G and Trypan Blue decreases, but ability of binding the other three dyes increases, because polyampholytes on the left side are more hydrophilic and have higher ability to form electrostatic interaction, so they have higher ability to bonding with dyes with multi-charges by electrostatic interaction, but have poorer ability to bind singly-charged dyes. In contrast, polyampholytes on the right side in Figure 4.10 have weaker electrostatic interaction but higher hydrophobicity, they have preference to bond with single-charge dyes by hydrophobic interaction. There is some variation out of the general trend like the

PDA49 has highest ability to bond with Trypan Blue and the PMcN48 is the worst to bond with every single dye compare with other polyampholytes, however the general trend supports the notion of electrostatic interaction and hydrophobicity affecting dye binding.

Different from the traditional polyampholytes dye bonding work which invokes electrostatic interaction at either high or low pH.[8,9] This work shows that polyampholytes are a new option for water purification at neutral pH by combination of both electrostatic and hydrophobicity interaction. This suggests potential applications of polyampholytes to mediate dyes pollution from the textile industry.[59]

4.5 Conclusion

In water, stoichiometric polyampholyte phase separations were controlled by both electrostatic interaction and polymer hydrophobicity. Hydrophilic polyampholytes with strong electrostatic interaction can have liquid to liquid phase separation to form coacervate; while those with weaker electrostatic interaction can form soluble polyampholytes even at pH(I). When the polyampholytes have large hydrophobic groups like aromatic rings, the strong hydrophobicity together with electrostatic interaction promotes the liquid to solid separation to form hydrogel. Hence, the phase separation properties depend on both electrostatic and hydrophobic interactions. We also find by selecting comonomers, polyampholytes can have LCST or (weak) UCST, and show selective binding with different dyes. This work reveals interesting properties of polyampholytes as well as the principles to control them, which may be beneficial to development of new polyampholyte

based materials, including water purification materials, thermo-responsive drug delivery systems, non-fouling materials, pH sensitive materials and physical hydrogels.

4.6 Acknowledgements

The authors would like to acknowledge funding for this research from NSERC.

4.7 References

1. Narayanan Nair, A. K.; Uyaver, S.; Sun, S. *J Chem. Phys.* **2014**, *141*, 134905 (1-11).

2. Rabiee, A.; Ershad-Langroudi, A.; Jamshidi, H. *Rev Chem Eng* **2014**, *30*, 501-519.

3. Kudaibergenov, S. E. *Adv. Polym. Sci.* **1999**, *144*, 116-192.

4. Zurick, K. M.; Bernards, M. *J. Appl Polym. Sci.* **2014**, *131*, 40069 (1-9).

5. Das, M.; Kumacheva, E. *Colloid Polym. Sci.* **2006**, *284*, 1073-1084.

6. Ciferri, A.; Kudaibergenov, S., Ciferri, A.; Kudaibergenov, S. *Macromol. Rapid. Comm.* **2007**, *28*, 1953-1968.

7. Ezell, R. G.; McCormick, C. L. *J. Appl. Polym. Sci.* **2007**, *104*, 2812-2821.

8. Kudaibergenov, S. E.; Tatykhanova, G. S.; Klivenko, A. N. *J. Appl. Polym. Sci.* **2016**, *133*, 43784 (1-9).

9. Deen, G. R.; Wei, T. T.; Fatt, L. K. *Polymer*, **2016**, *104* 91-103.

10. Song, J.; He, A.; Jin, Y.; Cheng, Q. *RSC. ADV.* **2013**, *3*, 24586-24592.

11. Schroeder, M. E.; Zurick, K. M.; McGrath, D. E.; Bernards, M. T. *Biomacromolecules* **2013**, *14*, 3112-3122.

12. Mi, L.; Jiang, S. *Angew, Chem, Int, Ed.* **2014**, *53*, 1746-1754.

13. Barcellona, M. N.; Johnson, N.; Bernards, M. T. *Langmuir*, **2015**, *31*, 13402-13409.

14. Liu, E. J.; Sinclair, A.; Keefe, A. J.; Nannenga, B. L.; Coyle, B. L.; Baneyx, F.; Jiang, S. *Biomacromolecules* **2015**, *16*, 3357-3361.

15. Das. A.; Ghosh. S.; Ray, A. R. *Polymer*, **2011**, *52*, 3800-3810.

16. Kitano, H.; Gemmei-Ide M. *J Biomater Sci Polym Ed.* **2010**, *21*, 1877-1893.

17. Xia, Y.; Gao, M.; Chen, Y.; Jia, X.; Liang, D. *Macromol. Chem. Phys.* **2011**, *212*, 2268-2274.

18. Edwards, S. F.; King, P. R.; Pincus, P. *Phys. Rev. Lett.* **1992**, *6*, 61-64.

20. Tanaka, M.; Tanaka, T. *Phys. Rev. E* **2000**, *62*, 3803-3816.

21. Higgs, P. G.; Joanny, J.-F. *J. Chern. Phys*. **1991**, *94*, 1543-1554.

22. Ulrich, S.; Seijo, M.; Stoll, S. *J. Phys. Chem. B* **2007**, *111*, 8459-8467.

23. Cheong, D. W.; Panagiotopoulos, A. Z. *Mol. Phys.* **2005**, *103*, 3031-3044.

24. McCormick, C. L.; Johnson, C. B. *Macromolecules* **1988**, *21*, 694-699.

25. Fevola, M. J. Kellum, M. G.; Hester, R. D.; McCormick, C. L. *J. Polym. Sci., Part A: Polym. Chem.* **2004**,

42, 3252-3270.

26. Ohlemacher, A.; Candau, F.; Munch, J. P.; Candau, S. J. *J. Polym. Sci., Part B: Polym. Phys.* **1996**, *34*, 2747-2757.

27. Corpart, J. M.; Candau, F. *Macromolecules* **1993**, *26*, 1333-1343.

28. McCormick, C. L.; Salazar, L. C. *Macromolecules*, **1992**, *25*, 1896-1900.

29. Masuda, S.; Minagawa, K.; Tsuda, M.; Tanaka, M. *Eur. Polym. J.* **2001**, 37, 705-710.

30. Dubey, A.; Burke, N. A. D.; Stöver, H. D. H. *J. Polym. Sci Pol. Chem.* **2014**, *53*, 353-365.

31. Abdilla, A.; Shi, S.; Burke, N. A. D.; Stöver, H. D. H. *J. Polym. Sci., Part A: Polym. Chem.* **2016**, *54*, 2109-2118.

32. Xiao, L.; Vyhnalkova, R.; Sailer, M.; Yang, G.; Barrett, C. J.; Eisenberg; A. *Langmuir*, **2014**, *30*, 891-899.

33. Canning, S. L.; Neal, T. J.; Armes, S. P. *Macromolecules*, **2017**, *50*, 6108-6116.

34. Zhang, X.; Ma, J.; Yang, S.; Xu, J. *Soft Mater.* **2013**, *11*, 394-402.

35. Takeoka, Y.; Berker, A. N.; Du, R.; Enoki, T.; Grosberg, A.; Kardar, M.; Oya, T.; Tanaka, K.; Wang, G.; Yu, X.; Tanaka, T. *Phys. Rev. Lett.* **1999**, *82*, 4863-4865.

36. Shao, Q.; Jiang, S. *Adv. Mater.* **2015**, *27*, 15-26.

37. Shao, Q.; Jiang, S. *J. Phys. Chem. B* **2014**, *118*, 7630-7637.

38. Zhu, Y.; Noy, J. M.; Lowe, A. B.; Roth, P. *Polym. Chem*. **2015**, *6*, 5705-5718.

39. Lappan, U.; Scheler, U. *Macromolecules* **2017**, *50*, 8631-8636.

40. Fu, J.; Fares, H. M.; Schlenoff, J. B. *Macromolecules* **2017**, *50*, 1066-1074.

41. Požar, J.; Kovačević, D. *Soft Matter*, **2014**, *10*, 6530-6545.

42. Sadman, K.; Wang, Q.; Chen, Y.; Keshavarz, B.; Jiang, Z. Shull, K. R. *Macromolecules*, **2017**, *50*, 9417-9426.

43. Kotov, N. A. *Nanostruct. Mater.* **1999**, *12*, 789-796.

44. Yi, S.; Lin, C.; Leon, W.; Vezenov, D.; Regen, S. L. *Langmuir*, **2016**, *32*, 12332-12337.

45. Zhao, J.; Burke, N. A. D.; Stöver, H. D. H. *RSC Adv.* **2016**, *6*, 41522-41531.

46. Luo, F.; Sun, T., Nakajima, T.; Kurokawa, T.; Li, X.; Guo, H.; Huang, Y.; Zhang, H.; Gong, J. *Polymer*, **2017**, *116*, 487-497.

47. Sun, T.; Kurokawa, T.; Kuroda, S.; Ihsan, A. B.; Akasaki, T.; Sato, K.; Haque, Md. A.; Nakajima, T.;

Gong, J. *Nat. Mater.* **2013**, *12*, 932-932.

48. Comert, F.; Malanowski, A. J.; Azarikiab, F. Dubin, P. L. *Soft Matter*, **2016**, *12*, 4154-4161.

49. Pathak, J.; Rawat, K.; Aswal, V. K.; Bohidar, H. B. *J. Phys. Chem. B* **2014**, *118*, 11161-11171.

50. Pathak, J.; Rawat, K.; Rawatb, K.; Bohidar, H. B. *Int. J. Biol. Macromol.* **2014**, *63*, 29-37.

51. Brzozowska, A. M.; Parra-Velandia, F. J.; Quintana, R.; Zhu, X.; Lee, S. S. C.; Chin-Sing, L.; Jańczewski, D.; Teo, S. L.-M.; Vancso, J. G. *Langmuir* **2014**, *30*, 9165-9175.

52. Rodriguez, A. M. B.; Binks, B. P.; Sekine, T. *Soft Matter*, **2018**, *14*, 239-254.

53. Zhao, J.; Johnson, M.; Burke, N. A. D.; Stöver, H.D.H. Synthetic Polyampholytes as Macromolecular Cryoprotective Agents. unpublished results.

54. Kaibara, K.; Okazaki, T.; Bohidar, H. B.; Dubin, P. L. *Biomacromolecules* **2000**, *1*, 100-107.

55. Zhang, Q.; Hoogenboom, R. *Chem. Commun*. **2015**, *51*, 70-73.

56. Kitano, H.; Takaha, K.; Gemmei-Ide, M. *Phys. Chem. Chem. Phys.* **2006**, *8*, 1178-1185.

57. Azzaroni, O.; Brown, A. A.; and Huck, W. T. S. *Angew. Chem. Int. Ed.* **2006**, *45,* 1770-1774.

58. Parasuraman, D.; Serpe, M. J. *ACS Appl. Mater. Interfaces* **2011**, *3*, 4714-4721.

59. Singh, K.; Arora, S. *Crit. Rev. Environ. Sci. Technol.* **2011**, *41*, 807-878.

4.8 Appendix

4.8.1 Reactivity Ratio Determination

The reactivity ratios were measured by ^{1}H-NMR using a method previously reported.[1] Solution copolymerizations were carried out in 5 mm NMR tubes at 55 °C in a water bath, with ethylene carbonate used as the internal NMR standard. The pH of mixtures of AA and AMPS with all three amines were between 2 to 3, without adjusting pH, and the pH of mixtures of NaSS with all amines were adjusted to pH 7. The monomer ratios used were 10:90, 30:70, 40:60, 50:50, 60:40, 70:30 and 90:10. Samples were removed from the water bath every several minutes, cooled in water and analyzed by ^{1}H-NMR. Conversion of each step was controlled between 5 to 20 %. The decrease of the integrated vinyl peaks reveals the conversion of the two monomers and also the instantaneous monomer and polymer concentrations. The reactivity ratios were then calculated by fitting the instantaneous monomer concentrations to the copolymerization equation.

4.8.2 Polymer Purification

For precipitation, and NMR, the polyampholytes with AA and AMPS were adjusted to pH around pH 2, for PMN45 and PDN50 to pH 10, and for PMcN48 to pH 1, in order to give the polyampholytes free charges to increase their solubility in water but decrease the solubility in water / acetone mixture.

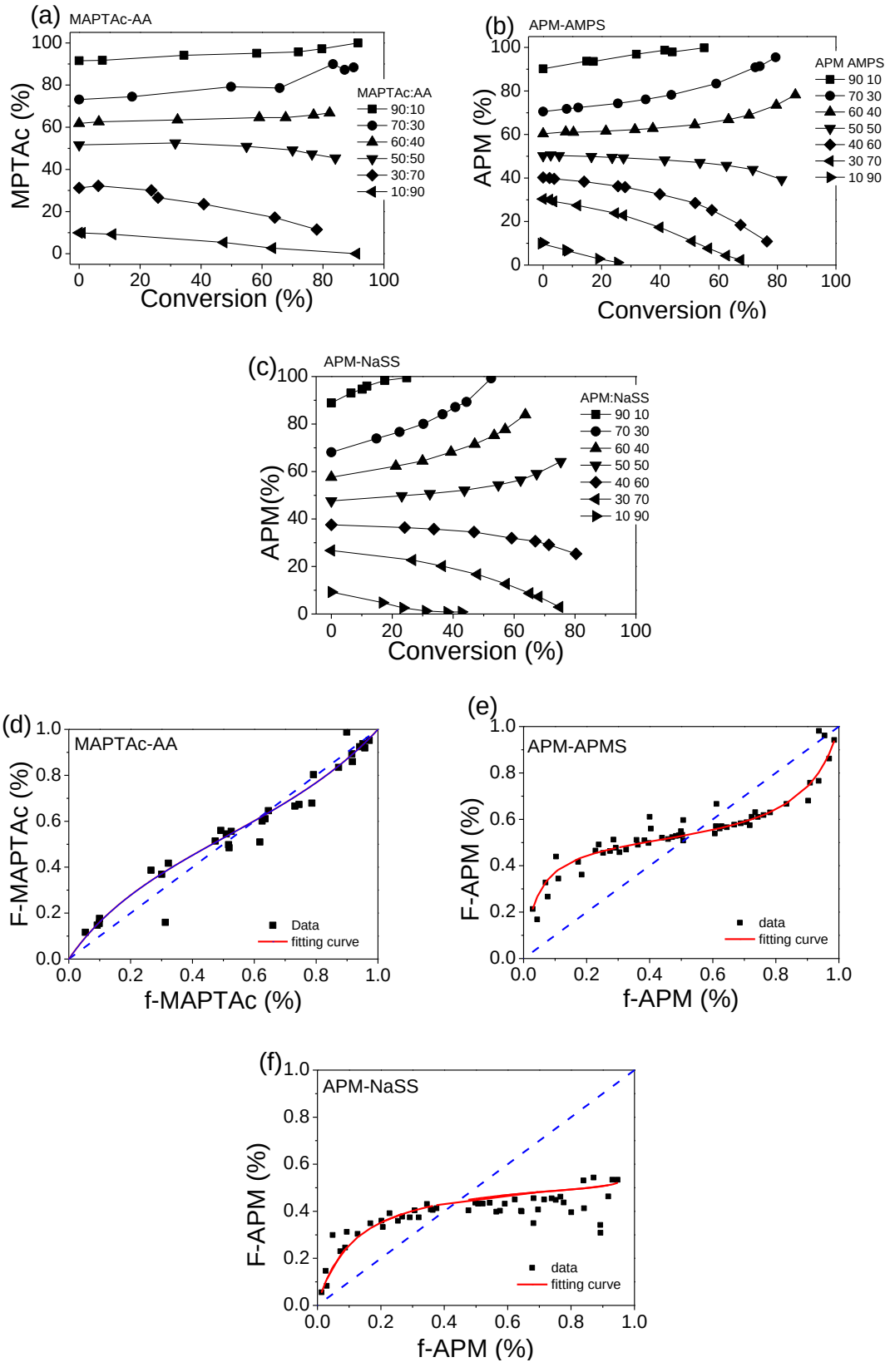
(a)
MAPTAc-AA
MPTAc (%)
Conversion (%)
MAPTAc:AA
90:10
70:30
60:40
50:50
30:70
10:90
(b)
APM-AMPS
APM (%)
Conversion (%)
APM AMPS
90 10
70 30
60 40
50 50
40 60
30 70
10 90
(c)
APM-NaSS
APM(%)
Conversion (%)
APM:NaSS
90 10
70 30
60 40
50 50
40 60
30 70
10 90
(d)
MAPTAc-AA
F-MAPTAc (%)
f-MAPTAc (%)
Data
fitting curve
(e)
APM-APMS
F-APM (%)
f-APM (%)
data
fitting curve
(f)
APM-NaSS
F-APM (%)
f-APM (%)
data
fitting curve

Figure 4A.1 (a), (b) and (c) show the cationic monomer percentage in total monomer during the polymerization, determined by ^{1}H-NMR. (d), (e) and (f) show instantaneous copolymer composition of cationic monomers for copolymerization with different initial mole ratios, fitted with the instantaneous copolymer composition equation.

Table 4A.1 The drift of APM mol% during coplymerization estimated from reactivity ratios for a series of 10% conversion steps.

	Conv(%)	0-10	10-20	20-30	30-40	40-50	50-60	60-70	70-80	80-90
APM:AA	50:50	53	53	52	52	52	51	50	49	47
APM:AMPS	50:50	53	53	53	53	52	52	52	51	50
APM:NaSS	30:70	48	49	49	49	50	-	-	-	-

Table 4A.2 The pH(I) of polyampholytes, calculated from titration curves.[1]

Polyampholyte	**pH(I)**
PMA 50	7.3
PDA 49	6.6
PMAs 49	7.2

1. The pH(I) was calculated as the midpoint between the pH of the half-maximum turbidity points on the leading edges of the forward and back titration curves.

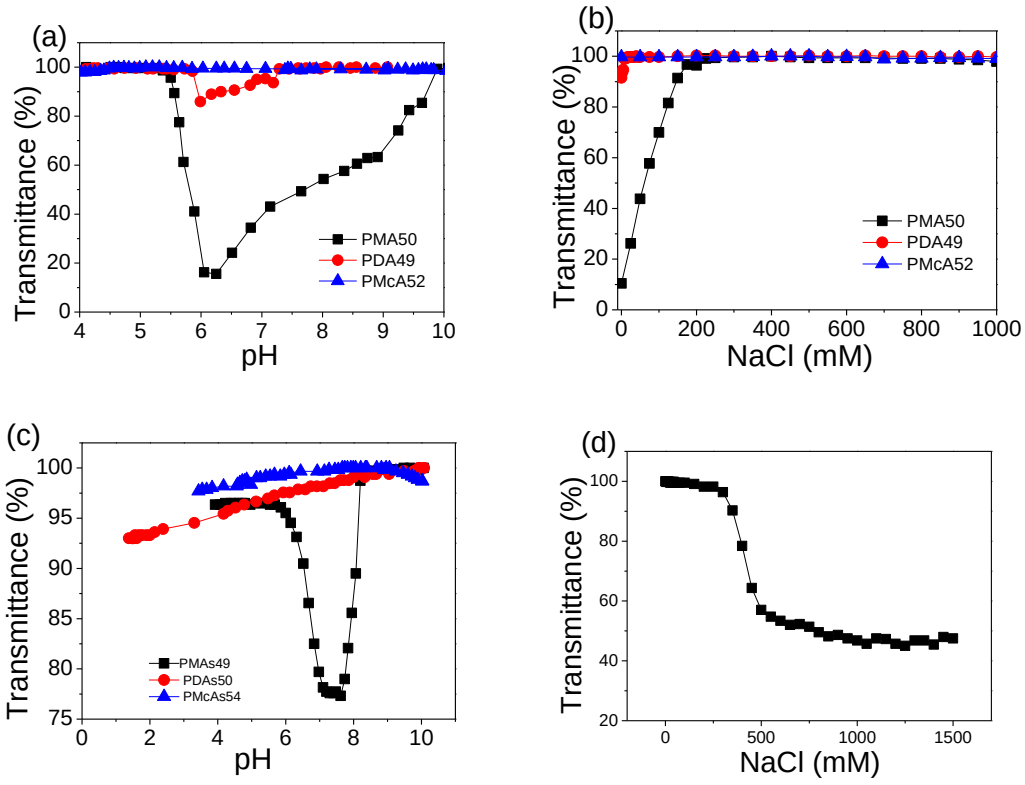

Figure 4A.2. The titration curves: polyampholytes 1 mg/ml with AA and different cationic monomers titrated by (a) NaOH and (b)NaCl; (c) polyampholytes 1 mg/ml with AMPS and different cationic monomers titrated by NaOH, and (d) NaCl titration of PMN45 0.5 mg/ml.

Table 4A.3 The molecular weight of polyelectrolytes

	Mn (kDa)	Mw (kDa)	PDI
PAA	32	105	3.27
PAMPS	77	205	2.70
PNaSS	44	95	2.15
PAPM	151	232	1.53
PDMAPMA	20	50	2.60
PMAPTAc	36	59	1.63

Table 4A.4 The transmittance of polyelectrolyte complex at pH 7.

	PAPM	**PDMAPMA**	**PMAPTAc**
PAA	0.40	0.88	1.47
PAMPS	0.95	0.89	0.66
PNaSS	0.43	0.42	0.57

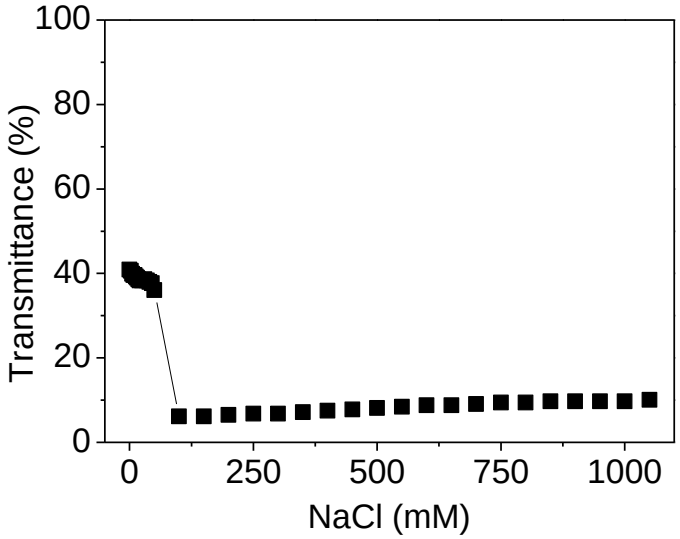

Figure 4A.3 The NaCl titration of PAPM / PAA complex (total 1mg/ml, 1:1 (n:n)) at pH 7, during the polyelectrolyte complex formation, the pH increased from pH 2 to pH7.

4.8.3 References

1. Zhao, J.; Burke, N. A. D.; Stöver, H. D. H. *RSC Adv.* **2016**, *6*, 41522-41531.

Chapter 5. Synthetic Polyampholytes as Macromolecular Cryoprotective Agents

J. Zhao, M. Johnson, R. Fisher, N.A.D. Burke, H.D.H. Stöver

To be submitted.

Contributions: I designed all experiments and performed: synthesis of polybetaines, fluorescent labelling of APM, ^{1}H-NMR, GPC, DSC, most of the polyampholytes synthesses, cryomicroscopy experiments, and part of the cell culture and cryoprotection. Mitchell Johnson did some of the cell culture, cryoprotection and cryomicroscopy experiments. Robert Fisher carried out part of the polyampholyte syntheses and cell cryoprotection experiments. I also wrote the manuscript, with editorial help and feedback from Dr. Stöver.

5.1 Abstract

A series of polyampholytes based on *N*,*N*-dimethylaminopropyl methacrylamide (DMAPMA), acrylic acid (AA) and optionally, *N*-*tert*-butylacrylamide (*t*-BuAAm), were prepared by free radical copolymerization, and tested as cryoprotective agents for 3T3 fibroblast cells by using a freeze-rethaw protocol, using 10% DMSO as control. Polybetaines prepared by reaction of DMAPMA homo and copolymers with 1,3-propanesultone, where used as additional controls. Results showed all of the copolymer composition, molecular weight, polymer concentration and NaCl concentration improved

post-thaw cell viability. Binary (DMAPMA/AA) copolymers gave best cell viability of 70% at 40 mol% excess AA, while introduction of 9 mol% *t*-BuAAm further increased post-thaw cell viability to 90%, all in absence of DMSO, anti-freeze proteins and any other additive. The results show polyampholytes decrease ice crystal size and provide an ice-free local environment for cells because of liquid-liquid phase separation, which reduces cell damage from intercellular ice crystals during the freezing step and may inhibit recrystallization during thawing. The polyampholytes also dehydrate cells during freezing which protects cells from damage due to intracellular ice crystal formation.

5.2 Introduction

Cryopreservation is the process of long term storage of cells, tissues and organs at cryogenic temperatures. To successfully freeze and re-thaw such samples, cryoprotective agents are needed that can protect cell walls from injury through ice crystals formed within or outside of cells. Natural cryoprotective agents include antifreeze proteins found in certain vertebrates, plants, fungi and bacteria, which can inhibit harmful ice growth and recrystallization.[1] Besides natural antifreeze proteins, small molecules such as glycerol and DMSO are commonly used as cryoprotective agents. Glycerol at 10-20 wt% was shown to protect cock spermatozoa at -80 ^{o}C,[2] and is now used at up to 40 wt% for freezing red blood cells.[3] DMSO at 10% is used as a component in cryoprotective media used for many different cell lines.

Anti-freeze proteins are not easily accessed in larger amounts, and have immunological issues where cell transplantation is anticipated.[4,5] Both glycerol and DMSO are considered

cell-penetrating cryoprotectants,[6] which can cause toxicity and require removal immediately after thawing to minimize both cell death and changes in differentiation ability in, e.g., cardiac myocytes, neuron-like cells, and granulocytes.[7-9] As well, removal of glycerol from thawed red blood cells requires additional time to permit out-diffusion from within cells.

Recent research into new cryoprotective agents has focused on both low molecular weight recrystallization inhibitors based on modified sugars,[10-12] anti-freeze proteins mimic polymers[13-17] and polyampholytes.[14,15,18,19] These new cryoprotective agents have lower or no cytotoxicity, can be active in lower concentration of up to 10 wt%, and do not require animal-derived proteins such as fetal bovine serum (FBS). Polyampholyte cryoprotective agents can protect red blood cells,[15] L929, HT-1080,[18,19] certain stem cells,[20] mouse oocytes[21] and mouse embryos,[22] with cell viabilities close to or better than those found with traditional methods.

Polyampholytes are copolymers that carry cationic and anionic groups on different monomer units, and that typically show an anti-polyelectrolyte effect and isoelectric points pH(I), where their net charge is zero. The properties of polyampholytes can be further tuned by incorporating different types of charged[23] as well as hydrophilic or hydrophobic comonomers.[24]

There is a large body of general background knowledge on polyampholytes owing to their significant uses in, e.g., water purification,[25] paper strength enhancement,[26] oil recovery,[27] as non-fouling surfaces,[28] as well as in drug delivery and cell adhesion.[29-31] On the other hand, the use of polyampholytes as cryoprotectants is quite recent, and the mechanisms involved are still being explored. Gibson et al. suggested they act as ice recrystallization

inhibitors, and that a one to one charge ratio is crucial for anti-freezing activity.[14,15] Matsumura et al. found polyampholytes to coat the surface of cells, which can help dehydrate cells during freezing, and protect the cell membrane from damage by interstitial ice crystals.[18,20,32]

The freezing methods using polyampholytes vary, depending on the cell types and polyampholytes, and include different cooling speed, sample volume and cryoprotective agent compositions. For example, polyampholytes can serve as single component cryoprotective agent, requiring high ionic strength with slow freezing, e.g. at 1 degree/min in a -80 ^{o}C freezer.[18,20,32-34] Elsewhere, polyampholytes have been combined with other cryoprotective agents, including hydroxyethyl starch,[15] and ethylene glycol,[21,22,35,36] in processes based on rapid freezing in liquid nitrogen. Some studies claim that polyampholytes require excess anionic charges,[20,21,33-36] while others are reported good results with stoichiometric polyampholytes having 1:1 charge ratios,[15,18,34] with molecular weights ranging from 4 to 311 kDa.

It is clear that polyampholytes have significant potential to complement or even replace DMSO and other small molecule cryoprotectants, serving as non-penetrating agents. In this work, we aim to investigate the potential of a group of polyampholytes to serve as single cryoprotective agents, and explore their fundamental mechanism. Specifically, we prepared binary and ternary polyampholytes with different molecular weights by free radical copolymerization of *N*,*N*-dimethylaminopropyl methacrylamide (DMAPMA), acrylic acid (AA) and optionally, *t*-butyl acrylamide (*t*-BuAAm), and explored their ability to act as cryoprotective agents for 3T3 mus musculus fibroblast cells. We focused on cationic/anionic comonomer ratios of 30/70 and 50/50 mol% DMAPMA / AA prepared as

described recently,[37] with low compositional drift and three different molecular weights, using a standard freezing protocol involving freezing at about 1 degree/minute in a -80 ^{o}C freezer and thawing at 37 ^{o}C, and using 10% wt DMSO as control.[38,39] In addition, polybetaines were prepared by quantitative reaction of the tertiary amines in PDMAPMA homopolymer and P(DMAPMA-*co*-AA) (60:40) with 1,3-propanesultone, and used as secondary controls.

We first compared the cryoprotective properties of the binary P(DMAPMA-*co*-AA) copolymers containing 30 and 50 mol% cationic groups, and the polybetaines, and subsequently took the best candidates from these screens to test the effects of polymer concentration, ionic strength and incorporation of hydrophobic comonomer *t*-BuAAm on cell post-thaw viability. Finally, differential scanning calorimetry (DSC) and optical cryomicroscopy were used to study the polymer phase separation behavior and the interaction between polymer, ice crystals and cells during the freezing and thawing processes.

5.3 Materials and Experiments

5.3.1 Materials:

Acrylic acid (AA, 99%) was purchased from Sigma-Aldrich, and distilled before use. *N*,*N*-Dimethylaminopropyl acrylamide (DMAPAM, 99%) from Sigma-Aldrich was neutralized using concentrated HCl, with stirring in an ice bath, the concentration was measured by ^{1}H-NMR. *N*-(3-Aminopropyl)methacrylamide hydrochloride (APM), ethylene carbonate (98%), *N*-*tert*-butylacrylamide (*t*-BuAAm 97 %), 1,3-propanesultone (98 %) 2,2'-

azobis(2-methylpropionamidine)dihydrochloride (Vazo-56), L-cysteine hydrochloride monohydrate (98%), 2-(cyclohexylamino)ethanesulfonic acid (99%), fluorescein isothiocyanate isomer 1 (FITC, ≥90%), *N*,*N*-dimethylformamide (DMF, reagent grade) from Sigma-Aldrich were used as received. Deuterium oxide (D_2O) was purchased from Cambridge Isotope Laboratories (Andover, MA). Sodium hydroxide and hydrochloric acid solutions (0.10 and 1.0 M each) were obtained from LabChem Inc. Dulbecco's Modified Eagle Medium (DMEM) (high glucose), phosphate-buffered saline (PBS), bovine calf serum (BCS), Trypsin-EDTA (0.05%) and Trypan Blue (0.4 % wt) were obtained from ThermoFisher Scientific. Polypropylene cryo tubes with external thread screw caps (2 ml) were obtained from Sarstedt AG & Co (Germany).

5.3.2 Batch Free Radical Solution Copolymerization

5.3.2.1 Synthesis of Polyampholytes

Solution copolymerizations were carried out at 55 °C in 60 mL Nalgene bottles on a set of horizontal steel rollers fitted with an enclosure and a thermostatted heater pad, with 10% (w/v) total monomer loading, 1 mol% initiator (Vazo-56, relative to total monomer), in distilled water. Batch comonomer feed ratios for DMAPMA: AA of 45:55 and 30:70 were used to form the binary copolymers. Different amounts of chain transfer agent (CTA, L-cysteine hydrochloride monohydrate): 0 mol%, 1 mol% and 5 mol% were added to control the molecular weight. For the DMAPMA/AA/*t*-BuAAm ternary copolymers, 5, 10 and 30 mol% *t*-BuAAm were used, with the DMAPMA/AA ratio held at 30:70, using a 1:1 (v:v) water/methanol mixture with 1 mol% chain transfer agent. Fluorescently labelled

polyampholytes were synthesized as above, with adding 1 mol% of fluorescently modified APM, as described in detail in the supporting information.

The copolymerizations were monitored by removing small aliquots by glass pipette, diluting these with D_2O, and determining conversion by ^{1}H-NMR on a Bruker Avance 600. The areas of the vinyl signals of AA at 5.5 ppm and of DMAPMA at 5.3 ppm relative to an internal standard (ethylene carbonate) were used to determine the conversion of the two monomers, and polymerizations were stopped at 60-80% conversion. After polymerization, the cooled reaction mixtures were added into a 4.5-fold excess of acetone in order to precipitate the polymers, then the mixture was centrifuged at 4000 rpm for 10 min, and the supernatant removed. The polymers were re-dissolved in distilled water and the precipitation repeated a total of four times. The polymers were dialyzed against distilled water in cellulose tubing (3.5 kDa MW cutoff) for 4 days with daily water changes. Finally, the purified polymers were isolated by freeze drying.

5.3.2.2 Synthesis of Polybetaines

PolyDMAPMA and poly(DMAPMA-*co*-AA) (60:40) were prepared in presence of 1% chain transfer agent, as described above. The purified polymers were dissolved at 5 wt% in distilled water, the solution adjusted to pH 10 by addition of small amounts of NaOH, and 1.1 equivalents of 1,3-propanesultone relative to tertiary amine groups were added and the reaction mixture stirred for 24 hrs at room temperature.[40] The resulting polybetaines were purified by quadruple precipitation into excess acetone as described above.

The nomenclature used to describe the binary copolymers is based on: PDA_x, where D, A, and x stand for DMAPMA, AA, and mol% DMAPMA in the polymer. Analogously, $PDAt_x$ is used for the ternary copolymers, where D, A, t and x stand for DMAPMA, AA, *t*-BuAAm and mol% *t*-BuAAm in the polymer, the ratio of DMAPMA and AA are kept at 3:7, the detailed ratio are shown in Table 5.1. The polybetaines are poly[3-((3-methacrylamidopropyl)dimethylammonio)propane-1-sulfonate] or PSPB, and poly[3-((3-methacrylamidopropyl)dimethylammonio)propane-1-sulfonate]-*co*-acrylic acid or $PSPBA_{60}$, where 60 is the mol% betaines in the polymer.

5.3.3 ^{1}H-NMR Analysis of Copolymers

Copolymer (10 mg) was dissolved in 1 mL D_2O, and the ^{1}H-NMR spectra measured using a Bruker AV 600 NMR spectrometer, to detect any residual monomer left after purification. In addition, the comonomer ratios in PDA_x were calculated from the areas of the DMAPMA methylene signals between 2.5 and 3.5 ppm (4H) compared to the combined signals of DMAPMA and AA between 0.5 to 2.5 ppm (13H of DMAPMA and 3H of AA). For other copolymers, the comonomer ratios were calculated from the monomers consumed during polymerization, by tracking the monomer signals, as illustrated in Figure 5A.2.

5.3.4 GPC Analysis

The molecular weights (MWs) of the polymers were measured using an aqueous gel permeation chromatography (GPC) system consisting of a Waters 515 HPLC pump, Waters 717plus auto-sampler, three columns (Waters Ultrahydrogel-120, -250, -500; 30 cm, 7.8 mm dia.; 6 μm particles; 0-3, 0-50, 2-300 kDa MW ranges), and a Waters 2414 refractive index detector calibrated with narrow disperse poly(ethylene glycol) standards (Waters). The mobile phase was 1 M sodium acetate/acetic acid buffer adjusted to pH 4.7 for PDMAPMA and polybetaine, 0.025 M CHES buffer adjusted to pH 10 and containing 0.5 M $NaNO_3$ for other polyampholytes.

5.3.5 Cell Culture, Cryoprotection and Proliferation

NIH 3T3 cells were cultured in Dulbecco's modified Eagle's medium (DMEM) supplemented with 10% BSA. Cells were cultured at 37 °C in a 5% CO_2 incubator. When the cells were 70-80% confluent they were washed 3 times with PBS and then treated with trypsin solution (0.25% [w/v] trypsin containing 0.02% [w/v] ethylenediaminetetraacetic acid in PBS), and incubated for 5 mins to detach the cells. The cells were centrifuged at 500 g for 5 min, then the pellet was resuspended with fresh DMEM without BSA.

Polymer solutions with different polymer compositions, polymer concentrations, and NaCl concentrations were prepared in DMEM without BSA and adjusted to pH 7.3 - pH 7.6. All polymer solutions were syringe-filtered through 0.22 μm filters and stored at 4 ^{o}C. One million 3T3 cells were mixed in 1 mL cryoprotection solution in a 2 ml polypropylene cryo tube, the cryo tubes were placed in a Mr. Frosty container filled with isopropanol, which

was then transferred to a -76 °C freezer without controlling the cooling rate (approximate 1 °C/min) for 24 h. For longterm cryostorage, the vials were subsequently transferred into liquid nitrogen. Frozen vials were thawed in a 37 °C water bath for approximately 3 to 5 min, immediately diluted 10-fold with DMEM containing BSA, and mixed well at room temperature. The resulting cell suspensions were centrifuged at 500 g for 5 min, and the pellets resuspended in 1 mL fresh DMEM with BSA. To count cells, 200 µl of cell suspension were stained with 20 µl trypan blue solution and counted on a hemocytometer. Cell viability was calculated as the ratio of viable cells to the total number of cells.

After freezing, cells with 70 to 90% viability (except the sample frozen by 2% DMSO which had 0% viability) were seeded at a cell density of $1 \times 10^4/cm^2$ per well in 12 well-plate with 2 ml of DMEM with 10% BSA. Cells were monitored after 1 and 3 days growing by Zeiss Axiovert 200 optical microscope fitted with an AxioVs40 V 4.8.2.0 software.

5.3.6 Statistical Analysis

All cell data are expressed as the mean ± standard deviation (SD). A two-tailed Two-Sample Assuming Unequal Variances T-test was used. Differences were considered statistically significant at a P value of <0.05.

5.3.7 Cryomicroscopy Experiments

FITC-labeled polymers were dissolved in DMEM (10% wt) (with/without cells and without BSA) and the pH adjusted to 7.3-7.6. 20 µl of the polymer solutions with/without

cells were dropped on a glass cover slide, and covered with another cover slide, without use of any spacer. Samples were cooled and heated at 1 ^{o}C/ min on a Linkam THMS 600 microscopy stage (CI 94 control unit, Linksys32 software, cooling was done using a stable flow of liquid nitrogen by teflon tubing into the thermal stage) attached to a Nikon ECLIPSE LV100ND optical microscope fitted with an ANDOR ZYLA-5.5-CL10 digital camera and NIS-Elements AR 4.30.02 software.

5.4 Results and Discussion

5.4.1 Copolymerization

In copolymerizations of two or more comonomers, knowledge of the reactivity ratios helps assess the drift in the instantaneous copolymer composition with increasing conversion, and gives some insight into comonomer sequence distributions.

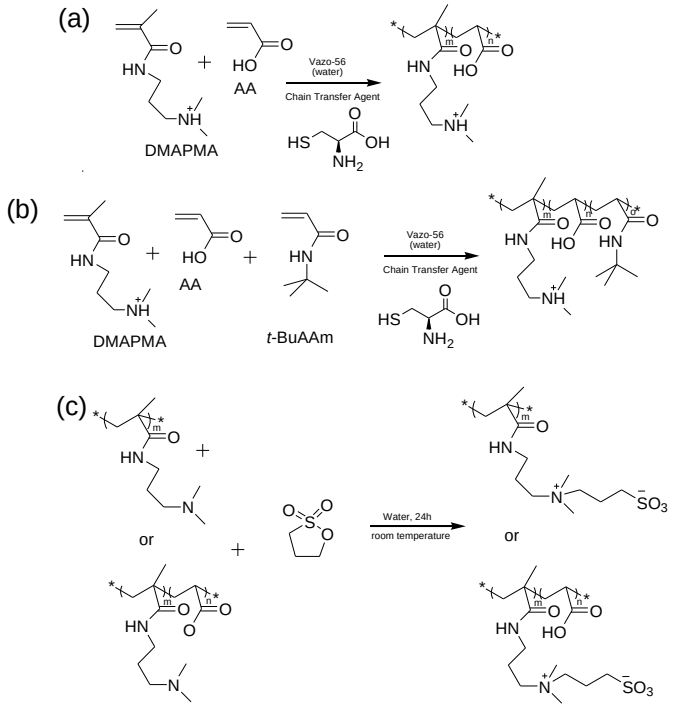

Scheme 5.1 Synthesis of (a) Poly(DMAPMA-*co*-AA) (b) Poly(DMAPMA-*co*-AA-*co*- *t*-BuAAm), (c) Polybetaine formed by modification of PDMAPMA and P(DMAPMA-*co*-AA).

The reactivity ratios of DMAPMA and AA in the binary copolymerizations were measured by ^{1}H-NMR during copolymerization, using a method described in previous work,[37] and found to be r_1(DMAPMA) = 0.59 and r_2(AA) = 0.42, suggesting a tendency towards alternating copolymerization with relatively little compositional drift during the copolymerization. The instantaneous DMAPMA content as function of DMAPMA feed ratio is shown in Figure 5A.1, showing a crossover point at 60 mol% DMAPMA. In order to ensure a net anionic charge and minimize cationic patches, the initial comonomer feed ratios were set at 30:70 and 45:55. Table 5A.1 shows the estimated corresponding drifts in instantaneous copolymer composition, indicating that the DMAPMA content decreases from 38% to 30%, and from 49% to 46%, respectively, as conversion increases from 10% to 70%. The slight tendency towards alternation for DMAPMA and AA leads to low calculated incidences of DMAPMA block of 4% and 12%, respectively, which is expected to contribute to low cell toxicity and low binding to media proteins.[41,42] Table 5.1 summarizes the compositional and MW information of the polyampholytes and polybetaines.

Table 5.1 Polyampholyte characterization

	Feed ratio (DMAPMA:AA)	CTA[b] (%)	Conversion (%)	%DMAPMA (NMR)	Mn (kDa)	Mw (kDa)	PDI
PDA_{30} 1	31:69	0	89	32:68	133	306	2.3
PDA_{30} 2	30:70	1	57	35:65	49	116	2.4
PDA_{30} 3	31:69	5	89	33:67	11	19	1.7
PDA_{45} 1	46:54	0	70	47:53	128	271	2.1
PDA_{45} 2	46:54	1	58	47:53	31	68	2.2
PDA_{45} 3	46:54	5	67	47:53	9	15	1.8
$PDAt_3$	28.5:66:5.5[a]	1	67	32:65:3	43	107	2.5
$PDAt_9$	27:63:10[a]	1	62	31:60:9	46	99	2.2
$PDAt_{20}$	21:49:20[a]	1	76	29:52:20	24	48	2.0
PDMAPMA	-	0	-	-	20	51	2.6
PDA_{60}	61:39	1	78	59:41	25	57	2.3
PSPB	-	-	-	-	51	156	3.1
$PSPBA_{60}$	-	-	-	-	35	70	2.0

a: feed ratios for DMAPMA: AA:*t*-BuAAm.

b. CTA: chain transfer agent

In Table 5.1, the binary polyampholytes prepared from DMAPMA and AA have average compositions within 5% of initial comonomer ratios. L-cysteine was used successfully as chain transfer agent to adjust MW, without affecting the comonomer ratio in the copolymers. Ternary copolymers with DMAPMA, AA and *t*-BuAAm also showed copolymer compositions within 5% of initial comonomer feed ratios. Figure 5A.2 shows ^{1}H-NMR spectra of a PMA_{30} copolymerization, taken before and after polymerization, and after purification. All other polymerizations were done in the same way, by determining the actual initial feed ratio from the pre-polymerization ^{1}H-NMR signals of the monomers, while comonomer conversion and copolymer composition were determined from the

decrease of the monomer signals relative to an internal standard. Conversions were limited to 60% to 80% in order to reduce compositional drift during copolymerization. The purified polymers were analyzed by ^{1}H-NMR, to confirm the absence of small molecules such as monomers, initiator and chain transfer agents.

The polybetaines were formed by betainization of poly(DMAPMA) homopolymer and DMAPMA/AA copolymers. Figure 5A.3 shows the ^{1}H-NMR spectra of PDMAPMA homopolymer before and after betainization (Figure 5A.3a), and of PDA_{60} and the corresponding betainization product, $PSPBA_{60}$ (Figure 5A.3b). After betainization, there are the expected new peaks g, h, i from the side chain of the betaine, and the *N*-methyl peak has moved from δ 2.9 (F) to δ 3.2 (f), both indicating that the betainization has proceeded with close to 100% yield.[40]

The monomers and the polymerization method in this work were carefully selected. The tertiary amine in DMAPMA is believed to give better anti-freezing activity compared with the primary amine in, e.g., *N*-(3-Aminopropyl)methacrylamide hydrochloride (APM).[14] As well, we recently reported that the stoichiometric polyampholytes comprised of AA with APM show liquid-liquid phase separation over a broad range about their pH(I) of about 7, at [NaCl] below 200 mM,[37] with even stronger phase separation observed for the corresponding APM/methacrylic acid copolymers.[24,29] In order to increase the anti-freezing activity and avoid the phase separation, DMAPMA and AA were selected as cationic and anionic comonomers.

DMAPMA and AA are known to form almost drift-free copolymers based on the reactivity ratio and average molecular weight was controlled by chain transfer agents, leading to

molecular weight dispersity is similar to those used in previous studies on polymer cryoprotection agents.[15,16,43,44]

5.4.2 Cryoprotection

The above copolymers were tested as cryoprotectants for 3T3 cells in DMEM media without BCS. Figure 5.1 shows cell viability after a freeze-thaw cycle in presence of 10 wt% PDA_{30} and PDA_{45} with different molecular weights, using 10 wt% DMSO in DMEM as control.

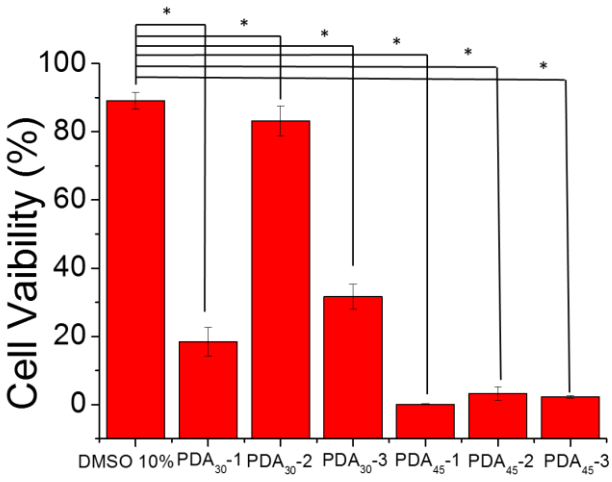

Figure 5.1 Cell viability of 3T3 cells after a freeze-thaw cycle in presence of PDA_{30} and PDA_{45} with three molecular weights, at 10 wt% polymer, and [NaCl]=150 mM in DMEM. PDA_{30}-1,-2,-3 stand for PDA_{30} with Mn of 133, 49 and 11 kDa, respectively, while PDA_{45}-1,-2,-3 stands for PDA_{45} with Mn of 128, 31 and 9, respectively. Data are expressed as the mean ± SD for three independent experiments (each sample was counted twice). *P <0.05.

Figure 5.1 shows a significant dependence of cryoprotectant effectiveness on both composition and molecular weight. One striking finding was that PDA_{30} conveyed up to 80% post-thaw viability, similar to DMSO, while the PDA_{45} regardless of molecular weight did not show any cryoprotective activity. This will be discussed in detail further below.

Another surprising finding was how strongly the cryoprotective abilities of PDA_{30} depended on the molecular weight, with post-thaw cell viability at a maximum at intermediate MW (Figure 5.1) around 40 kDa, which is in agreement with other polymer cryoprotective agents.[17,44,45] Several mechanisms may be involved in this strong effect of molecular weight on cell viability: ice nucleation, polymer phase separation, and cell-polymer interactions. It is known that polyampholytes can interfere with ice nucleation,[18,15] and it is thus possible that this property depends on polyampholyte molecular weight, as was recently shown for poly(vinyl alcohol).[46] Second, the interaction between polymer and cell membranes has been shown to play an important role in cell cryoprotection,[18] and this effect may also be dependent on polymer molecular weight.

The strong effect of polymer composition on cell viability is in agreement with some literature reports stating that non-stoichiometric polyampholytes with net negative charges are better cryoprotectants than stoichiometric, neutral polyampholytes.[20-22,34-36] Some stoichiometric polyampholytes gave good viability but only when used together with additives such as hydroxyethyl starch.[15]

On the other hand, there are also reports stating that in some cases non-stoichiometric and stoichiometric polyampholytes work equally well, or where the non-stoichiometric one works even a little better.[19,32,33] Others have used stoichiometric poly(DMAEMA-*co*-

MAA).[18,34] It is possible that these, formally stoichiometric, copolymers, actually had a net negative charge during use: the pKa values of the amine and acid groups in poly(DMAEMA-*co*-MAA) are 8.3 and 4.65,[29,47] giving a calculated isoelectric pH for the stoichiometric poly(DMAEME-co-MAA) of about 6.5, which means it should have a small, negative charge at pH 7 or 7.4. In addition, it is known that DMAEMA can partly hydrolyze during the polymerization in aqueous media, leading to more, anionic, MAA units in the copolymer than expected.[48] Finally, DMAEMA was found to undergo transesterification in methanol or methanol mixture during polymerization[49] and form a noticeable amount of methyl methacrylate, which would end up replacing some of the cationic groups in the polymer with neutral hydrophobic groups. These reasons together suggest that the net charge of a nominally 1:1 DMAEMA-MAA copolymer can easily become negative at pH 7.4, and may explain why these formally stoichiometric polyampholytes work as well as the non-stoichiometric polyampholytes. In this context, it may be useful to emphasize that reactivity ratios and degree of conversion can also significantly affect the final comonomer ratio, and hence charge balance, and should thus be reported.

To further explore the effect and role of negative charges in cryoprotection, a polybetaine (PSPB) as a neutral polymer,[50,51] as well as a polybetaine ($PSPBA_{60}$) containing 40 mol% net anionic charges, were compared with polyampholytes as shown in Figure 5.2. The PSPB with zero net charge gave cell viabilities of less than 10%, similar to those for PDA_{45}. On the contrary, the post-thaw cell viability increased to 60% in presence of $PSPBA_{60}$. $PSPBA_{60}$ has 40% anionic groups at pH 7.4, and hence a net charge close to that of $PDA_{30.}$ Of course, there exist natural antifreezing proteins with net anionic and with net cationic charges, so the need for excess anionic charges shown for the two groups of polymers

described here may not be general, in particular as natural anti-freeze proteins may work by a range of mechanisms not limited to reducing ice crystal size.

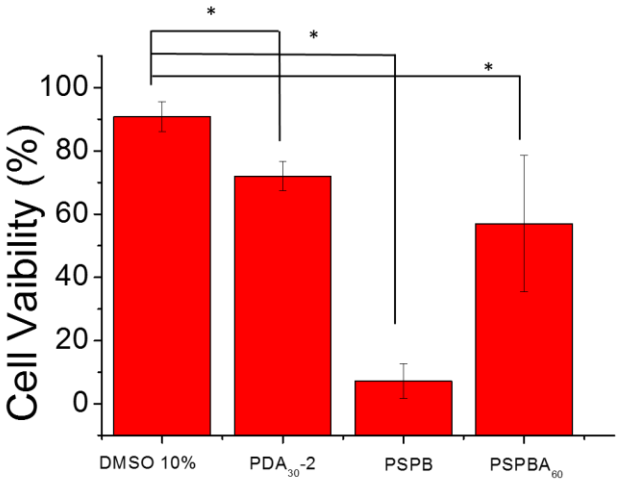

Figure 5.2 The post-thaw cell viabilities for polyampholyte PDA_{30}-2, betaine homopolymer PSPB, and betaine/AA copolymer $PSPBA_{60}$, for [polymer] = 10% wt, and [NaCl]=150 mM. Data are expressed as the mean ± SD for three independent experiments (each sample was counted twice). *P <0.05.

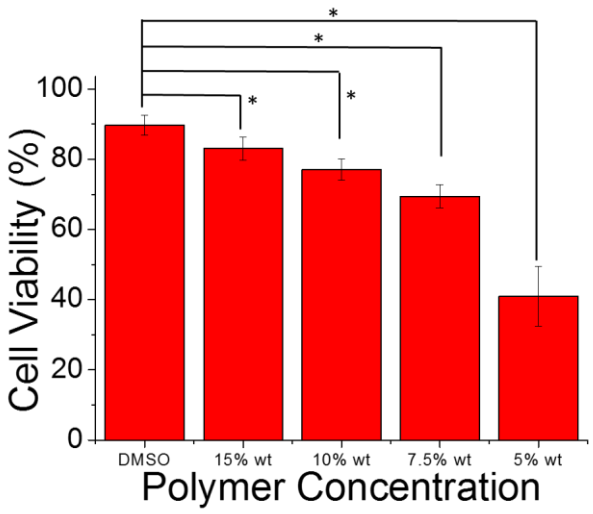

Figure 5.3 Cryoprotective properties of PDA_{30}-2 at different concentrations, with [NaCl] = 150 mM. Data are expressed as the mean ± SD for three independent experiments (each sample was counted twice). *P <0.05.

The cell viability was also found to depend on the polymer concentration. Figure 5.3 shows the cell viability decreasing from 83% to 41% with PDA_{30}-2 concentration decreasing from 15% to 5%. The effect of polymer concentration may come from at least two parts. First, higher polymer concentration may produce smaller ice crystals,[17,20,52] or inhibit recrystallization of ice during thawing, second, the as known before, for slow freezing process, the concentration of extracellular solute increases during freezing, the high viscosity solute solution separates the ice crystals and maybe inhibit recrystallization.[39] However, 10 %wt is a preferable concentration compared with 15%wt, because cell suspensions containing 10 %wt copolymer have lower viscosity, making them easier to handle.

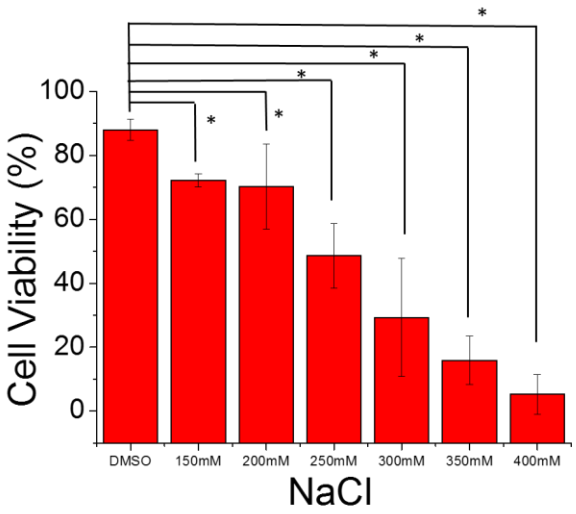

Figure 5.4. Cryoprotective properties of PDA_{30}-2 at various NaCl concentration. [Polymer] =10 %wt. Data are expressed as the mean ± SD for three independent experiments (each sample was counted twice). *P <0.05.

Because the dehydration rate is a key factor of cell cryoprotection, increase NaCl concentration should help cells dehydrate, and so higher NaCl concentrations are often reported to increase post-thaw cell viability.[18-21] The effect of NaCl concentration on post-thaw cell viability was measured here by adding aliquots of 5M NaCl solution into DMEM media. In Figure 5.4, the cell viability in presence of 10% PDA_{30}-2 was not affected going to 200 mM NaCl, and then decreased with further increases of NaCl concentration. Hence it appears that the polymer itself is sufficient for cells to dehydrate during freezing, while excessively high NaCl concentrations are detrimental.

However, the best cell viabilities are still lower than those for 10 wt% DMSO. In attempts to further increase the cell viabilities, small amounts of hydrophobic comonomer *t*-BuAAm were incorporated into the PDA_{30} copolymer while keeping the DMAEMA: AA ratio constant. Increasing the hydrophobicity of polyampholytes has previously been found to improve the cell viability.[18,34]

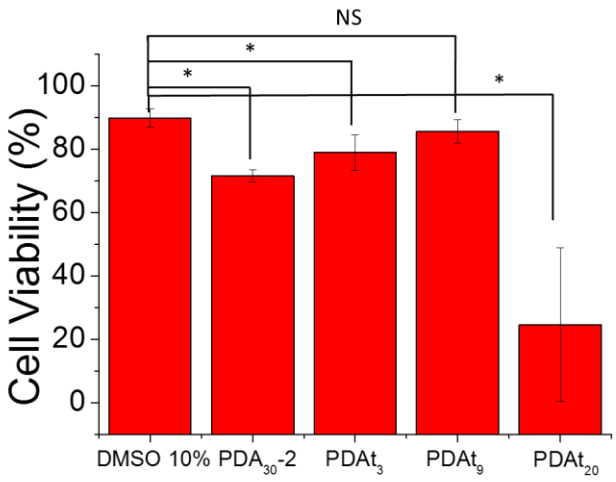

Figure 5.5 Cryoprotective properties at increasing *t*-BuAAm concentrations. [Polymer]=10% wt, [NaCl]=150 mM. Data are expressed as the mean ± SD for three independent experiments (each sample was counted twice). *P <0.05.

As shown in Figure 5.5, incorporating 3 and 9 mol% *t*-BuAAm increases the viability to 80 and 86%, respectively. Further increases in *t*-BuAAm to 20 mol% caused the viability to drop again, to 24%. This suggests the cryoprotection of 3T3 cells is related to the hydrophobicity of the polyampholyte, possibly involving improved polymer binding to the cell membrane.[20,53] As well, hydrophobic groups have been shown to decrease the size of the ice crystals.[18] Both PDA_{30}-2 and $PDAt_9$ after storage in liquid nitrogen for one month, (Figure 5A.4) have high viability.

To study the mechanism of cryoprotection of these polyampholytes, PDA_{30}-2 was selected as standard cryoprotectant for cryomicroscopy experiments using the same cooling rate as in cell freezing of 1 ^{o}C/min. As shown in Figure 5.6 B and C, after freezing, the average

ice crystal size for PDA_{30}-2 is about an order of magnitude smaller than those in DMEM media (Figure 5.6A), indicating that PDA_{30}-2 decreases the size of ice crystal, as reported for other polyampholytes.[14,15,18] Fluorescence optical microscopy (Figure 5.6C) shows distinct bright polymer-rich and dark ice-rich phases. The cryoprotectant solutions phase separate upon freezing into a polymer-rich liquid and solid ice. Figure 5A.5 shows the DSC curves of PDA_{30}-2 solutions and DMEM media, similar to previous findings,[13,54,58] both have sharp exothermic peaks, but the crystallization of water in PDA_{30}-2 solution only goes to 80% completion at -25 ^{o}C, compared with DMEM media, suggesting that about 10% of the water is not frozen in presence of 10 wt% polyampholyte. The lower freezing point of PDA_{30}-2 also indicates anti-freezing properties of the polymer.[54] DSC results show that when the temperature goes below -25 ^{o}C, some residual water in the polymer rich phase does not freeze, but rather stays in the liquid state by bonding to polymer and further decreasing the vitrification temperature of this phase.

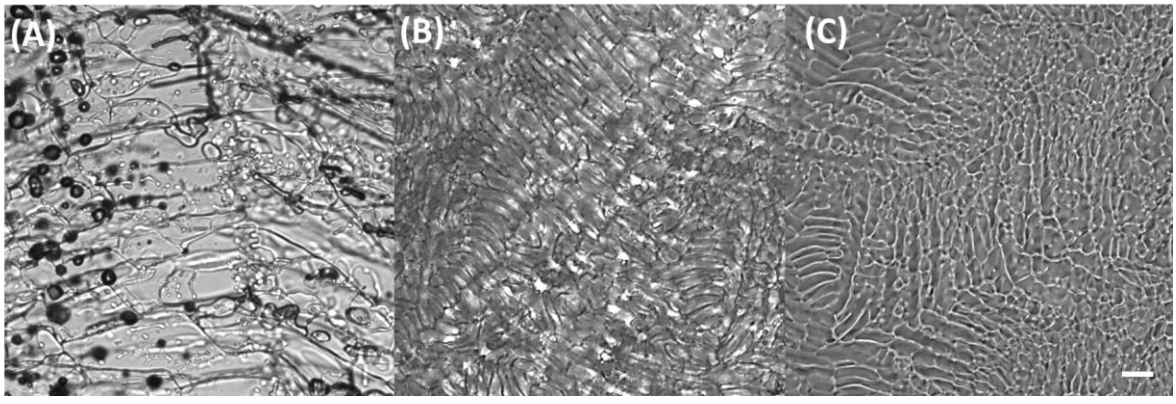

Figure 5.6 The transmission microscope images of (A) DMEM media at -43.5 ^{o}C; (B) PDA_{30}-2 at -40.6 ^{o}C; (C) PDA_{30}-2 at -44.6 ^{o}C; (A), (B): optical microscopy images and

(C): fluorescence microscopy images. Cooling rate: 1 °C/min. Length bar: 50 µm. Polymer concentration 10 %wt.

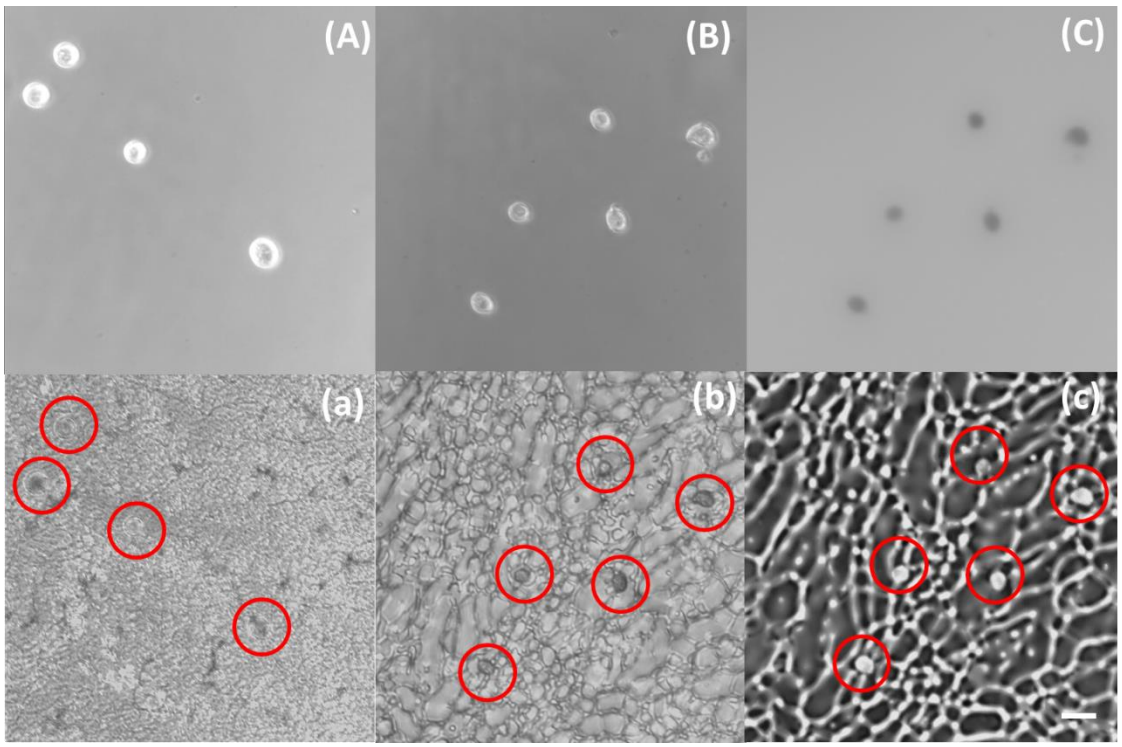

Figure 5.7 The transmission microscope images of DMEM media with 3T3 cells (A) at 0 °C before freezing, (a) at -30 °C; PDA_{30}-2 with 3T3 cells (B) at 8.2 °C before freezing, (b) at -31.2 °C; (C) at 10.4 °C after thawing, (c) at -30.2 °C. (A), (a), (B), (b): optical microscopy images and (C), (c): fluorescence microscopy images. Cooling rate: 1 °C/min. Length bar: 25 µm. Polymer concentration 10 %wt.

In Figure 5.7a, 3T3 cells frozen in DMEM media are indistinguishable from the surrounding ice, but cells frozen in 10 wt% PDA_{30}-2 solution are much more easily found. In Figure 5.7C cells appeared dark before freezing because only the polymer was

fluorescently labeled, while the cells where not. That means before freezing there was no polymer bonding to, or entering into, cells. After freezing, in Figure 5.7b and c, cells are located in the polymer-rich phase, and appear bright, indicating they are coated with, or surrounded by, polymer, and located in the interstitial spaces between ice crystals. Because the water in the polymer-rich phase does not crystallize down to at least -25 ^{o}C, there are three ways these polymers may work to cryoprotect the cells: the polymer leads to smaller ice crystals in the bulk sample, provides an ice-free local environment immediately around the cells, and facilitates cell dehydration to inhibit ice crystallization within cells. (In Figure 5A.6 the cells in PDA_{30}-2 are smaller both before and after freezing than in DMEM media).

Figure 5.8 shows the thawing process of PDA_{30} solution, with analogous results for DMEM media shown in Figure 5A.7. During freezing, ice near cells melts faster, creating a buffer zone between cells and remaining ice. The polymer concentration in the interstitial, polymer-rich phase around cells during thawing is higher than 10 wt%, given the presence of significant residual ice, and both the buffer zone and the high polymer concentration can protect cells from ice recrystallization during the thawing stage, which is thought the most harmful factor for cryoprotection.[55,56] In contrast in Figure 5A.7, in DMEM, cells are closely surrounded by ice, making it hard to distinguish cells and ice, in Figure 5A.7 1-6, which suggests again the cells and ice are in close proximity to each other, and hence more liable to damage from recrystallization. The thawing of PDA_{30}-2 also appears faster than for DMEM in Figure 5A.5b, which is also helpful to protect cells.

This phenomenon is called the "pre-melting water",[57] and was closely studied by Raman and broadband dielectric spectroscopy for frozen hydrogels containing poly(methyl vinyl ether). It was observed that heating from the frozen state at -60 ^{o}C increased the mobility

of polymer, and the polymer will facilitate early melting of ice near it, through hydrogen bonding with the molten water molecules. So during melting, before the bulk ice starts to melt, ice near the polymer-rich phase has already melted and bonded with cells, so the cells in the polymer phase are covered by concentrated polymer solution. This polymer solution resists recrystallization and thus protects cells from the ice crystals and ice recrystallization during the melt phase. After thawing, the cells are all back to dark in Figure 5A.8b, same with Figure 5.7C indicating no polymer is retained on or within cells.

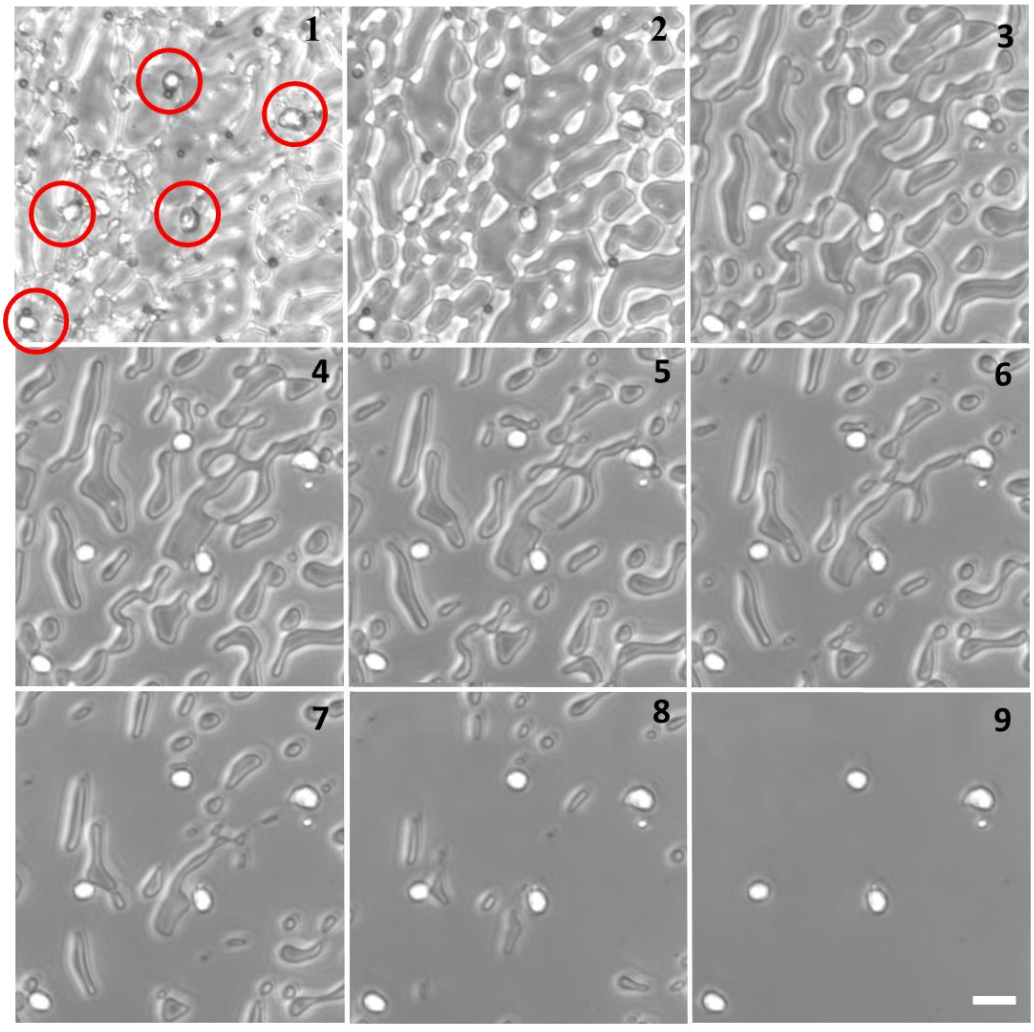

Figure 5.8 The transmission microscope images of 3T3 cells thawing in PDA_{30}-2, Polymer concentration 10 %wt. From 1 to 9, temperature from -30 ^{o}C to room temperature under passive warming over 5 minutes, size bar: 25 μm.

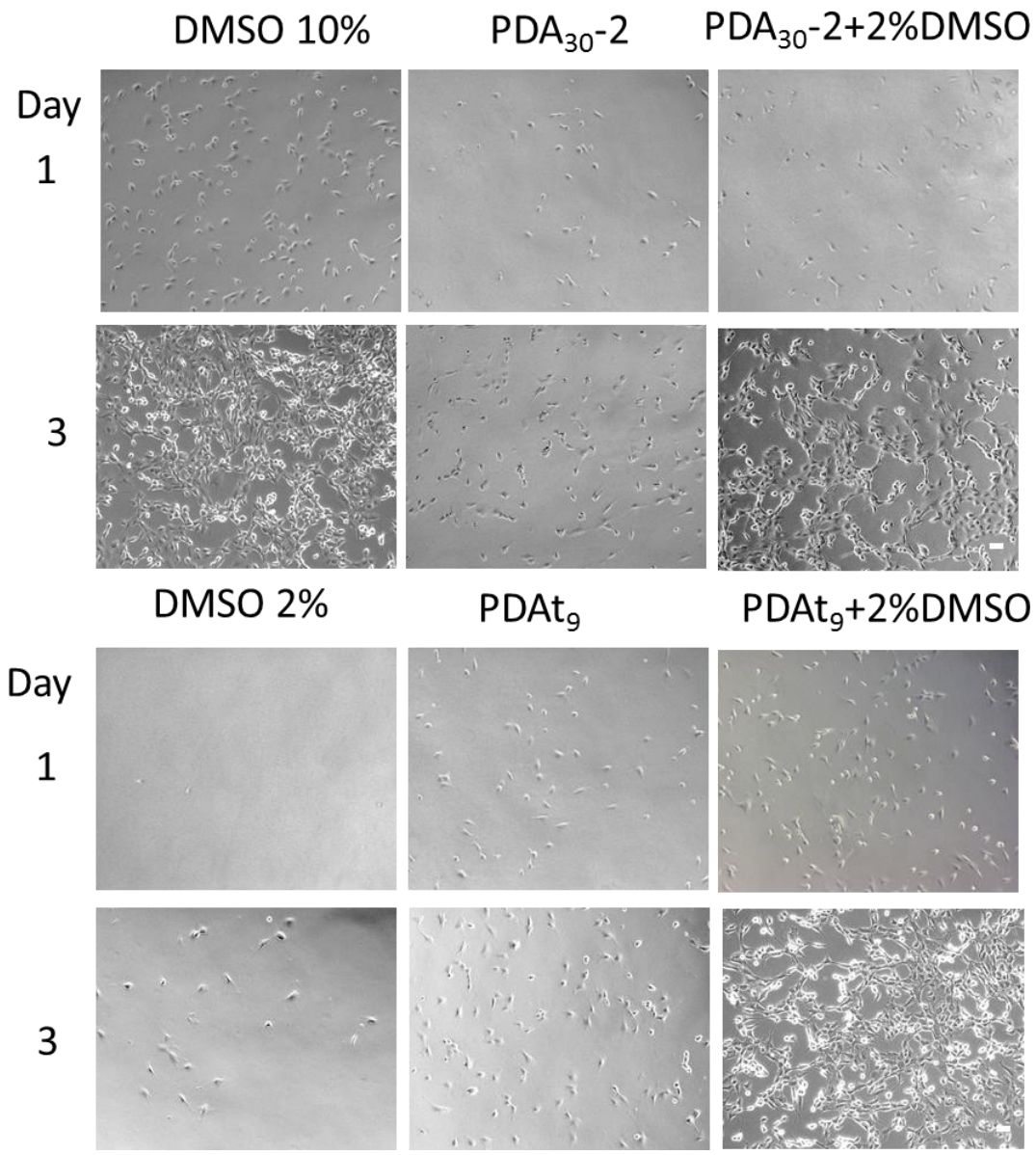

Figure 5.9 The microscope pictures of 3T3 cells culture after thawing. DMSO 10 %wt，polymer concentration 10 %wt, and polymer 10 %wt with DMSO 2 %wt. Cell number is $1 \times 10^4/cm^2$ in 12 well-plate with 2 ml growth medium, Scale bar: 50 μm.

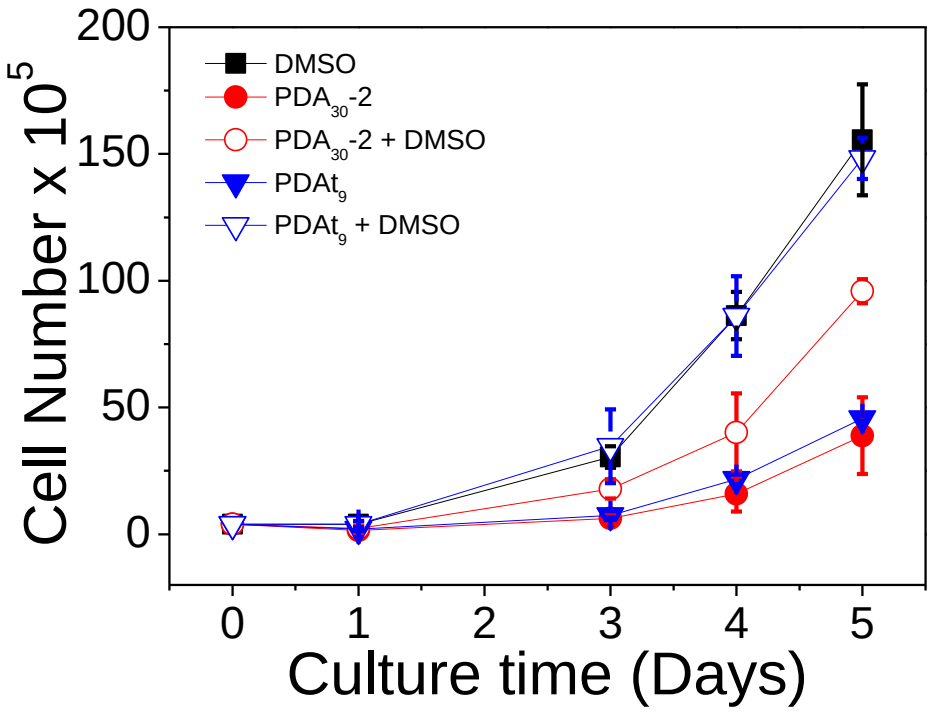

Figure 5.10 Growth curves of 3T3 cells frozen by DMSO and polyampholytes for 5 days. Data are expressed as the mean ± SD for three independent experiments.

The results above show the polyampholytes are very effective as a non-permeable cryoprotective agents, as judged by cell viability immediately after thawing. Another important measure of cryoprotection is long term health of thawed cells including ability to attach and proliferate. Figure 5.9 indicates that, at the same seeding densities of live cells of $1 \times 10^4/cm^2$, cells frozen in presence of PDA_{30}-2 or $PDAt_9$ have much lower degrees of attachment after 24hs and much lower cell numbers after 3 days of culturing, compared with cells frozen with 10% DMSO. To improve the cell attachment and viability after thawing, 2% DMSO was added with 10% PDA_{30}-2 and $PDAt_{27}$. 2% DMSO is not enough to protect cells by itself, as shown in Figure 5.9 with only a few cells attached after 3 days

culture. However, PDA_{30}-2 and $PDAt_{27}$ together with 2% DMSO lead to significantly improved cell attachment and proliferation, comparable to results obtained using 10% DMSO shown in Figure 5.10.

The good cell viability but low cell attachment observed when using only polyampholytes as cryoprotectants suggest these non-permeant polyampholytes only work to protect cells from extracellular damage, and help maintain overall cell integrity. However, the dehydration from polyampholytes may not sufficient to protect the cells from intracellular ice formation during recrystallization, so 2% of DMSO is needed to increase the intracellular protection. While not able to completely replace DMSO as cryoprotectants at this point, the polyampholytes studied here do permit decreasing the use of DMSO from 10 to 2 wt%, which represents a significant step in the direction of eliminating DMSO entirely.[38,43-45,58]

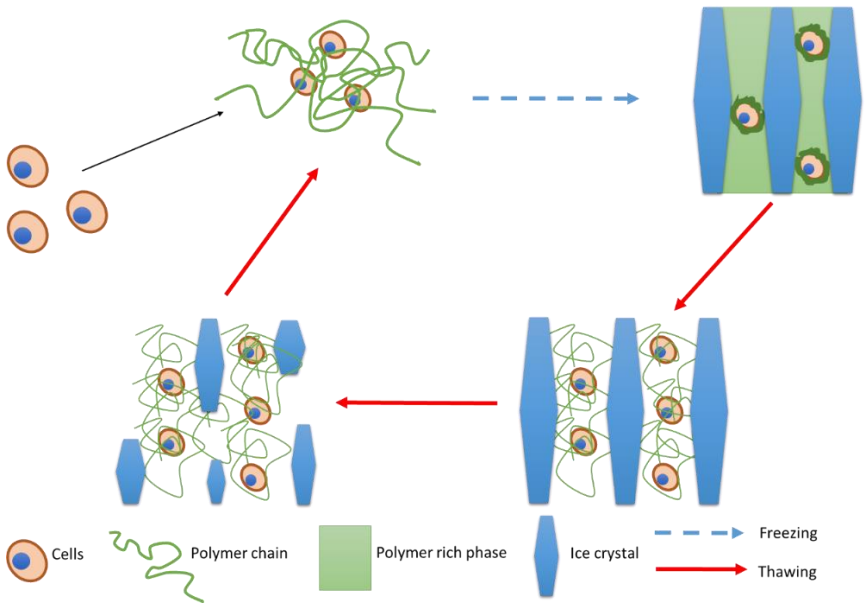

Scheme 5.2 The mechanism of cell cryoprotection.

The proposed mechanism of cryoprotection of cells is summarized in Scheme 5.2. During the slow freezing, the polymer phase separates with the cells from ice and ice size is decreased simultaneously. The polymer-rich phase around cells becomes more concentrated during freezing, which promotes cell dehydration and finally leads to extracellular vitrification at low enough temperatures. During the thawing step, the pre-melting processes cause extracellular vitrified domains to melt first, which maintains a liquid, polymer-rich phase around cells that protects cells from damage through ice recrystallization. The polyelectrolytes also appear to dehydrate cells during freezing, as indicated by decrease in cell size during freezing. This process may not be sufficient to prevent intracellular ice damage, though this can be rectified by addition of 2 wt% DMSO as a supplemental permeant cryoprotectant.

5.5 Conclusion

In this work, we found the synthetic DMAPMA-AA polyampholytes are effective as non-permeant cryoprotective agents in slow freezing protocols, decreasing the need for added DMSO from 10% to 2%. The cryoprotective properties are strongly dependent on polymer composition, molecular weight, polymer concentration, polymer hydrophobicity and the ionic strength in solution. We found that excess negative charge with the appropriate molecular weight are important factors to achieve effective cryoprotection for the copolymers studied. Our results support the notion that polyampholytes play multiple roles during cryoprotection, including anti-freezing properties, forming polymer-rich phases

separating cells from ice, dehydration of cells and the pre-melting of the polymer-rich phase around cells during thawing.

Future work will aim to explore the cryoprotective behavior of polyampholytes with stem cells under the vitrification process with fast freezing. The effect of permeant additives like DMSO, ethylene glycol as well as sucrose will be explored. In conclusion, this study provides a new group of polyampholytes useful to minimize cryo damage, and permitting a significant decrease of DMSO as co-cryoprotectant. We believe this work also helps further our understanding of cryopreservation mechanisms and provides information and guidelines for developing new polymer cryoprotective agent working for different conditions.

5.6 Acknowledgments

The authors acknowledge funding for this project from the Natural Sciences and Engineering Research Council of Canada through its Discovery Grant and CREATE programs, and from the Ontario Centres of Excellence through the OCE-RE program, and also thanks Dr. Paul J. Berti and Dr. Philip Britz-Mckibbin for providing the -80 ^{o}C freezer, and Dr. Heather Sheardown for providing the initial 3T3 cells.

5.7 References

1. Fletcher, G. L.; Hew, C. L.; Davies, P. L. *Annu. Rev. Physiol*. **2001**, *63*,359-390.

2. Polg, C. Smith, A. U.; Parkes, A. S. *Nature* **1949**, *164*, 666-666.

3. Miloš Bohoněk (2012). Cryopreservation of Blood, Blood Transfusion in Clinical Practice, Dr. Puneet Kochhar (Ed.), ISBN: 978-953-51-0343-1, InTech, Available from: http://www.intechopen.com/books/blood-transfusionin-clinical-practice/cryopreservation-of-blood

Henkelman, S.; Noorman, F.; Badloe, J. F.;Lagerberg, J. W. M. *Vox Sanguinis* **2015**, *108*, 103-112

4. Liu, S.; Wang, W.; von Moos, E.; Jackman, J.; Mealing, G.; Monette, R.; Ben, R. N. *Biomacromolecules*, **2007**, *8*, 1456-1462.

5. Wang, T.; Zhu, Q.; Yang, X.; Layne Jr., J. R.; Devries, A. L. *Cryobiology* **1994**, *31*, 185-192.

6. Methods in Molecular Biology, 2007 vol. 368: Cryopreservation and Freeze-Drying Protocols, Second Edition Edited by: J. G. Day and G. N. Stacey © Humana Press Inc., Totowa, NJ page 39.

Hoffman, A. S. In *Biomaterials Science*, 2nd ed.; Ratner, B. D., Hoffman, A. S., Schoen, F. J., Lemon, J. E., Eds.; Elsevier Academic Press: San Diego, CA, 2004; p 107.

7. Young, D. A.; Gavrilov, S.; Pennington, C. J.; Nuttall, R. K.; Edwards, D. R.; Kitsis, R. N.; Clark, I. M. *Biochem. Biophys. Res. Commun.* **2004**, *322*, 759-765.

8. Oh, J. E.; Raja, K. K.; Shin, J. H.; Pollak, A.; Hengstschlager, M.; Lubec, G. *Amino Acids* **2006**, *31*, 289-298.

9. Jiang, G.; Bi, K.; Tang, T.; Wang, J.; Zhang, Y.; Zhang, W.; Ren, H.; Bai, H.; Wang, Y. *Int. Immunopharmacol.* **2006**, *6*, 1204-1213.

10. Capicciotti, C. J.; Kurach, J. D. R.; Turner, T. R.; Mancini, R. S.; Acker, J. P.; Ben, R. N. *Sci Rep.* **2015**, *5*, 9692 (1-10).

11. Briard, J. G.; Jahan, S.; Chandran, P.; Allan, D.; Pineault, N.; Ben, R. N. *ACS Omega* **2016**, *1*, 1010-1018.

12. Chaytor, J. L.; Tokarew, J. M.; Wu, L. K.; Leclère, M.; Tam, R. Y.; Capicciotti, C. J.; Guolla, L.; von Moos, E.; Findlay, C. S.; Allan, D. S.; Ben, R. N. *Glycobiology* **2012**, *22*, 123-133.

13. Mitchell, D. E.; Lovett, J. R.; Armes, S. P.; Gibson, M. I. *Angew. Chem. Int. Ed*. **2016**, *55*, 2801-2804.

14. Stubbs, C.; Lipecki, J.; Gibson, M. I. *Biomacromolecules* **2017**, *18*, 295-302.

15. Mitchell, D. E.; Cameroncd, N. R.; Gibson, M. I. *Chem. Commun.* **2015**, *51*, 12977-12980.

16. Deller, R. C.; Vatish, M.; Mitchell, D. A.; Gibson, M. I. *Nat. Commun.* **2014**, *5*, 3244.

17. Congdon, T.; Notman, R.; Gibson, M. I. *Biomacromolecules* **2013**, *14*, 1578-1586.

18. Rajan, R.; Hayashi, F.; Nagashima, T.; Matsumura, K. *Biomacromolecules* **2016**, *17*, 1882-1893.

19. Jain, M.; Rajan, R.; Hyonc, S.; Matsumura, K. *Biomater. Sci.* **2014**, *2*, 308-317.

20. Matsumuraa, K.; Hayashi, F.; Nagashimab, T.; Hyon, S. H. *J. Biomater. Sci. Polym. Ed.* **2013**, *24*, 1484-1497.

21. Watanabe, H.; Kohaya, N.; Kamoshita, M.; Fujiwara, K.; Matsumura, K.; Hyon, S. H.; Ito, J.; Kashiwazaki, N. *Plos one* **2013**, *8*, e83613.

22. Hyon, S. H.; Ito, J.; Kashiwazaki, N.; Shibao, Y.; Fujiwara, K.; Kawasaki, Y.; Matsumura, K. *Cryobiology* **2014**, *68*, 200-204.

23. Zurick, K. M.; Bernards, M. *J. Appl Polym. Sci.* **2014**, *131*, 40069 (1-9).

24. Abdilla, A.; Shi, S.; Burke, N. A. D.; Stöver, H. D. H. *J. Polym. Sci., Part A: Polym. Chem.* **2016**, *54*, 2109-2118.

25. Shao, H.; Wang, C.; Chen, S.; Xu, C. *J. Polym. Sci., Part A: Polym. Chem.* **2014**, *52*, 912-920.

26. Song, J.; He, A.; Jin, Y.; Cheng, Q. *RSC. Adv.* **2013**, *3*, 24586-24592.

27. Ezell, R. G.; McCormick, C. L. *J. Appl. Polym. Sci.* **2007**, *104*, 2812-2821.

28. Yu, B.; Zheng, J.; Chang, Y.; Sin, M.; Chang, C.; Higuchi, A.; Sun, Y. *Langmuir* **2014**, *30*, 7502-7512.

29. Dubey, A.; Burke, N. A. D.; Stöver, H. D. H. *J. Polym. Sci Pol. Chem.* **2014**, *53*, 353-365.

30. Schroeder, M. E.; Zurick, K. M.; McGrath, D. E.; Bernards, M. T. *Biomacromolecules* **2013**, *14*, 3112-3122.

31. Huang, Y.; Tang, Z.; Zhang, X.; Yu, H.; Sun, H.; Pang, X.; Chen, X. *Biomacromolecules*, **2013**, *14*, 2023-2032.

32. Matsumura, K. Hyon, S. H. *Biomaterials* **2009**, *30*, 4842-4849.

33. Matsumura, K.; Bae, J. Y.; Hyon, S. H. *Cell Transplantation.* **2010**, *19*, 691-699.

34. Rajan, R.; Jain, M.; Matsumura, K. *J. Biomater. Sci. Polym. Ed.* **2013**, *24*, 1767-1780.

35. Matsumura, K.; Kawamoto, K.; Takeuchi, M.; Yoshimura, S.; Tanaka, D.; Hyon. S. H. *ACS Biomater. Sci. Eng.* **2016**, *2*, 1023-1029.

36. Matsumura, K.; Bae, J. Y.; Kim, H. H.; Hyon, S. H. *Cryobiology* **2011**, *63*, 76-83.

37. Zhao, J.; Burke, N. A. D.; Stöver, H. D. H. *RSC Adv.* **2016**, *6*, 41522-41531.

38. Hunt, C. J. *Transfus. Med. Hemother*. **2011**, *38*, 107-123.

39. Meryman, H. T. *Transfusion* **2007**, *47*, 935-945.

40. Bütün, V. *Polymer*, **2003**, *44*, 7321-7334.

41. Hoet, P. H. M.; Gilissen, L.; Nemery, B. *Toxicol. Appl. Pharm.* **2001**, *175*, 184-190.

42. Fischer, D.; Li, Y.; Ahlemeyer, B.; Krieglstein, J.; Kissel, T. *Biomaterials* **2003**, *24*, 1121-1131.

43. McCullough, J.; Haley, R.; Clay, M.; Hubel, A.; Lindgren, B.; Moroff, G. *Transfusion* **2010**, *50*, 808-819.

44. Pellerin-Mendes, C.; Million, L.; Marchand-Arvier, M.; Labrude, P.; Vigneron, C. *Cryobiology* **1997**, *35*, 173-186.

45. Thirumala, S.; Wu, X.; Gimble, J. M.; Devireddy, R. V. *Tissue Eng. Part C Methods*, **2010**, *16*, 783-792.

46. Congdon, T.; Dean, B. T.; Kasperczak-Wright, J.; Biggs, C. I.; Notman, R.; Gibson, M. I. *Biomacromolecules* **2015**, *16*, 2820-2826.

47. van de Wetering, P.; Moret, E. E.; Schuurmans-Nieuwenbroek, N. M. E.; van Steenbergen, M. J.; Hennink, W. E. *Bioconjugate Chem*. **1999**, *10*, 589-597.

48. Carlsson, L.; Fall, A.; Chaduc, I. Wågberg, L.; Charleux, B.; Malmström, E. D'Agosto, F.; Lansalot, M.; Carlmark, A. *Polym. Chem*. **2014**, *5*, 6076-6086.

49. Bories-Azeau, X.; Armes, S. P. *Macromolecules* **2002**, *35*, 10241-10243.

50. Schlenoff, J. B. *Langmuir*, **2014**, *30*, 9625-9636.

51. Shao, Q.; Jiang, S. *Adv. Mater.* **2015**, *27*, 15-26.

52. Budke, C.; Thomas Koop, T. *Chem. Phys. Chem.* **2006**, *7*, 2601-2606.

53. Inui, O.; Teramura, Y.; Iwata, H. *ACS Appl. Mater. Inter*. **2010**, *2*, 1514-1520.

54. Baruch, E.; Mastai, Y. *Macromol. Rapid Commun.* **2007**, *28*, 2256-2261.

55. Fowler, A.; Toner, M. *Ann. N. Y. Acad. Sci*. **2006**, *1066*, 119-135.

56. Bank, H. L.; Brockbank, K. G. M. *J. Card. Surg.* **1987**, *2*, 137-143.

57. Pastorczak, M.; Dominguez-Espinosa, G.; Okrasa, L.; Pyda, M.; Kozanecki, M.; Kadlubowski, S.; Rosiak, J. M.; Ulanski, J. *Colloid. Polym. Sci.* **2014**, *292*, 1775-1784.

58. Hayakawa, J.; Joyal, E. G.;Gildner, J. F.; Washington, K. N.; Phang, O. A.; Uchida, N.; Hsieh, M. M.; Tisdale, J. F. *Transfusion* **2010**, *50*, 2158-2166.

5.8 Appendix

5.8.1 Experiment Section

5.8.1.1 Reactivity Ratio Determination

Solution copolymerizations were carried out at 55 °C in a water bath, on 1 mL scale with 10% (w/v) total monomer loading, 1 mol% initiator (Vazo-56) relative to total monomer, and ethylene carbonate (10 mg/ml) as internal NMR standard in D_2O, in a 5 mm NMR tube. The monomer ratios used were DMAPMA:AA=10:90, 30:70, 40:60, 50:50, 60:40, 70:30 and 90:10. Samples were removed from the water bath every several minutes (90:10, 70:30 is 10 mins, 60:40, 50:50 is 5 mins, 30:70 is 3 mins and 10:90 is 2 mins), cooled in ice water and analyzed by ^{1}H-NMR using a Bruker Avance 600 spectrometer. The decrease of the integrated peaks representing the vinyl protons of AA at 5.5 ppm and DMAPMA at 5.3 ppm reveal the conversion of the two monomers. The reactivity ratios were then calculated by fitting the instantaneous monomer concentrations to the terminal model of the copolymerization equation as described previously.[1]

5.8.1.2 Fluorescent Labelling of APM

In a 20 mL screw cap glass vial, 100 mg of the APM was dissolved in 10 mL of a 0.1M $NaHCO_3$ buffer at pH 9 and the pH adjusted back to pH 9 by addition of 1 M NaOH. A 5 mg/ml FITC solution in DMF was prepared and added to the stirred polymer solution. After reaction for 2 hrs, the FITC-APM was precipitated by centrifugation from the $NaHCO_3$ buffer, and the precipitate washed with water to remove unreacted APM and FITC, following which the water was removed by freeze drying. FITC labeled polymers,

incorporporating 0.5 mol% FITC-APM, were prepared as described above but in a 1:1 v/v water/methanol mixture.

5.8.1.3 DSC Experiment

Polymer solutions were prepared with 10 %wt polymer in DMEM, and added into the aluminum crucibles. Then the polymer solutions were measured on a TA Q200 from 20 ^{o}C to -40 to 30 ^{o}C with cooling/heating rate at 2 ^{o}C/min.

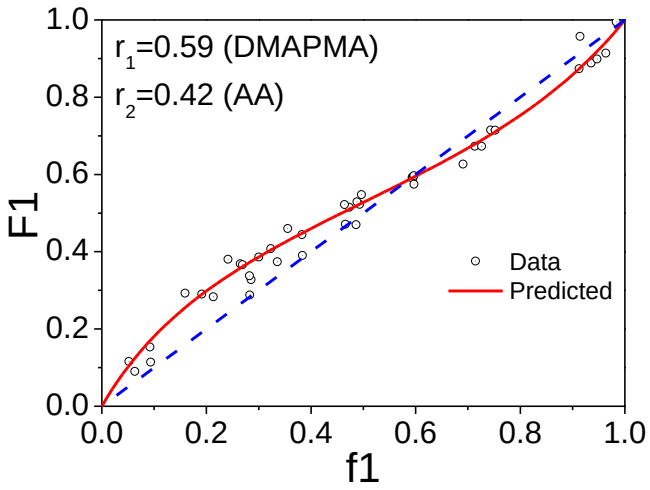

Figure 5A.1 The instantaneous copolymer composition of DMAPMA from a copolymerization of DMAPMA and AA with different initial mole ratios. Experimental data from ^{1}H-NMR: hollow circles; fitted red line calculated using instantaneous copolymer composition equation.

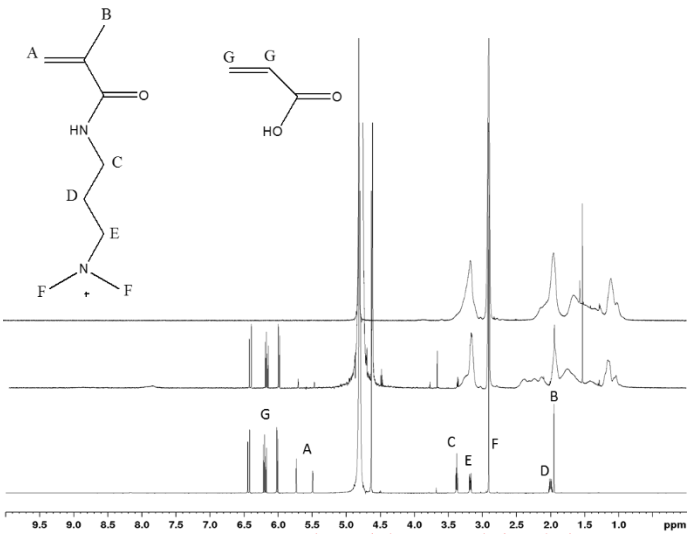

Figure 5A.2 ^{1}H-NMR (600 MHz) spectra of PDA_{30} copolymerization mixture with increasing heating time at 55 °C. From bottom to above: the comonomer mixture before polymerization, after polymerization and after purification.

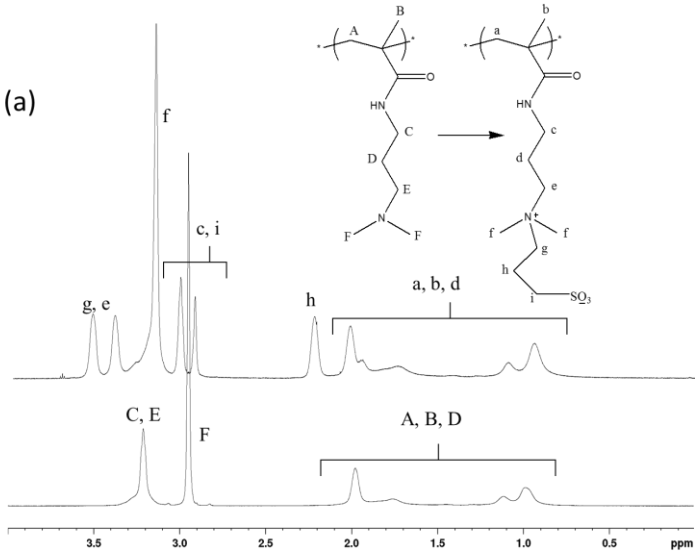

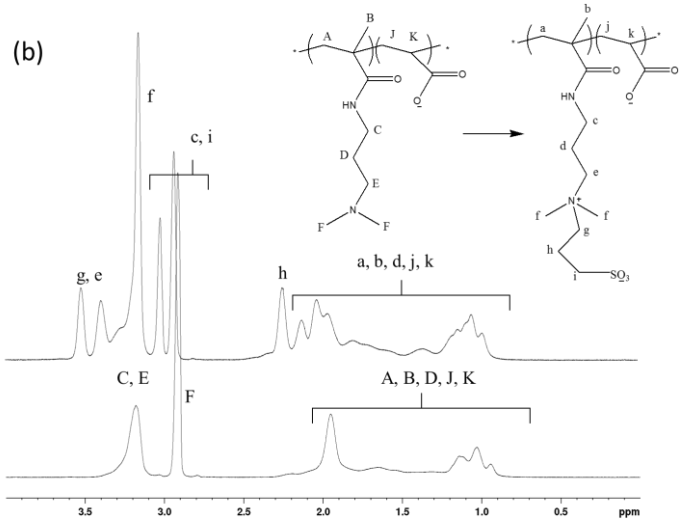

Figure 5A.3 ^{1}H-NMR spectra (in D_2O) before and after betainization, (a) PDMAPMA and PSPB; (b) PDA_{60} and $PSPBA_{60}$.

Table 5A.1 Predicted drift in composition during preparation of PMAx, starting from 30:70 (PDA_{30}) and 45:55 (PDA_{45}) DMAPMA/AA monomer mixtures, estimated using a series of 10% Conversion Steps. Predicted Comonomer Sequence Distributions calculated by the method of Igarashi.[2]

% DMAPMA in polymer											Blockiness (%)		Alternation (%)
Conversion (%)	0-10	10-20	20-30	30-40	40-50	50-60	60-70	70-80	80-90	90-100	DMAPMA	AA	
PDA30	38.4	37.6	36.7	35.6	34.2	32.4	30.0	26.5	20.5	8.1	3.9	43.9	52.2
PDA45	49.3	49.0	48.6	48.1	47.5	46.7	45.7	44.1	41.3	30.0	12.1	22.1	65.8

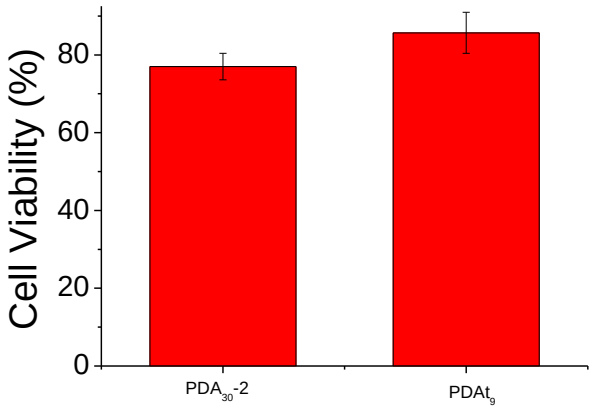

Figure 5A.4 Cell viability after cryostorage for one month. [Polymer]=10% wt, [NaCl]=150 mM. Data are expressed as the mean ± SD for three independent experiments (each sample was counted twice).

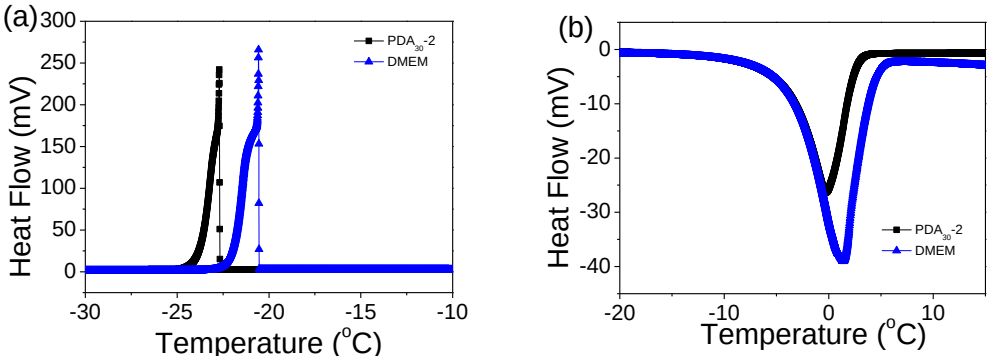

Figure 5A.5 DSC curves of DMEM and PDA_{30}-2 solution, (a) cooling, (b) heating.

Table 5A.2 The heat flows of DMEM and PDA_{30}-2 cooling and heating.

	Freezing point (°C)	Melting point (°C)	Heating Flow (J/g) (Cooling)	Heating Flow (J/g) (Heating)	Crystallization (%) (Cooling)	Crystallization (%) (Heating)
DMEM	-20.7	-3.36	314	346		
PDA_{30}-2	-23.8	-3.98	262	278	83%	80%

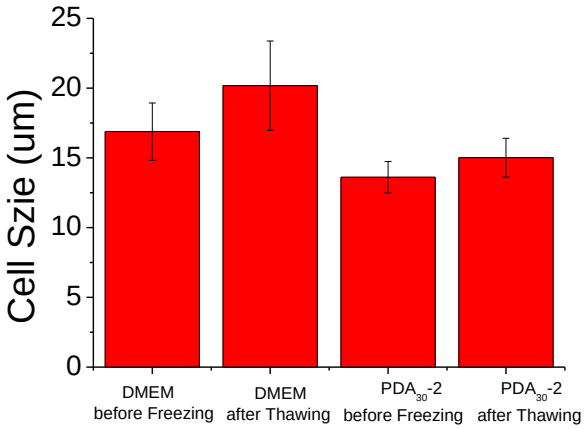

Figure 5A.6 3T3 cells size before freezing and after thawing. Data are expressed as the mean ± SD for 10-20 cells.

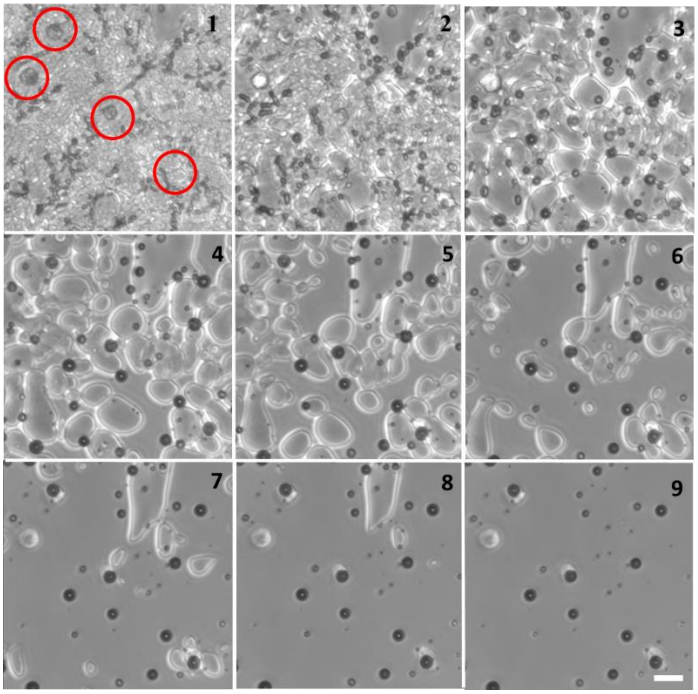

Figure 5A.7 The microscope transmission microscope images of 3T3 cells thawing in DMEM. From 1 to 9, temperature rises ballistically (no active temperature control) from -30 ^{o}C to room temperature over about 5 min, scale bar: 25 µm. (the rounds dark spots are air bubbles).

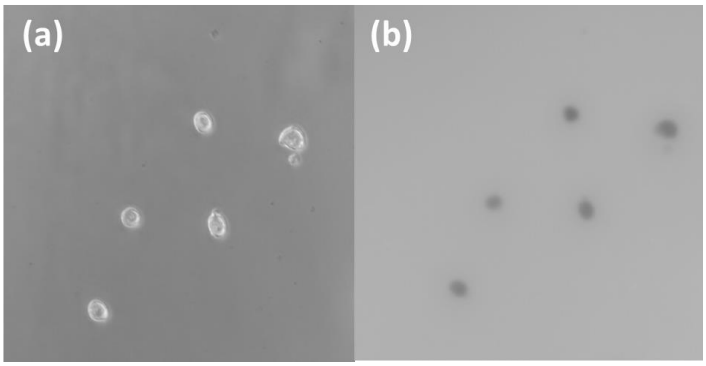

Figure 5A.8 The microscope pictures of PDA_{30}-2 with 3T3 cells at room temperature after thawing (A) optical microscopy images and (B): fluorescence microscopy images. Polymer concentration 10% wt.

5.8.2 References

1. Zhao, J.; Burke, N. A. D.; Stöver, H. D. H. *RSC Adv.* **2016**, *6*, 41522-41531.

2. Igarashi, S. *J. Polym. Sci., Part C Polym. Lett*. **1963**, *1*, 359-363.

Chapter 6: Summary and Future Work

6.1 Summary

Polyampholytes are amphipathic polymers with interesting properties, due to the presence of cationic and anionic charges. Polyampholytes with zero net charge have significant attractive electrostatic interactions, which can cause phase separation or viscosity increases in aqueous solution. When there is net free charge, polyampholyte behavior will shift towards polyelectrolyte behaviour. For polyampholytes incorporating weak acidic and basic groups, the net charge can be adjusted through both comonomer ratio and pH. Polyampholytes have an isoelectric pH, or pH(I), which is the pH at which their net charge is zero. The pH(I) depend on the pKa of both cationic and anionic groups as well as on their ratio, and can be theoretically predicted.[1]

The ionic strength of the medium will affect polyampholytes in two ways. If there are net charges on polyampholytes then small increases in the ionic strength will shield the electrostatic repulsion and decrease the solubility, while larger increases of the ionic strength will also shield the intra-molecular electrostatic interaction of polyampholytes and increasing their solubility, an effect known as the anti-polyelectrolyte effect.

This thesis explores the properties of high charge density binary (and some ternary) polyampholytes comprising weak acid and base monomers, which have not been systematically studied to date. This includes studying the phase separation properties of stoichiometric polyampholytes comprising different types of ionic groups to explore the

effect of hydrophobic interactions on polyampholyte behaviour. Finally, the cryoprotective properties of synthetic polyampholytes are studied in detail.

The following summarizes the results of each chapter in this thesis:

6.1.1 Chapter 2

A series of new polyampholytes with weak acid and base, acrylic acid (AA) and *N*-(3-aminopropyl)methacrylamide hydrochloride (APM) were synthesized. The reactivity ratio of these two monomers were measured by ^{1}H-NMR, by monitoring the ratio of APM and AA during copolymerization and fitting the results with the copolymerization equation, giving reactivity ratios of APM and AA of 0.68 and 0.48. These reactivity ratio were then used to guide the synthesis of polyampholytes with different charge ratios ranging from 6% to 88% APM with little compositional drift.

The pH(I) of these polyampholytes moves to higher pH with increasing APM concentration, and increasing [NaCl] at pH(I) will increase the solubility. While the pH(I) and anti-polyelectrolytes properties are also seen in other polyampholytes, the difference found in this work is that the neutral monomer units of non-stoichiometric polyampholyte at pH(I) have a big effect on polyampholyte properties. In presence of excess AA, at pH(I) the hydrogen bonding between AA units works together with electrostatic interaction, leading to stronger phase separation. Specifically, PMA_{52} (52% cationic APM) has liquid to liquid phase separation, PMA_{35} has liquid to solid phase separation and requires much higher [NaCl] than PMA_{50} to redissolve the polymer, and PMA_{12} shows both salting-in and salting-out with increasing [NaCl]. However, on the other side, excess APM increases the

solubility of polyampholytes at pH(I) so that polyampholytes containing more than 60% APM do not show phase separation at pH(I).

Exploring the temperature responses of APM-AA polyampholytes showed that these polyampholytes can have both LCST and UCST under different conditions. The stoichiometric polyampholytes solubilized by addition of NaCl at pH(I) show LCST behaviour. The polyampholytes with less than 10% APM have UCST behavior at pH values just below their pH(I), which is attributed to the hydrogen bonding of AA units.

6.1.2 Chapter 3

The third chapter focusses on the properties of stoichiometric APM-AA polyampholytes with different molecular weights. A series of stoichiometric polyampholytes with MW ranging from 15 to 460 kDa were synthesized by free radical polymerization in presence of chain transfer agent. The moleular weight does not affect the pH(I), but has significant effects on other polyampholyte solution properties. With decreasing molecular weight the transmittees of polyampholytes at pH(I) increases and finally reaches 100%, while the [NaCl] needed to make the solutions clear decreases. Fluorescently labelled polyampholytes were used to measure the phase separation efficiency. High molecular weight polyampholytes were found to have high phase separation efficiency, becoming independent of [polymer] above a threshold MW.

The LCST-related cloud point temperatures are also molecular weight dependent. Polyampholytes with different molecular weights all have LCST, no matter what the phase separation efficiency is at pH(I). The polyampholyte with highest molecular weight were

thermally coacervated and crosslinked with THPC. The results show low crosslink density produces the crosslinked gel, and high crosslink density will give the crosslinked coacervates. Finally, absorption of organic dyes was explored using the polyampholyte with highest molecular weight, and it was found that polyampholytes at pH(I) strongly bind multi-charge organic dyes from water by electrostatic interaction.

6.1.3 Chapter 4

The fourth chapter is aimed at understand the effect of polyampholyte structures on phase separation from aqueous solutions. Three anionic monomers, AA, AMPS and NaSS, and three cationic monomers, APM, DMAPMA and MAPTAc, were seleted with the charge density decreasing but the hydrophobicity increasing in those orders. Then the reacticity ratio of different monomer pairs were measured and nine different polyampholytes were synthesized by free radical copolymerization resulting in binary copolymers with near alternating sequence distribution and with 50±5% cationic units.

Both the electrostatic interaction and polymer hydrophobicity affect the polyampholyte phase separation. When polyampholytes are hydrophilic, as with 50% AA, the electrostatic interaction is the dominating force of the phase separation, with the transmittance increasing when the charge density on the amine decreases, and the [NaCl] needed to make the solution clear also decreasing. When the hydrophobicity increases, as in presence of AMPS, the electrostatic interaction decreases, so phase separation is controlled by both factors, with PMAs49 and PDAs50 showing similar phase separation behavior. However, when the hydrophobicity keeps increasing as in the polyampholytes with NaSS, phase

separation was mainly controlled by hydrophobic interactions, with liquid to solid phase separation, compared to liquid to liquid phase separation seen in other polymers. As well the [NaCl] needed to clarify the solution are higher than for other polymers, and PNM45 even shows salting-out instead of the anti-polyelectolyte effect.

To better understand the phase separation of polyampholytes, the polyelectrolyte complexes made by corresponding polyelectrolyte homopolymers are compared with the polyampholytes. The phase separations of polyelectrolyte complexes are stronger than those of the corresponding polyampholytes, which is because of the low efficiency of charge-charge complexation in polyampholytes, and the free ionic groups on polyampholytes. Increasing the [NaCl] to 1 M cannot make the PAPM PAA complex dissolve but can make the PMA50 solution clear, suggesting only some of the electrostatic interaction of polyampholytes are shielded by NaCl.

Then, the different polyampholytes can have either LCST or weak UCST depending on the structure. Polyampholytes also have select bonding with organic dye from water, which depends on the electrostatic interaction and hydrophobic interactions between polyampholytes and dyes.

6.1.4 Chapter 5

The last chapter explores the application of polyampholytes as a cryoprotective agent. This work found the polyampholyte cryoprotectants need excess negative charge at physiological conditions, with zero net charge polyampholytes not showing cryoprotective properties. Slight increases in hydrophobicity improves the cell freeze-thaw viability,

probably because the hydrophobic groups will help polyampholytes bind to cell surfaces. With proper conditions, the freeze-thaw viability can reach 80%, comparable with DMSO.

Cryomicroscopy experiments found that the polyampholytes phase separate with cells from during freezing, protecting the cells from the ice crystal and also helping cells dehydrate. During thawing, the polyampholyte rich phase melts first, protecting cells from ice recrystallization.

However, the percentage cell attachment after thawing was much lower than DMSO, showing the cell viability after thaw decreases over time. That may be because of lack of sufficient intracellular cryoprotection. Because the polyampholytes are a nonpermeable cryoprotective agent, they can only protect the cell exterior. To prove this assumption and improve the cell attachment after thawing, 2% DMSO were added with polyampholytes, and the cell attachment improved and was comparable with DMSO.

6.2 Future Work

6.2.1 Polyampholyte Physical Crosslinked Hydrogel as the Adsorbent of Organic Dyes

Based on chapter 4, polyampholytes prepared by monomers with significant hydrophobicity will form hydrogels at zero net charge. The hydrogel will have hydrophobic groups and free charges, so theoretically, polyampholytes should have an ability to bind organic dyes with both electrostatic and hydrophobicity interaction. Chapter 3 and 4 have

proved that polyampholytes at pH(I) can bind with organic dyes. Polyampholytes physically crosslinked hydrogel have been made and found to bind with both cationic and anionic polyelectrolyte hydrogel.[2,3]

Future work will combine these two findings, using hydrophobic ionic monomers to prepare hydrogels, and use these hydrogel as the organic dye adsorbent. Preliminary experiments found the one to one ratio polyampholyte NaSS and VBTEAc can form hydrogels in situ during free radical copolymerization without crosslinker. The hydrogel was found to bind Orange II dye from water at higher [NaCl]. Future work will explore the hydrogel's swelling properties, and the ability of dye binding under different conditions.

6.2.2 Polyampholytes with UCST

Chapter 2 and 3 show polyampholytes made soluble by addition of NaCl at their pH(I) have LCST behaviour. However, theoretical research predicted such polyampholytes should have UCST, where the polyampholyte solubility would increase at high temperature at pH(I) or with zero next charge.[4] However, as far as we know, there is no polyampholyte showing UCST in water, though a few studies found polyampholytes showing UCST in water/organic solvent mixtures.[5,6] In chapter 4, we found the stoichiometric polyampholytes based on DMAPMA and NaSS show weak UCST, the solution transmittance increases with heating though not reaching 100%, even with lower molecular weight (data not shown). However, we found the stoichiometric polyampholyte with NaSS and VBTEAc with lower molecular weight (around 10 kDa, data not shown), have UCST. The hypothesis is the large hydrophobicity of these monomers increases the polymer-

polymer interaction, which promotes polyampholyte phase separation at low temperature. However, the electrostatic interaction is weak and can be broken by heating, so the polyampholytes present the UCST. Future work will focus on these temperature responses and try to explore the underlying mechanisms.

6.3 References

1. Patrickios, C. S. *J. Colloid Interface Sci.* **1995**, *175*, 256-260.

2. Sun, T.; Kurokawa, T.; Kuroda, S.; Ihsan, A. B.; Akasaki, T.; Sato, K.; Haque, M. A.; Nakajima, T.; Gong, J. *Nat. Mater.* **2013**, *2*, 932-937.

3. Roy, C. K.; Guo, H.; Sun, T.; Ihsan, A. B.; Kurokawa, T.; Takahata, M.; Nonoyama, T.; Nakajima, T.; Gong, J. *Adv. Mater.* **2015**, *27*, 7344-7348

4. Tanaka, M.; Tanaka, T. *Phys. Rev. E* **2000**, *62*, 3803-3816.

5. Zhang, Q.; Hoogenboom, R. *Chem. Commun*., **2015**, *51*, 70-73.

6. Takeoka, Y.; Berker, A. N.; Du, R.; Enoki, T.; Grosberg, A.; Kardar, M.; Oya, T.; Tanaka, K.; Wang, G.; Yu, X.; Tanaka, T. *Phys. Rev. Lett.* **1999**, *82*, 4863-4865.